

Surface Mediated Reduction of Chlorinated Solvents by Zero-Valent Iron

Timothy Lee Johnson
B.S. Geology, University of Arkansas, 1989

A dissertation submitted to the faculty of the
Oregon Graduate Institute of Science and Technology
in partial fulfillment of the
requirement for the degree of
Doctor of Philosophy
in
Environmental Science and Engineering

September 1997

This dissertation "Surface Mediated Reduction of Chlorinated Solvents by Zero-Valent Iron" by Timothy Lee Johnson has been examined and approved by the following examination committee:

Dr. Paul Tratnyek, Dissertation Advisor
Associate Professor

Dr. William Fish
Associate Professor

Dr. Carl Palmer
Associate Professor

Dr. Yuri Gorby
Battelle, Pacific Northwest National Laboratory

DEDICATION

I dedicate this work to my family, who have been very supportive during the many years I have followed my dreams.

ACKNOWLEDGEMENTS

I would first like to thank Paul Tratnyek for his example of never ending devotion to science. He has provided a example of what it is like to truly love your work. I would also like to thank the faculty of the Department of Environmental Science and Engineering who have at various stages of my time at OGI given me input and encouragement.

Thanks to Leah Matheson and Abinash Agarwal who have been great comrades from my early days at OGI to the present. Michelle Scherer has been my friend now for at least two lives, UCONN and OGI. I thank her for her support which has been crucial throughout.

Many good friends at OGI have been on numerous great adventures. I thank them for the good times we have had and the many to come.

TABLE OF CONTENTS

Dedication	iii
Acknowledgements	iv
List of Tables	ix
List of Figures	x
Abstract.....	xi

Chapter 1. Passive Treatment Zones of Iron Metal: A Review of the Science and Technology

1.1 Abstract.....	1
1.2 Introduction	1
1.3 The In-Situ Treatment Barrier Alternative	2
1.3.1 Reactive Media.....	2
1.3.2 Barrier Designs.....	2
1.4 Chronology of Zero-Valent Iron Based Remediation	3
1.5 Existing Treatment Walls of Zero-Valent Iron	4
1.5.1 Base Borden, Ontario, Canada.....	4
1.5.2 Intersil, Sunnyvale, CA.....	4
1.5.3 SGL Circuit, Wayne, NJ.....	5
1.5.4 Hill AFB, Utah.....	5
1.5.5 Nortel, Belfast, Ireland.....	5
1.5.6 U.S. Coast Guard Air Station, Elizabeth City, NC.....	5
1.5.7 Portsmouth Gaseous Diffusion Plant, OH.....	6
1.5.8 Moffet Federal Airfield, CA.....	6
1.5.9 Coffeyville, KS.....	6
1.5.10 Other sites.....	6
1.6 Cost of In-Situ Barriers.....	6
1.7 Chemistry of Zero-Valent Iron Based Remediation	6
1.8 Long-Term In-Situ Performance of Treatment Walls	8
1.8.1 Precipitation and Other Geochemistry.....	8
1.8.2 Microbiological Effects.....	9
1.9 Treatment of Surface Water	10

1.9.1	Industrial Waste Streams.....	10
1.9.2	Acid Mine Drainage.....	10
1.10	Organic Contaminants Treatable by Zero-Valent Iron.....	10
1.10.1	Halogenated Aliphatics.....	10
1.10.2	Halogenated Aromatics.....	10
1.10.3	Nitroaromatics.....	11
1.10.4	Azo-Compounds.....	11
1.11	Inorganic Contaminants Treatable by Zero-Valent Iron.....	11
1.11.1	Contaminant Metals.....	11
1.11.2	Non-Metal Inorganic Ions.....	13
1.12	Reduction by Bi-Metallic Systems and Other Zero-Valent Metals.....	13
1.12.1	Bi-Metallic Systems.....	13
1.12.2	Zero-Valent Metals Other Than Iron.....	14
1.13	The Future of In-Situ Reactive Treatment Barriers.....	14
1.14	References.....	28

**Chapter 2. A Column Study of Geochemical Factors Affecting Reductive
Dechlorination of Chlorinated Solvents by Zero-Valent Iron**

2.1	Abstract.....	36
2.2	Introduction.....	37
2.2.1	Chemical Background.....	37
2.3	Experimental Section.....	39
2.3.1	Chemicals.....	39
2.3.2	Column Design.....	40
2.3.3	Analyses.....	40
2.4	Results and Discussion.....	41
2.4.1	Chemistry of the Fe-H ₂ O-Sand System.....	41
2.4.2	Iron Surface Analysis.....	42
2.4.3	Dechlorination of Solvents.....	42
2.5	Implications for In-Situ Remediation.....	43
2.6	References.....	51

Chapter 3. Kinetics of Halogenated Organic Compound Degradation by Iron Metal

3.1	Abstract	52
3.2	Introduction	53
3.3	Methods.....	54
3.4	Results and Discussion	55
3.4.1	Pseudo-First-Order Rate Data.....	55
3.4.2	Surface Area Normalized Kinetics.	55
3.4.3	Factors Effecting k_{SA}	56
3.4.4	Apparent Deviations from the Kinetic Model.	58
3.4.5	Relating Batch to Column Kinetics.....	59
3.4.6	Indirect Effects on the Second-Order Model.	60
3.4.7	Correlating Representative Rate Constants.....	61
3.5	List of Symbols.....	62
3.6	References.....	77

Chapter 4. Degradation of Carbon Tetrachloride by Iron: Complexation Effects on the Oxide Surface

4.1	Abstract	81
4.2	Introduction	82
4.3	Experimental Information.....	83
4.3.1	Chemicals and Solutions.	83
4.3.2	Batch Systems.....	84
4.3.3	Analyses.....	84
4.4	Results and Discussion	84
4.4.1	Kinetics of Dehalogenation.	84
4.4.2	Kinetics of Iron Dissolution.	85
4.4.3	Passivation by Borate.....	87
4.4.4	Depassivation by Chloride.	87
4.4.5	Modeling Inhibition by Catechol.	88
4.4.6	Comparison of Catechol, Ascorbate, and Acetate.....	89
4.4.7	Effect of EDTA.....	90
4.4.8	The Role of Surface-Bound Fe^{2+}	91

4.5 Conclusions	92
4.6 List of Symbols	93
4.6 References	105

LIST OF TABLES

1.1	Reactive media hypothesized for permeable barriers.....	22
1.2	Installation techniques of permeable barriers.....	23
1.3	Chlorinated compounds aside from aliphatics degraded by iron.....	24
1.4	Metal and inorganic ions reduced by zero-valent iron.....	25
1.5	Capital costs of field scale installations	26
1.6	Surface area of several commonly used iron metals.....	27
2.1	Pseudo-first-order rate constants for chloroform degradation in a column	50
3.1	Experimental conditions	70
3.2	Representative kinetic data for dehalogenation by iron metal.....	71
3.S1	Batch data for halogenated alkane reduction.....	72
3.S2	Batch data for halogenated alkene reduction.....	73
3.S3	Column data for halogenated alkane reduction.....	75
3.S4	Column data for halogenated alkene reduction.....	76
4.1	Model parameters for inhibition of the CCl_4 reaction with Fe^0	103
4.2	Comparison of reduction rates by Fe^{2+} with and without Fe^0	104

LIST OF FIGURES

1.1	Schematic of in-situ passive treatment zone for groundwater contamination.....	16
1.2	Chronology of development of zero-valent iron for groundwater remediation.....	17
1.3	Field sites in operation include Base Borden (sheet pile (a)), SGL, NJ (above ground (b)), Nortel (funnel and gate (c)), and Elizabeth City (trencher (d)).	18
1.4	Evolution of hypothesized reactive interface with time.....	19
1.5	Geochemistry of natural groundwater will be affected by iron-zone	20
1.6	SEM of precipitates formed by CCl ₄ transformation.....	21
2.1	Pourbaix diagram of Fe-H ₂ O system showing possible precipitates.	44
2.2	Schematic of column utilized in geochemical studies.....	45
2.3	Steady state profile of pH across an iron-bearing zone.	46
2.4	Profile of Fe ²⁺ in solution across an iron-bearing zone.....	47
2.5	SEM of precipitates formed after 6 months of CCl ₄ degradation.	48
2.6	Kinetics of chloroform degradation.	49
3.1	Distribution of k _{obs} data from the literature.....	63
3.2	Distribution of surface area normalized kinetic data	64
3.3	Range of surface areas as measured by BET.....	65
3.4	Effects of pretreatment and media composition on k _{SA}	66
3.5	Effect of initial concentration on reaction rate.	67
3.6	Comparison of k _{SA} between batch and column experiments.....	68
3.7	Correlation between k _{SA} and 2-electron reduction potential.....	69
4.1	Schematic of oxide surface on Fe ⁰	94
4.2	Effect of [P] ₀ on k _{CCl₄}	95
4.3	Zero-order dissolution of Fe ²⁺ from Fe ⁰	96
4.4	Effect of [P] ₀ on k _{Fe²⁺}	97
4.5	Effect of borate and chloride on k _{CCl₄}	98
4.6	Effect of catechol on k _{CCl₄} and k _{Fe²⁺}	99
4.7	Effect of acetate and ascorbate on k _{CCl₄}	100
4.8	Effect of EDTA on k _{CCl₄}	101
4.9	Conceptual model of inner-and outer sphere adsorption.....	102

ABSTRACT

In-situ barriers of zero-valent iron (Fe^0) have become one of the most attractive options for remediation of chlorinated solvents in groundwater due to their simplicity of application and ability to remediate a wide range of contaminants. This study clarifies the geochemistry associated with the reaction of Fe^0 and chlorinated aliphatic compounds. The focus (and chapters) proceed from the macro scale to the molecular scale.

Column experiments were used to simulate a cross-section of a permeable barrier with an iron-bearing zone, an up-gradient, and a down-gradient zone of sand. The columns showed that (i) water flowing from the treatment zone is anoxic, alkaline, and high in ferrous iron, (ii) the kinetics of dechlorination vary with flow rate, and (iii) there is a correlation between the initial concentration of CCl_4 ($[\text{P}]_0$) and the concentration of Fe^{2+} in solution.

To further explore the mechanism of dechlorination by Fe^0 , a combination of new and previously reported kinetic data was subjected to an analysis of factors effecting contaminant degradation rates. Rate constants from batch and column studies vary widely, but normalization to concentration of iron surface area yields a specific rate constant (k_{SA}) that varies by only 1 order of magnitude for individual halocarbons. Correlation analysis using k_{SA} reveals that dechlorination is generally more rapid at saturated carbon centers than unsaturated carbons, and high degrees of halogenation favor rapid reduction. It was concluded from this study that the unexplained order of magnitude variability in k_{SA} reflects differences in surface oxide composition.

To evaluate the role of the surface oxide film in mediating the reduction of chlorinated solvents, CCl_4 was used as a probe of degradation by Fe^0 under the influence of various anions, ligands, and $[\text{P}]_0$. The reaction kinetics were pseudo-first order for CCl_4 disappearance (k_{CCl_4}), and zero order for the appearance of Fe^{2+} in solution ($k_{\text{Fe}^{2+}}$). Values of k_{CCl_4} and $k_{\text{Fe}^{2+}}$ exhibit saturation kinetics with respect to $[\text{P}]_0$, suggesting that CCl_4 is transformed via reaction with a limited number of specific reactive sites, and that it is the dominant oxidant contributing to corrosion in these systems.

Chapter 1

Passive Treatment Zones of Iron Metal: A Review of the Science & Technology

1.1 ABSTRACT

The use of granular iron metal to remediate groundwater contamination has evolved into an accepted technology in the last few years. The reaction was discovered by accident and its potential went unnoticed for several years, but increasing concern in the late 1980's over chlorinated solvents in groundwater lead to interest in alternative remediation technologies. The chemistry of zero-valent iron metal as a reductant of environmental contaminants has evolved from the asking of basic questions to asking sophisticated questions about the mechanisms of the reaction. It is now understood by most that the reaction can be thought of as analogous to common corrosion reactions with the contaminant, often a chlorinated solvent, serving as the oxidant. Along with a better understanding of the reaction mechanism came an acceptance of the technology from the regulatory community, which has led to the many field sites that are now in progress.

1.2 INTRODUCTION

The perspective of this review of in-situ barriers focuses on the use of zero-valent iron and proceeds from the large scale to the small scale. The concept of permeable barriers as a means of groundwater remediation is discussed along with methods of installation and a discussion of materials which may be useful for various contaminants. A brief discussion of several field sites is presented along with an analysis of cost. The focus then shifts to the basics of how degradation by iron works, and what type of contaminants can be treated. This is meant to supplement the understanding of geochemical changes in a flow through system provided in Chapter 2 (Johnson and Tratnyek 1994), the thorough kinetic analysis

of chlorinated aliphatic compound degradation provided in Chapter 3 (Johnson *et al.* 1996b), and the discussion of surface chemical complexation in Chapter 4 (Johnson *et al.* 1996a).

1.3 THE IN-SITU TREATMENT BARRIER ALTERNATIVE

The approximately 300,000 sites estimated to be contaminated by chlorinated solvents, and the history of limited success with current treatment methods (Mackay and Cherry 1989), has forced the pursuit of new remediation strategies (Pankow and Cherry 1996). Currently in-situ barriers have become one of the most popular options for groundwater treatment (Fig 1.1). The concept of permeable reactive barriers for groundwater remediation has received attention due to its simplicity and the variety of treatment materials that can be used to remediate a wide range of contaminants (Gillham *et al.* 1994; Kovalick 1995; Morrison and Spangler 1995; Nyer and Suthersan 1996; Vidic and Pohland 1996). A host of media for use in barriers that utilize adsorption, precipitation, chemical, or biological treatment are in various stages of development. Several field scale in-situ demonstrations are also in progress using barriers to test biotic and abiotic scenarios for contaminant treatment (Kovalick 1995).

1.3.1 Reactive media. A large number of reactive media, both biotic and abiotic, have been suggested for use in treatment zones (Table 1.1). The reactions responsible for contaminant removal include oxidation/reduction, precipitation, adsorption, complexation, and cementation. Most of these remediation reactions involve surface chemistry but others attempt to stimulate microorganisms or inorganic reactions. One abiotic reaction that appears to be applicable to a wide range of contaminants is zero-valent iron. Several methods of utilizing zero-valent iron as an in-situ treatment are under development.

1.3.2 Barrier designs. After a reactive media has been chosen, an installation design and method must be configured. A few of the most common designs are briefly reviewed here and a list is provided in Table 1.2. The simplest application of an in-situ treatment zone is to shallow groundwater plumes underlain by a confining layer. To install the treatment zone, sheet piling is driven into the ground to form an enclosed cell in the path of the plume. The sheet pile cell is then excavated and backfilled with the reactive media. The sheet piling is removed and contaminated water flows through the wall with the existing hydraulic gradient. Bentonite slurry or sheet pile walls are sometimes used to ensure that the contaminant plume does not pass the treatment zone. Permeable reactive barriers may also employ the funnel and gate type system where sheet metal piling acts as

the sides of a funnel to direct naturally flowing groundwater through a reactive gate (Star and Cherry 1994). This gate can be made for easy removal to rejuvenate the reactive media.

Another method of in situ permeable barrier installation using a trencher modified with a hopper has recently proven successful. The machine simultaneously opens a trench and backfills it with reactive media. A full-scale barrier 150 feet long was installed in one day at the Coast Guard site in Elizabeth City, NC using this method, which provided cost savings over driving sheet piling and excavating.

Several other emplacement methods including colloid injection, horizontal trenching, and auguring of so called "fences", are in various stages of development. Emplacement of colloidal zero-valent iron into columns of sand has been achieved in laboratory tests (Kaplan *et al.* 1994; Kaplan *et al.* 1996) although the lifetime, reactivity, and transport of these colloids remains poorly defined. It has also been suggested that a series of large diameter augured holes, backfilled with reactive media could extend the depth of achievable treatment (Vidic and Pohland 1996). Other application ideas include treatment train systems, as an additive to clay liners at disposal facilities as a type of secondary containment, and as a proppant in hydro-fractured contaminated clays.

A particularly novel application for zero-valent iron has been as a part of the so called "Lasagna" process. In this process contaminants are forced by electroosmosis to flow through a treatment barrier. Electroosmotic gradients are directed by two electrodes installed into the ground which serve as anode and cathode for application of low direct current voltage that forces contaminants to migrate (Shapiro and Probststein 1993). Theoretically this approach could be used to force contaminants through an iron-bearing zone for treatment. Advantages of electroosmosis include uniform water flow and control of flow direction. Disadvantages include slow flow rates, unstable long-term operation due to soil consolidation and cracking, steep pH gradients, and precipitation of metals and minerals near the cathode (Acar and Alshawabkeh 1993; Ho *et al.* 1995). Combining electroosmosis with zero-valent metals will require careful consideration of chemical gradients inherent to both systems.

1.4 CHRONOLOGY OF ZERO-VALENT IRON BASED REMEDIATION

The chronology of development that lead to the wide spread use of iron metal for environmental remediation is presented as a timeline in Figure 1.2. It appears that the first use of iron metal to reduce environmental contaminants was by J. Z. Sweeny who was granted a patent titled "Decomposition of halogenated organic compounds using metallic couples" in 1973 (Sweeny and Fischer 1973). In the late 1970's and early 1980's Sweeny

published two symposium papers on the reduction of a wide range of organic compounds (Sweeny 1979; Sweeny 1981) and Gould reported the removal of cadmium and chromium from wastewaters by a process described as 'cementation' (Gould 1982). As the time line in Figure 1.2 shows, there was a resurgence in iron metal based remediation technology in the late 1980's. This resurgence was caused by a well casing study that was completed in 1985, but the significance of the results were only recognized a few years later (Gillham 1995; Gillham and O'Hannesin 1992; Gillham and O'Hannesin 1994; Gillham *et al.* 1993; O'Hannesin and Gillham ; O'Hannesin 1993) . Beginning about 1992, the interest in iron metal increased rapidly (Fairweather 1996; Tratnyek 1996; Wilson 1995).

1.5 EXISTING TREATMENT WALLS OF ZERO-VALENT IRON

Since 1991 there have been several field applications of reactive iron barriers and many more are planned in the near future at a variety of different types of sites. The permeable iron-barrier technology has recently been featured in news magazines such as *Chemical & Engineering News* (Wilson 1995), *Civil Engineering* (Fairweather 1996), and *Chemistry & Industry* (Tratnyek 1996). The Ground-Water Remediation Technologies Analysis Center (GWRTAC) has also compiled information on an electronic database (www.gwrtac.org). Additional information on the status of reactive barriers is available in the EPA technology status report on in situ barriers (Kovalick 1995).

1.5.1 Base Borden, Ontario, Canada. The first in situ application of an iron barrier was installed on June 10, 1991 at Canadian Base Borden, Ontario, Canada (Fig 1.3a) to treat an artificial spill of PCE and TCE (O'Hannesin 1993). A sheet pile cell constructed on the surface was driven to 32 feet and the material inside excavated. The cell was then filled with granular iron (22% w/w) and coarse sand (78%). The dimensions of the wall are 18 ft long, 5.2 ft thick, and 7.2 ft deep. This reactive barrier has continuously reduced greater than 90% of the initial contaminants for more than 5 years. Cores taken across the wall after 1 and 2 years of operation showed relatively little massive precipitate by scanning electron microscopy. Core material was enriched for several types of microbial activity with primarily null results (Matheson 1994).

1.5.2 Intersil, Sunnyvale, CA. Intersil Semiconductor Manufacturing, a subsidiary of General Electric in Sunnyvale California, was the first commercial full-scale field demonstration of an iron barrier, and was installed in December 1994 (Fig 1.3b). Approximately 220 tons of iron metal from Master Builder were placed by Geomatrix in a barrier that is 40 ft long, 4 ft thick and 13 feet deep which is intercepting a plume of TCE (Yamane *et al.* 1995). The cost of capital was \$770,000 and it has been estimated that

Intersil is saving about \$300,000 per year in operation and maintenance costs that were being spent on a pump and treat system (Fairweather 1996). The previous system also rendered the property unusable for the projected 30 year cleanup time, while the barrier has allowed the site to be leased and paved for a parking lot.

1.5.3 SGL Circuit, Wayne, NJ. A fixed bed reactor was installed at SGL Printed Circuit, a former industrial site, and used to treat PCE, TCE, and 1,2-DCE. The above ground reactor consisted of a 2.4 m diameter fiberglass tank filled to a depth of 1.7 m with granular iron. Contaminated water was pumped into a reservoir at the top of the tank and allowed to percolate through the iron and exit the bottom. Residence time of contaminated water in the tank was 24 hr, but it was found that the contaminants had been degraded to below detection limits by 12 hr (Bhattacharya and Subramanian 1996; Vogan *et al.* 1995).

1.5.4 Hill AFB, Utah. An above ground canister was used at the Hill AFB to treat a plume of approximately 2000 ug/L of TCE from June 2 to October 13, 1994. The reactor was 4.5 ft high and 1 ft in diameter and was filled with Master Builder granular iron (Blend B, GX-27). The reactor was found to degrade TCE and subsequent byproducts (cDCE and VC) to acceptable levels. After approximately 4 months of operation the canister was plugged by precipitation of carbonate compounds. Three difficulties at this site preclude full scale use of an in-situ barrier: (i) column plugging, (ii) the best location for installation of an in situ barrier is off site, and (iii) the Record of Decision came too early to include this technology (Searles 1995).

1.5.5 Nortel, Belfast, Ireland. An electronics manufacturing facility owned by Nortel and located in Northern Ireland has recently become the first site in Europe where Fe⁰ is being used to remediate a chlorinated organic plume (Wilson 1995). A small but concentrated (300 mg/L) plume of TCE is being funneled through a reactive iron gate (Fig 1.3c) by means of slurry walls (Thomas *et al.* 1995). Golder and Associates is the consulting company applying the technology.

1.5.6 U.S. Coast Guard Air Station, Elizabeth City, NC. A site used by the Navy and Coast Guard for chrome-plating engine parts is billed as being the first mixed waste (organic and inorganic) site to be treated by zero-valent iron (Fig 1.3d). The site contains a few parts per million Cr(VI) and TCE. Laboratory tests found the most effective metal for this site to be that from Peerless Metal Powders and Abrasives, (Detroit, MI). A modified horizontal trenching machine was recently able (June 22, 1996) to install this barrier which is 150 feet in length 18 feet deep and 2 feet thick in one day (Puls *et al.* 1995; Vardy 1996).

1.5.7 Portsmouth Gaseous Diffusion Plant, OH. A field scale experiment at the Portsmouth gaseous diffusion plant is testing three types of reactive media in an above ground facility. Three reactors with parallel test columns contain Master Builder iron, Peerless iron, and palladized Fisher iron. Flow rates were set to provide uniform retention times in all canisters. All three canisters reduced the concentration of TCE from 170 ppb to below detection (2 ppb) with the palladized iron providing the most rapid degradation. Rates of degradation have slowed slightly in all canisters with time perhaps as a result of iron-sulfide precipitation (Liang *et al.* 1996b).

1.5.8 Moffet Federal Airfield, CA. In March 1996 an iron barrier was constructed to treat a plume of TCE. The iron zone is 3.2 m wide by 3.2 m thick and 8.2 m deep with wing walls consisting of 6.5 m long interlocking sheet piles to direct contaminated water into the barrier. Water sampling conducted in June 1996 indicated that the initial concentrations of 850-1180 $\mu\text{g/L}$ of TCE were mostly degraded. Estimated cost of this installation is \$300,000 (Vidic and Pohland 1996).

1.5.9 Coffeyville, KS. The plume being treated at this facility is approximately 800 m long and consists of PCE, TCE, TCA, and 1,2-DCE at concentrations of 100's $\mu\text{g/L}$. The barrier, installed in January 1996, consists of two 150 m long slurry walls directing water into an iron-zone that is 6 m long, 3.8 m wide and 1 m thick (Vidic and Pohland 1996).

1.5.10 Other sites. Other sites that are under consideration but have limited information available are in Colorado, New Hampshire, Michigan, and Toronto.

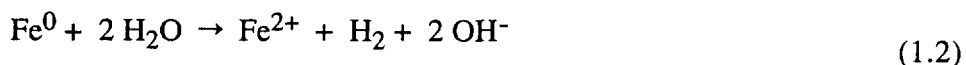
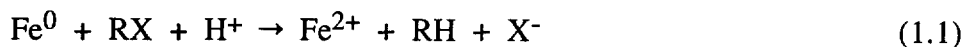
1.6 COST OF IN-SITU BARRIERS

Costs of remediation utilizing in-situ iron-barriers have been estimated to be half of conventional methods (Fairweather 1996). The capital cost for installation of a barrier is similar to that of a pump and treat system, but operation and maintenance are very low. This alone can lead to savings of hundreds of thousands of dollars per year. The capital cost of most of the barriers in the preceding section is presented in Table 1.3.

1.7 CHEMISTRY OF ZERO-VALENT IRON BASED REMEDIATION

Reduction of chlorinated aliphatic hydrocarbons (CAH) by zero-valent iron is a surface mediated reaction equivalent to corrosion. To have facile reduction of oxidized contaminants in groundwater a high solid to solution ratio is needed. This is accomplished by placing a large mass of granular iron with high surface area iron into the contaminated

aqueous environment. Introduction of Fe^0 into aqueous solution results in corrosion of the metal and dissolution of Fe^{2+} into solution (eq 1.2). As the CAH is reduced on the surface of iron metal (eq 1.1), Fe^{2+} is produced by corrosion and liberated into solution. The Fe^{2+} produced may also be oxidized to Fe^{3+} (eq 1.3).



The kinetics of chlorinated solvent degradation have been found to be first order by numerous researchers. Kinetic rates depend on surface area of iron, condition of surface area, pH, solution composition, contaminant concentration, and mixing. Varying the initial CAH concentration reveals that the rate of CAH reduction exhibits saturation type behavior (Chapter 3). The plateau of reaction rate with increasing contaminant concentration is consistent with evidence for reactive site saturation. This suggests that the dechlorination reaction is taking place at a limited number of reactive sites. As the reduction reaction proceeds the surface of the metal changes due to dissolution and precipitation of Fe^{2+} .

Heterogeneous chemical reactions including CAH reduction by Fe^0 and the dissolution of Fe^{2+} must be mediated by the solid-water interface. When metal is exposed to the environment it begins to corrode and a film of oxides cover the surface (Fig 1.4). If the amount of corrosion of iron is measured during CAH dechlorination one finds a correlation between the amount of CAH degraded and the amount of ferrous iron in solution. Plots of Fe^{2+} concentration in solution versus time are linear suggesting that the kinetics of the dissolution reaction are zero-order, consistent with most data on metal oxide dissolution (Biber *et al.* 1994). If the surface becomes passivated with a film of iron-oxides this may inhibit the degradation of chlorinated solvents.

The difference between laboratory and industrial grade iron metal is surface condition. Most laboratory grade metals are relatively clean and possess only a small amount of oxide. Industrial grade metal is often covered with cutting oil which has been charred, leaving a complex film containing carbon and crystalline oxides due to the heating. The carbon layer on the surface could affect the adsorption of contaminants as well as surface reactivity. A large amount of impurities could also lead to differences in the degradation pathway. Table 1.4 contains surface area and other information on several types of iron metal that have been used in CAH- Fe^0 studies.

1.8 LONG-TERM IN-SITU PERFORMANCE OF TREATMENT WALLS

Despite recent interest and activity in this area, some uncertainties remain over factors controlling field performance of iron barriers. These uncertainties range from the macroscopic scale to the molecular scale and are represented by the following frequently asked questions: Will biofilms or precipitation of iron oxides reduce the porosity of the barrier such that ground water will flow around it rather than through it? Will zones of massive precipitates clog the aquifer down-gradient of the barrier? What role does the oxide film on the surface of the iron metal play in the reduction reaction? Does the reaction take place at the metal surface or at the oxide/electrolyte interface? Does the oxide film act as a mediator of the electron transfer reaction? Under what conditions might reaction products form that are regulated contaminants?

Perhaps the most frequently asked questions about iron barriers are: Will the iron wall corrode away and how long will it remain reactive? The answers depend on the contaminant and geochemistry of the specific site but some generalizations are possible based on laboratory batch and column tests, along with long term field data from the Waterloo barrier. Data from column investigations provide information on the inorganic chemistry of the reactions (Johnson and Tratnyek 1994) and the relationship between the process of dechlorination and the spatial and temporal variations in geochemistry that develop in systems containing iron metal. Results from column tests show that treated water emerges from the iron-bearing zone anoxic, alkaline, and high in ferrous iron. The geochemistry is controlled by interfaces from the molecular level to the macroscopic level and is important in order to develop relationships among batch, column, and field studies.

1.8.1 Precipitation and other geochemistry. The focus of this section is how natural geochemical conditions influence the iron-bearing zone and how the iron-bearing zone affects the natural geochemistry (Fig 1.5). Chemical characteristics of input water to an iron-bearing zone can affect the degradation of solvents through transport or chemical mechanisms. Topics discussed include effects of oxygen, ferrous iron, carbonate, salinity, and various trace ions.

Highly oxygenated water may cause precipitation of iron-hydroxides that result in clogging of pore space and lowering of the permeability (Mackenzie *et al.* 1995b). Precipitation of large amounts of oxide can also cover reactive sites making the metal less reactive to the environmental contaminant of interest. Laboratory tests (Johnson, unpublished data) show little effect of water with high initial concentrations of ferrous or ferric iron. It is also possible that part of that iron will precipitate out in the barrier. This could result in slightly increased rates of fouling. The pH of the treated water is controlled

by the precipitation of amakinite (FeOH_2) with a pK_a of 9.2. This means that the pH will rise due to corrosion to approximately 9.2, and then stabilize or even decrease due to precipitation removing OH^- . Water with high concentrations of carbonate results in precipitation of siderite (Agrawal *et al.* 1996; Mackenzie *et al.* 1995a). Excessive siderite precipitation, although slow, can reduce the reaction rate or physically plug pore space in the barrier. The metal surface may become inactive due to borate or other ions which form binuclear surface complexes on the metal surface. Conditions which may increase the rate of solvent degradation are high ionic strength and anion content such as that of brackish water. Brackish water may also result in a shorter lifetime of the barrier due to enhanced corrosion and dissolution.

1.8.2 Microbiological effects. Geochemical gradients generated by a reactive iron barrier create a wide range of conditions that could support a variety of microbial populations. Microbes that live within the iron bearing zone must be anaerobes that tolerate reducing conditions (pH values of 9 and approximately -300 mV). Immediately down-gradient of an iron bearing zone the pH will decrease due to precipitation and perhaps iron oxidizing bacteria. The length of the anoxic plume will be controlled by the redox capacity of the aquifer solids (Barcelona and Holm 1991). Where the plume of anoxic water encounters the natural sub-oxic groundwater, ferrous iron will oxidize to ferric iron with additional precipitation. Iron reducing bacteria should thrive in this environment. If bacteria proliferate, compounds that have been partially degraded could be mineralized.

The role of sulfur reducing bacteria (SRB) and methanogens in microbially assisted oxidation of iron has been documented in the corrosion literature (Iverson 1987; Lorowitz *et al.* 1992). Methanogenic microorganisms, which are known to dechlorinate CAHs, may also play an important role within the iron-bearing zone of some field sites. Laboratory experiments with a mixed methanogenic culture and steel wool examined the symbiotic effects of biotic and abiotic dechlorination (Weathers *et al.* 1995). Through these experiments it was shown that the rate of dechlorination of chloroform is faster in the presence of iron and a mixed methanogenic bacteria culture than with either treatment separately.

SRB immobilized on dolomite and metallic iron have also been found to reduce sulfate. Sulfate was reduced more rapidly in an experiment containing iron rather than dolomite as the carrier for SRB (Somlev and Tishkov 1994). The authors attribute the additional reduction of sulfate to increased biotic mechanisms but, it is likely that the use of iron as a carrier resulted in subsequent unrecognized abiotic reduction mechanisms. Sulfate reduction was accompanied in both systems by a decrease of arsenic and nitrate concentrations.

1.9 TREATMENT OF SURFACE WATER

1.9.1 Industrial waste streams. Industrial waste streams are currently difficult to treat with iron metal due to the large volume of water and relatively slow reaction rate as compared to chemical treatment (Senzaki 1991; Senzaki and Yasuo 1988; Senzaki and Yasuo 1989). Large volumes of iron must be used in order to provide the resident times need for complete solvent degradation. Application of mixed reactors rather than packed beds could help by improving bulk mass transfer and limiting clogging due to precipitation.

1.9.2 Acid mine drainage. Bacterially mediated oxidation of sulfide-rich mining waste results in waters with a low pH (~3), and high concentrations of metals such as Fe, Mn, and Al (Kimball *et al.* 1994). The utility of iron to neutralize acid mine drainage and precipitate metals as solid solutions of iron oxides is under investigation by several groups. The first study to appear in the literature using metallic iron to treat acidic water from a mine found that the pH was maintained at ambient environmental levels and the concentration of metals were reduced (Shelp *et al.* 1995). The dominant chemical reactions in removal of metals from acid mine drainage are from sorption, precipitation, and aqueous complexation (Kimball *et al.* 1994). The large amounts of ferrous iron generated from iron corrosion can enhance these removal processes.

1.10 ORGANIC CONTAMINANTS TREATABLE BY ZERO-VALENT IRON

1.10.1 Halogenated aliphatics. The wide spread interest in Fe⁰ has lead to a large amount of research on degradation of halogenated aliphatics (see reference list at http://www.ese.ogi.edu/ese_docs/tratnyek/ironrefs.html) and a substantial number of organic compounds have been tested. Studies of degradation of chlorinated aliphatic compounds by iron metal comprise approximately 80% of literature on this topic to date. Chapter 3 (Johnson *et al.* 1996b) compiles available kinetic data and synthesizes typical degradation rates for chlorinated methanes, ethanes, and ethenes. So far there is little data on degradation of propanes, or on brominated or fluorinated compounds in general.

1.10.2 Halogenated aromatics. Reduction of a few halogenated aromatic compounds by zero-valent iron has been demonstrated (Table 1.5) but has not been as successful as the application to aliphatic compounds. Pentachlorophenol (PCP) was found to be removed from solution by acid washed iron at neutral pH (Ravary and Lipczynska-Kochany 1995), but the process was shown to be slower at higher pH. Halogenated

aromatics require a stronger reductant than aliphatic compounds which suggests that reduction by iron metal is not feasible at environmental conditions. Dechlorination of PCB by iron was reported (Sweeny 1979), but an EPA review found the disappearance to be a function of chromatographic effects rather than reduction (Erickson and Estes 1978). Dechlorination of PCBs have been reported to occur rapidly at 300 °C on a pure iron bed (Chuang *et al.* 1995). Dehalogenation of aromatics in bi-metallic systems such as Fe-Pd have also been reported and will be discussed later (Section 6.2.1).

1.10.3 Nitroaromatics. Nitroaromatics such as nitrobenzene, parathion, trinitrotoluene (TNT), and some degradation products of these compounds, can be reduced by iron metal (Agrawal and Tratnyek 1994). In model systems, the kinetics of transformation reaction from nitrobenzene to nitrosobenzene are pseudo-first-order in substrate concentration and iron surface area. The primary transformation pathway of nitrobenzene by granular iron metal is sequential reduction to nitrosobenzene, and then to aniline. The complete transformation to aniline typically occurs in a few hours, and aniline appears to be the stable final product irrespective of the transformation pathway. Nitrobenzene reductions by granular iron are mass-transfer limited, surface reactions, similar to dechlorination, however, the products are not as benign (Burris *et al.* 1996). Since biodegradation of aniline is facile, the coupling of these two technologies should be beneficial, although there have been no reports of application to date.

1.10.4 Azo-Compounds. Azo-compounds, which are used to make dyes, are coming under scrutiny as a possible environmental contaminant. A study with 4-aminoazobenzene (4-AAB), an aromatic azo compound common in dye stuff, supported on saphrose beads was undertaken to determine if the iron reaction was surface mediated. By sequestering the 4-AAB and Fe⁰ it was shown that the substrate must come into contact with the Fe⁰ surface for reduction to occur. The rate of azo reduction was determined by measuring the rate of aniline production (Weber 1995; Weber and Adams 1995).

1.11 INORGANIC CONTAMINANTS TREATABLE BY ZERO-VALENT IRON

1.11.1 Contaminant metals. Some inorganic environmental contaminants can be treated with Fe⁰ (Table 1.6). Oxidized metals are especially likely to undergo sorption, precipitation, or reduction in the reducing conditions of an iron-bearing zone. The affinity of iron oxide and hydroxides for metals is well documented (Dzombak and Morel 1990). Some of the metals sequestered by zero-valent iron include Cr⁶⁺, CrO₄²⁻, MoO₄²⁻, TcO₄²⁻, UO₄²⁺, As, Mo, Se, Hg, and Ag.

Chromium. The wide spread disposal of chromate-bearing slag and runoff from chrome plating operations has resulted in numerous chromium-contaminated sites. The complex chemistry resulting from chromium-contaminated soils has made remediation difficult (James 1996). It has been recognized for some years that Fe^0 removes chromium from solution (Gould 1982). This reduction and immobilization of hexavalent chromium by Fe^0 has subsequently been studied in detail (Blowes and Ptacek 1992; Powell *et al.* 1994). It has been shown that the kinetics of this reaction are influenced by Cr^{6+} concentration, pH, surface area of iron, mixing rate, and ionic strength (Gould 1982). The removal of CrO_4^{2-} by siderite, pyrite, and metallic iron have also been studied, with metallic iron being most effective.

Radioactive metals. Many other oxidized metals such as MoO_4^{2-} , TcO_4^{2-} , and UO_4^{2+} may thermodynamically be reduced by iron metal. Laboratory experiments show that the removal rates decrease in the order $\text{Tc}_4^{2-} > \text{UO}_4^{2+} \gg \text{Mo}_4^{2-}$ (Cantrell *et al.* 1995). Results of extensive batch and column tests under numerous conditions using Fe^0 and other adsorbents have been reported (Bostick *et al.* 1995a; Liang *et al.* 1996a).

Selenium. Selenium is a common groundwater contaminant in arid parts of the southwest US. Due to the often large quantities of water contaminated, an efficient, inexpensive method of treatment is useful. Iron filings were found to remove selenium with some inhibition by nitrate (Epoc 1987). Additional studies of the mechanism of removal suggest that most Se is adsorbed to the iron oxide (Anderson 1989).

Mercury. The removal of mercury by zero-valent iron has been reported by several groups (Bostick *et al.* 1996; Gould *et al.* 1984; Grau and Bisang 1995). Gould also reported removal of mercury by iron (Gould *et al.* 1984). Grau found that mercury was efficiently removed by iron felt (compressed steel wool) under ambient conditions from solutions containing chloride ions. Further the mercury can be recovered and reused by chemical dissolution of the iron felt. Used fluorescent lamps containing mercury are currently disposed of in sanitary landfills if from the private market and if from government facilities must be treated as hazardous waste. The study of crushed fluorescent lamps shows that mercury solubilized with excess oxidant (hypochlorite) and stabilized by complexation with halide ions can, after removal of chloride, be cemented by steel wool (Bostick *et al.* 1996).

Silver. Removal of silver from spent photographic solutions has been well documented (Boulineau 1992). Gould also reported removal of silver by iron (Gould *et al.* 1984).

Cadmium. The presence of cadmium in the environment is of concern due to its toxicity at low levels. Recycled granular cast-iron was found to remove Cd(II) from batch

and fixed bed experiments (Smith 1995). Surface concentrations of Cd on Fe were found to be as high as 30 mg/g with initial Cd concentrations of 5 mg/L at pH 7.

1.11.2 Non-metal inorganic ions. Many inorganic compounds such as carbonate, nitrate, and sulfate are subject to reduction by zero-valent iron. Reduction of carbonate to methane was reported by Hardy (Hardy and Gillham 1996). Precipitation of siderite (Agrawal *et al.* 1996) also results in removal of carbonate (Mackenzie *et al.* 1995b). See additional discussion of carbonate in Section 1.8.1.

Nitrate. Reduction of nitrate, a common contaminant in agricultural areas and from septic systems, has been demonstrated (Siantar *et al.* 1995). Reduction of nitrate has also been reported by green rust (Hansen *et al.* 1994) a likely product of the dechlorination reaction (Johnson and Tratnyek 1995). Figure 1.6 shows an SEM image of green rust precipitated in a long term column experiment.

Sulfur. The role of several forms of sulfur, and its perhaps multifaceted function in the iron system have been investigated. Degradation of several chlorinated compounds by sulfur and ferrous iron in mineral systems such as pyrite, have also been reported (Kriegman-King and Reinhard 1992; Kriegman-King and Reinhard 1994). It has been suggested by some that S plays a crucial role in the reduction of chlorinated compounds by iron (Hassan and Wolfe 1995), while other researchers have shown that the reaction occurs when no sulfur is present (Korte *et al.* 1995). Reduction of the sulfur group on HEPES has also been suggested (Lipczynska-Kochany *et al.* 1994). Removal of sulfate from acid mine drainage has been shown (Shelp *et al.* 1995).

Phosphorus. Sorption of phosphorus by sand amended with steel wool has been reported (James *et al.* 1992).

1.12 REDUCTION BY BI-METALLIC SYSTEMS AND OTHER ZERO-VALENT METALS

1.12.1 Bi-metallic systems. Bi-metallic reductants are comprised of a base metal, often iron, with a second metal, usually Pd, plated at concentrations of a few percent. The use of bi-metallic reductants in environmental remediation could lead to a wider range of compounds that can be treated with this system. Bi-metallic reductants are generally stronger reductants than individual metals. Several factors remain to be worked out with this system including cost of exotic metals, cost of large scale preparation, field performance, and regulatory approval. Data are just now becoming available to explain the behavior and lifetime of pure iron barriers, suggesting that understanding bi-metallic systems, especially on a mechanistic basis, will take significant additional research.

Laboratory experiments using bi-metallic reductants have shown dechlorination of PCB congeners of Aroclor 1260, at ambient temperatures, in 5-10 minutes (Grittini *et al.* 1995). The system contained a solution mixture of methanol/water/acetone (1:3:1) and 0.05% w/w palladium/metallic iron. The only reaction products were biphenyl and chloride ions. In parallel experiments PCBs were found to adsorb but not degrade on the surface of unpalladized iron. Additional studies of PCB degradation have been performed using 2,3,2',5'-tetrachlorobiphenyl (TeCB) dissolved in a 20% acetone mixture with Fisher iron (100 mesh) palladized at 0.25 % (West *et al.* 1996).

Fe-Pd has been found to reduce compounds that are not degradable by zero-valent iron alone. One case of this reduction is dichloromethane which has been shown repeatedly to be recalcitrant to dechlorination by Fe⁰ (Korte *et al.* 1995). Other chloromethanes and chloroethenes have also been rapidly degraded (Muftikian *et al.* 1995). Most halogenated aliphatics should be susceptible to transformation by Fe-Pd.

1.12.2 Zero-valent metals other than iron. Some of the other zero-valent metals in consideration are corroding metals such as aluminum, zinc, brass, copper, and tin, and noble metals like palladium and nickel. Early experiments at Waterloo examined the rates of degradation of some halogenated aliphatics by galvanized steel, stainless steel, and aluminum. Reduction was most rapid with galvanized steel and slowest with stainless steel (Reynolds *et al.* 1990). Experiments using CCl₄ as a substrate found that reduction by Sn lead to CHCl₃, CO₂, SnO₂, and HCl as the main products. Using Zn as a reductant lead to CH₃Cl, CH₄, ZnCl₂, and Zn(OH)₂ (Boronina *et al.* 1995).

Zinc reduces parathion. One of the earliest reports of using a zero-valent metal to remove an organic contaminant can be attributed to Butler in 1981. He reported field disposal of methyl parathion using powdered zinc (Butler *et al.* 1981) but like the early work with Fe⁰ the idea was not widely acknowledged.

Zinc removes Cadmium. The presence of cadmium in the environment is of concern due to its toxicity at low levels. Removal of cadmium by cementation on zinc has been reported under varying ambient conditions (Gould *et al.* 1987). Cementation is an electrochemical reaction which involves reduction of more electropositive species (noble, like Hg, Cd) and by more electronegative species (sacrificial, like Fe, Zn) (Khudenko and Gould 1991).

1.13 THE FUTURE OF IN-SITU REACTIVE TREATMENT BARRIERS

The application of zero-valent iron barriers at field sites over the next few years will provide the definitive proof of concept that some seek. So far reaction rates have been

found to be surprisingly consistent with time (Johnson and Tratnyek 1994). The longest running site, Borden, shows consistent degradation, as does the one year old Intersil site. There are however four general scenarios in which a wall can fail: (i) it can completely corrode, (ii) become unreactive towards the contaminant of interest, (iii) become physically clogged with abiotic precipitates or bio-mass, or (iv) produce toxic degradation products. Very high concentrations of contaminants or aggressive anions, such as chloride, may shorten the wall lifetime due to rapid corrosion. Where the groundwater is high in oxygen or carbonate, the wall may fail from physical plugging. Waters high in borate or other binuclear ligands may lead to passivation, and little or no degradation of contaminants.

If the iron metal becomes passivated it will need to be replaced or rejuvenated. It might be possible, pending regulatory approval, to remove the passive film by flushing the iron-bearing zone with a dilute acid solution or a concentrated salt solution. Other means of rejuvenating the surface could include a strong reductant, such as ascorbate, coupled with a ligand such as EDTA (Johnson *et al.* 1996a). Physical clogging of the wall may require replacement which could be greatly facilitated if this consideration is taken into account in the original design calculations.

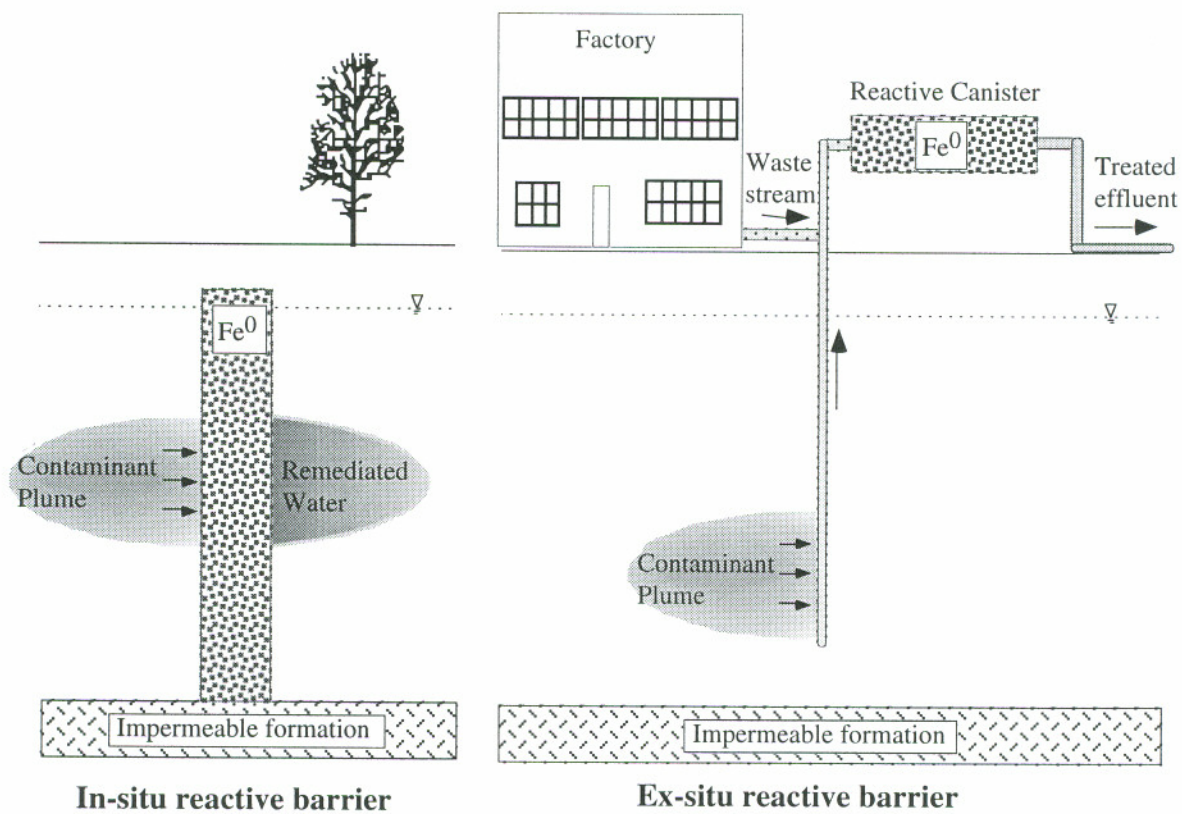


Figure 1.1 Reactive media such as Fe⁰ can be applied by in-situ passive treatment zones (left) or used to treat water from a waste stream or pump and treat system above ground in a mixed-reactor (right).

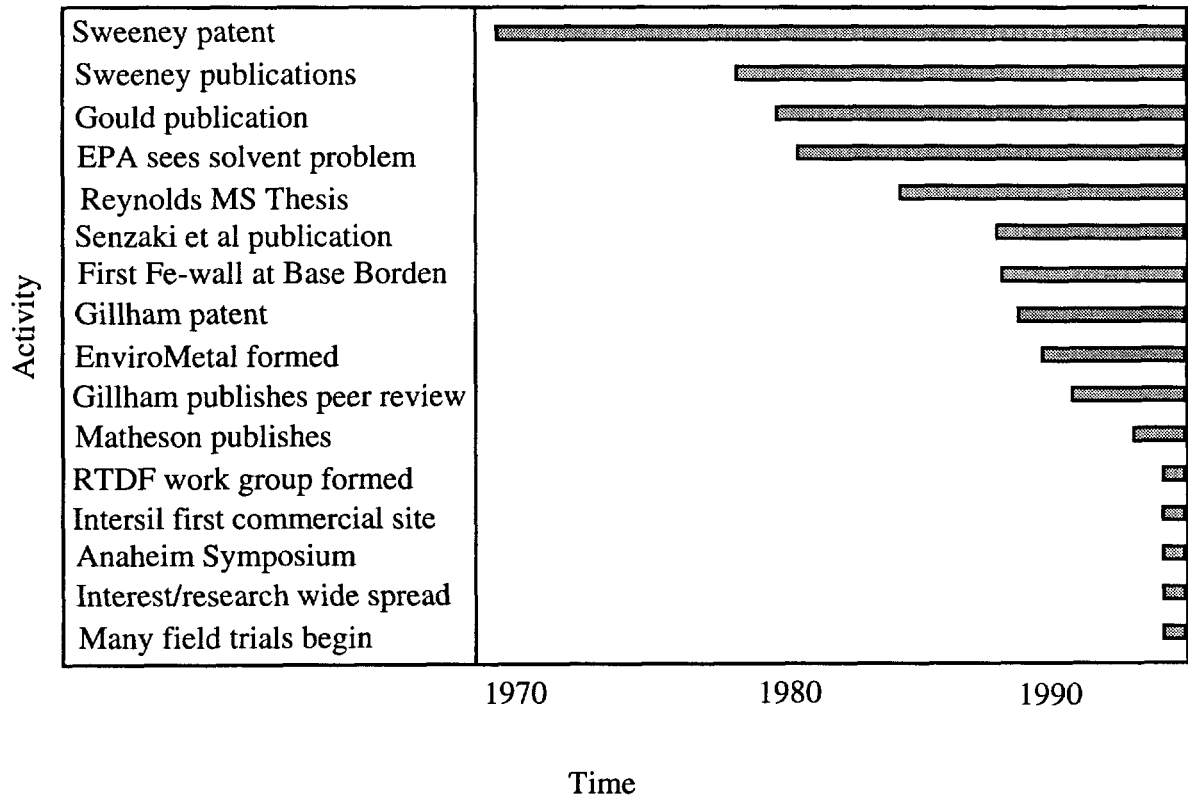


Figure 1.2 This timeline shows the chronology of major events that lead to the development of zero-valent iron for groundwater remediation.

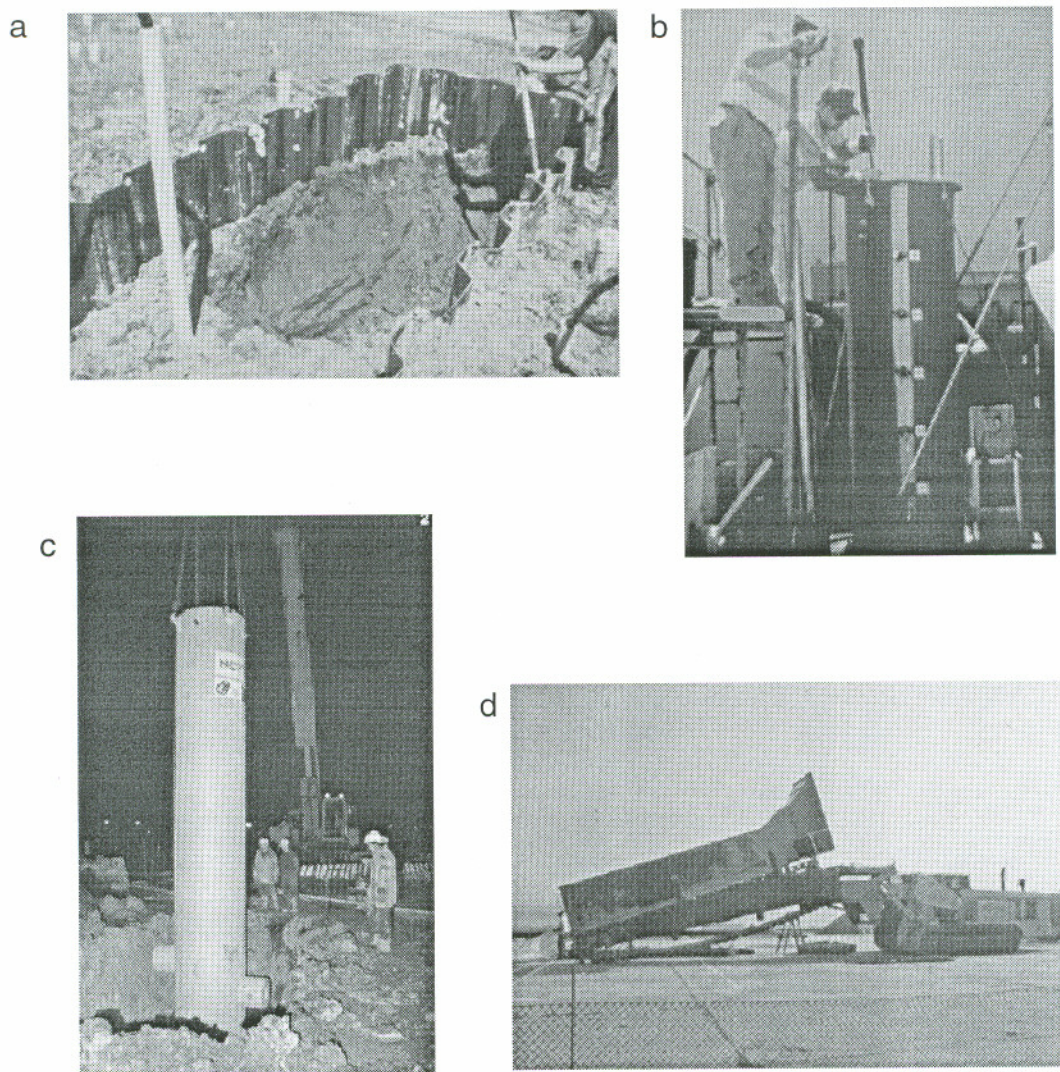


Figure 1.3 Field sites in operation include: (a) Base Borden, sheet pile; (b) SGI Circuit, above ground; (c) Nortel, funnel and gate; (d) Elizabeth City, trencher.

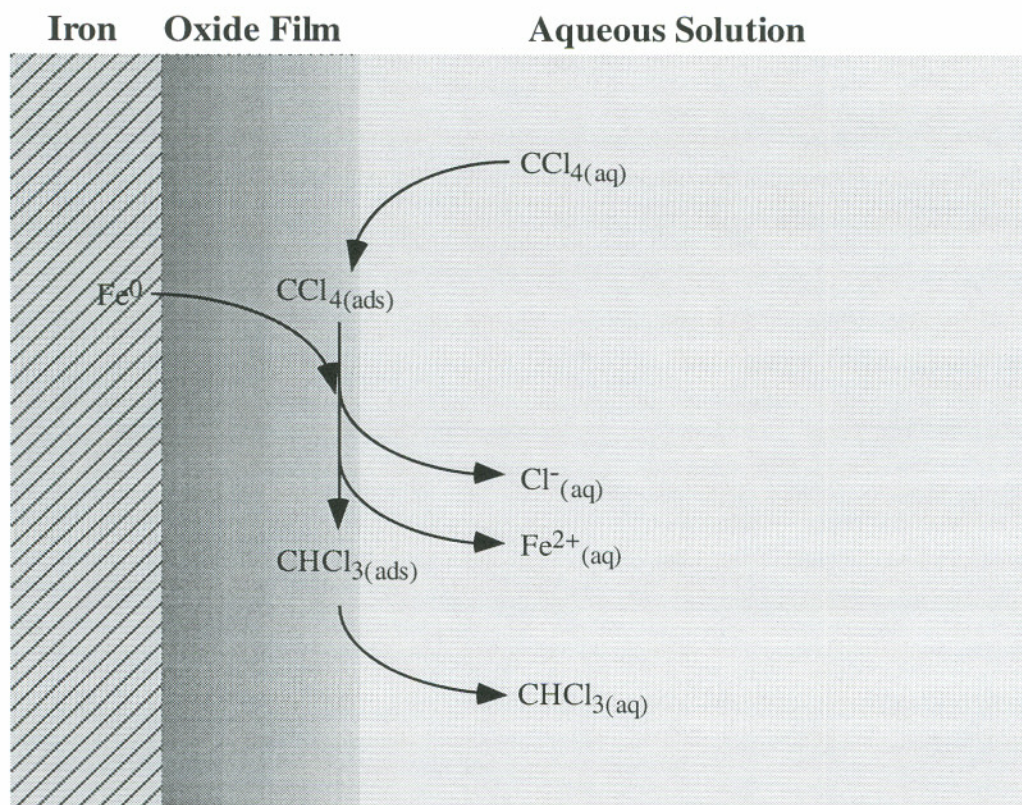


Figure 1.4 Iron metal exposed to the environment quickly develops a coating of iron oxides that mediates further surface reactions. This hypothesized reactive interface also evolves with time and changes in chemical conditions.

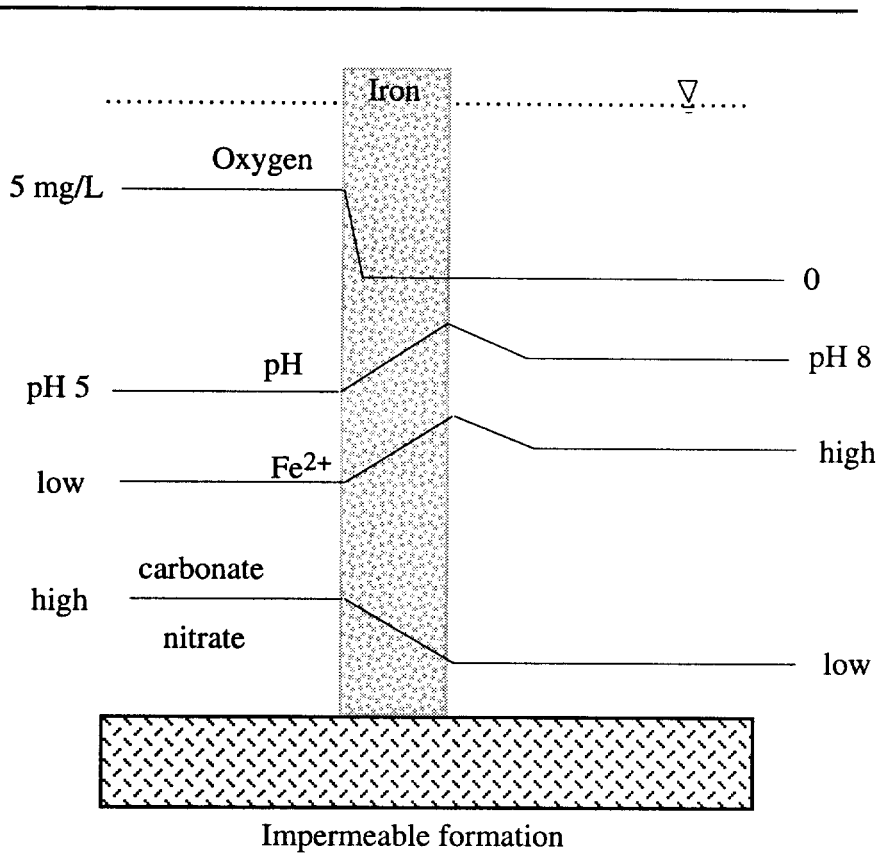


Figure 1.5 Groundwater which passes through an iron-bearing zone will become anoxic, alkaline, high in ferrous iron, and low in ions which precipitate readily with Fe^{2+} .

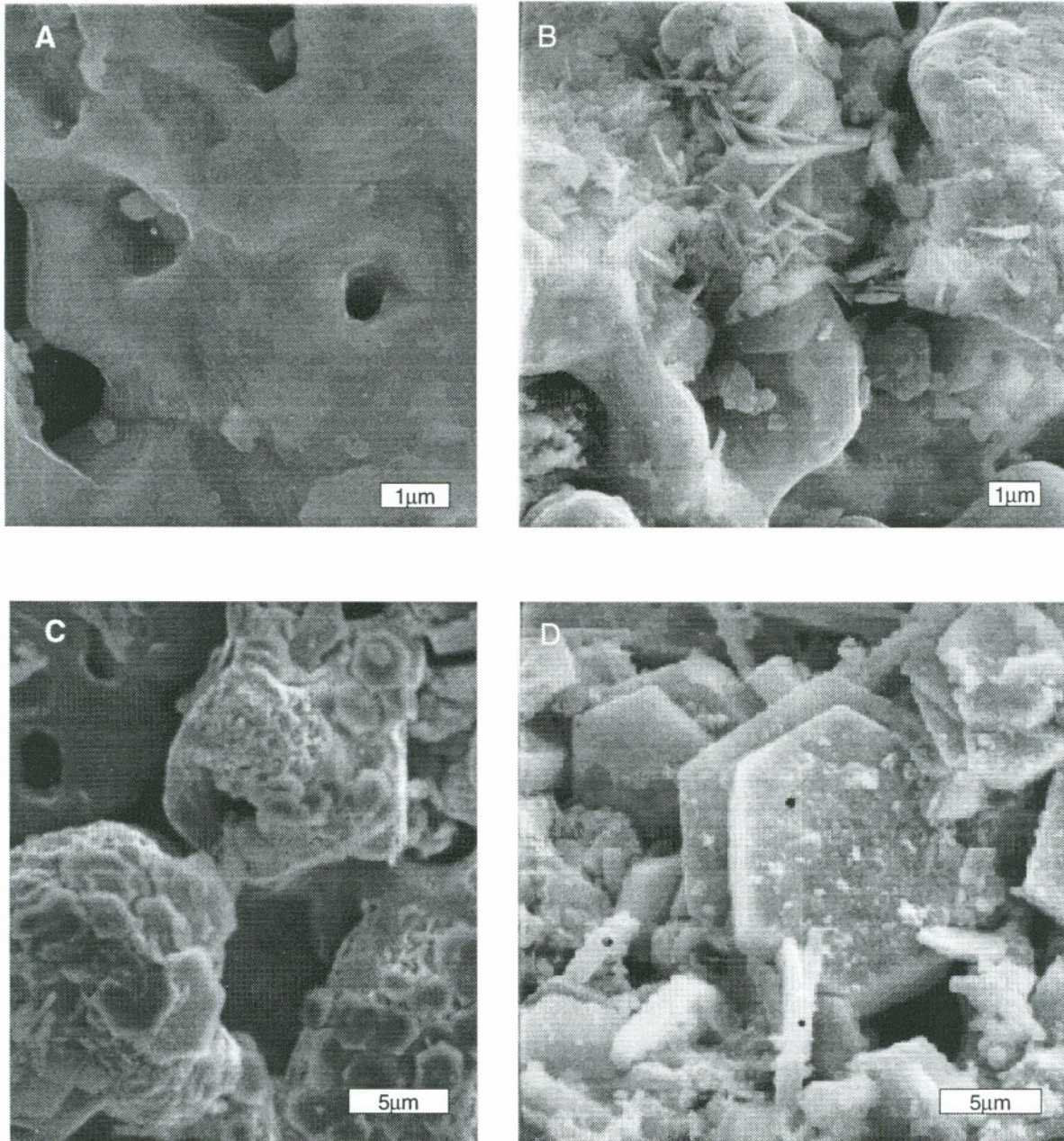


Figure 1.6 Scanning electron micrographs showing the effects of corrosion and precipitation in a continuous flow column: (A) unexposed metal sample, x8000; (B) iron grain from near the front of the iron-bearing zone after 9 months, x5000; (C) grain from the down-gradient end of the iron-bearing zone, x3000; (D) another grain from the down-gradient end of the iron bearing-zone, x3000. Black dots in D are where EDS was performed. The hexagonal crystals have tentatively been identified as green rust.

TABLE 1.1 REACTIVE MEDIA PROPOSED FOR PERMEABLE BARRIERS

Treat Inorganics		Treat Organics	
Sorption	Precipitation	Degradation	Sorption
Peat	Zero-valent iron	Zero-valent metals	Zeolites
Ferric oxyhydroxides	Ferrous hydroxide	Bi-metallic couples	Surfactant-modified silicates
Zeolites	H ₂	Iron-sulfide minerals	Activated carbon
AFO	Dithionite	Iron (II) porphyrins	Peat
Hydroxyapatite	Lime or Limestone	Resting-state microbes	Sawdust
Silica and Polymer gels			SMZ

Adapted from (Morrison and Spangler 1995)

TABLE 1.2 METHODS OF IRON UTILIZATION

Method	Reference
Funnel and gate	(Starr and Cherry 1994)
Biopolymer slurry machine	
Continuous trenching machine	(Vardy 1996)
Removable cassettes	
Tea-bag	
Mandrel based	
High pressure jetting	
Soil-mixing/auger	
Above ground reactor	(Vogan <i>et al.</i> 1995)
Colloidal injection	(Kaplan <i>et al.</i> 1996)
Cercona foam	

TABLE 1.3 CAPITAL COST SUMMARY FOR TREATMENT WALLS

Location	Dimensions (m)*	Contaminants	Cost (X1000)		
			Constr.	Iron	Total
Sunnyvale, CA	12 x 1.2 x 3.5 (6) m 75 m slurry walls	1-2 mg/L VC, <i>cis</i> -1,2- DCE, and TCE	550	170	720
Moffet Federal Air Field, CA	3.2 x 3.2 x 8.2 m 6.5 m sheet pile walls	1 mg/L TCE			300
Coffeyville, KS	6 x 1 x 3.8 (9) 150 m slurry walls	100's µg/L TCE	350	50	400
Elizabeth City, NC	45 x 0.6 x 5.5 m	TCE, Cr(VI)	220	200	420
Lowry AFB,CO	2.9 x 1.6 x 3.5 m 5 m cutoff walls	850 µg/L TCE 220 µg/L <i>cis</i> - 1,2-DCE	105	32.5	137.5
Proposed Sites					
New Hampshire	400-m long wall with several gates; 9 m deep	100's µg/L TCE, VC, <i>cis</i> -1,2- DCE	1,200	900	2,100
Michigan	90-m long with 3 gates; 6 m deep	10 - 100 mg/L TCE	300	135	435
Canada	45-m long with 2 gates; 4.5 m deep	50 - 100 µg/L TCE	130	52.5	182.5

* Dimensions are given as a length x width (thickness) x depth, if the top of the barrier is below ground surface the depth to the bottom is included in parenthesis

Adapted from (Vogan 1996)

TABLE 1.4 SURFACE AREA OF IRON

Source of Iron	Grain Size (mm)	Surface Area m ² /g	Reference
Master Builder (MBcs)	0.43	--	(Clausen <i>et al.</i> 1995)
Master Builder (MBfn)	0.23	3.3	(Focht 1994)
Fisher filings (Ffil)	0.15	--	(Gillham and O'Hannesin 1992)
Fisher Electrolytic (Felc)	0.15	0.287	(Gillham and O'Hannesin 1994)
Aldrich (Ald1)	0.10	2.4	(Helland <i>et al.</i> 1995)
EM Science (EMS)	0.15	0.14	(Johnson and Tratnyek 1994)
Felc	0.15	0.0567	Johnson, unpublished
Ffil	0.43	1.635	(Liang and Goodlaxson 1995)
Felc	<0.15	--	(Lipczynska-Kochany <i>et al.</i> 1994)
VWR	--	--	(Mackenzie <i>et al.</i> 1995b)
Felc	0.15	0.70	(Matheson and Tratnyek 1994)
Electrolytic	<0.15	--	(Milburn <i>et al.</i> 1995)
Kanmet Casting (KC)	--	--	(O'Hannesin 1993)
Felc	0.15	0.20	(Scherer and Tratnyek 1995)
Johnson Matthey (JM)	0.10	--	(Schreier and Reinhard 1995)
Kishida Electrolytic (Kelc)	0.075	--	(Senzaki and Yasuo 1989)
VWR	--	1.24	(Sivavec and Horney 1995)
MBcs	0.43	--	(Vogan <i>et al.</i> 1995)

TABLE 1.5 ORGANIC CONTAMINANTS DEGRADED BY ZERO-VALENT IRON¹

Contaminant	Fe ⁰	Fe-Pd
dichloromethane		(Korte <i>et al.</i> 1995)
PCP	(Ravary and Lipczynska-Kochany 1995)	
4-aminoazobenzene	(Weber 1996)	
nitrobenzene	(Agrawal and Tratnyek 1996; Burris <i>et al.</i> 1996)	
nitrosobenzene	(Agrawal and Tratnyek 1996; Burris <i>et al.</i> 1996)	
phenylhydroxylamine	(Burris <i>et al.</i> 1996)	
1,3-dinitrobenzene	(Agrawal and Tratnyek 1996)	
4-chloronitrobenzene	(Agrawal and Tratnyek 1996)	
4-nitroanisole	(Agrawal and Tratnyek 1996)	
4-nitrotoluene	(Agrawal and Tratnyek 1996)	
2,4,6-trinitrotoluene	(Agrawal and Tratnyek 1996)	
parathion	(Agrawal and Tratnyek 1996)	
chlorobenzene	(Sweeny 1981) ²	
Atrazine	(Pulgarin <i>et al.</i> 1995) ³	
PCB	(Chuang <i>et al.</i> 1995) ⁴	(Grittini <i>et al.</i> , 1995; West <i>et al.</i> , 1996)
Others		
Chlordane		2,4-D
Endrin		2,4,5-T
Heptachlor		Silvex
Kepone		Atrazine

¹Comprehensive list of references on chlorinated aliphatics in (Johnson *et al.* 1996b).

²later shown for some cmpds to be chromatographic retention (Erickson and Estes 1978)

³requires sunlight

⁴elevated temperature

TABLE 1.6 METALS AND INORGANICS REDUCED BY ZERO-VALENT IRON

Contaminant	Fe ⁰	Zn
aluminum	(Shelp <i>et al.</i> 1995)	
cadmium	(Shelp <i>et al.</i> , 1995; Smith, 1995)	(Gould <i>et al.</i> 1987)
chromium	(Blowes and Ptacek, 1992; Gould, 1982; Powell <i>et al.</i> , 1994)	
copper	(Shelp <i>et al.</i> 1995)	(Khudenko and Gould 1991)
mercury	(Bostick <i>et al.</i> , 1996; Grau and Bisang, 1995; Khudenko and Gould, 1991)	
molybdenum	(Cantrell <i>et al.</i> 1995)	
selenium	(Anderson 1989; Epoc 1987)	
silver	(Khudenko and Gould 1991)	
technetium	(Bostick <i>et al.</i> , 1995; Cantrell <i>et al.</i> , 1995)	
uranium	(Cantrell <i>et al.</i> 1995)	
Inorganics		
carbonate	(Agrawal <i>et al.</i> , 1995; Hardy and Gillham, 1996)	
nitrate	(Siantar <i>et al.</i> 1995)	
sulfate	(Somlev and Tishkov 1994)	

1.14 REFERENCES

- Acar, Y. B., and A. N. Alshawabkeh. 1993. Principles of electrokinetic remediation. *Environ. Sci. Technol.* 27 (13): 2638-2647.
- Agrawal, A., T. L. Johnson, M. M. Scherer, and P. G. Tratnyek. 1997. Effect of aqueous bicarbonate on contaminant transformation with zero-valent iron. *J. Contam. Hydrol.* : in prep.
- Agrawal, A., and P. G. Tratnyek. 1994. Abiotic remediation of nitro-aromatic groundwater contaminants by zero-valent iron. *207th National Meeting ACS. Preprint Extended Abstracts, Division of Environmental Chemistry.* San Diego, CA. Vol. 34, No. 1, pp. 492-494.
- Agrawal, A., and P. G. Tratnyek. 1996. Reduction of nitro aromatic compounds by zero-valent iron metal. *Environ. Sci. Technol.* 30 (1): 153-160.
- Agrawal, A., P. G. Tratnyek, P. Stoffyn-Egli, and L. Liang. 1995. Processes affecting nitro reduction by iron metal: Mineralogical consequences of precipitation in aqueous carbonate environments. *209th National Meeting ACS. Preprint Extended Abstracts, Division of Environmental Chemistry.* Anaheim, CA. Vol. 35, No. 1, pp. 720-723.
- Anderson, M. A. 1989. *Fundamental aspects of selenium removal by Harza process.* San Joaquin Valley Drainage Program. Report No. 7-CS-20-05170, pp. 1-18.
- Barcelona, M. J., and T. R. Holm. 1991. Oxidation-reduction capacities of aquifer solids. *Environ. Sci. Technol.* 25 (9): 1565-1572.
- Bhattacharya, S., and M. Subramanian. 1996. Synthesis, redox and electrochemical properties of new anthraquinone-attached micelle- and vesicle-forming cationic amphiphiles. *Journal of the Chemical Society Perkin Transactions 2* (9): 2027-2034.
- Biber, M. V., M. S. Afonso, and W. Stumm. 1994. The coordination chemistry of weathering: IV. Inhibition of the dissolution of oxide minerals. *Geochim. Cosmochim. Acta.* 58 (9): 1999-2010.
- Blowes, D. W., and C. J. Ptacek. 1992. Geochemical remediation of groundwater by permeable reactive walls: removal of chromate by reaction with iron-bearing solids. *Subsurface Restoration Conference.* Dallas, TX. pp. 214-216.
- Boronina, T., K. J. Klabunde, and G. Sergeev. 1995. Destruction of organohalides in water using metal particles: Carbon tetrachloride/water reactions with magnesium, tin, and zinc. *Environ. Sci. Technol.* 29 (6): 1511-1517.
- Bostick, W. D., D. E. Beck, K. T. Bowser, D. H. Bunch, R. L. Fellows, and G. F. Sellers. 1996. *Treatability study for removal of leachable mercury in crushed fluorescent lamps.* Oak Ridge National Laboratory. Report No. K/TSO-6.
- Bostick, W. D., P. E. Osborne, D. E. Beck, D. H. Bunch, R. L. Fellows, G. F. Sellers, J. L. Shoemaker, K. T. Bowser, and D. A. Bostick. 1995a. *Removal of technetium-99 from simulated Oak Ridge National Laboratory newly-generated liquid low-level waste.* Oak Ridge National Laboratory. Report No. K/TCD-1141.

- Bostick, W. D., P. E. Osborne, G. D. Del Cul, and D. W. Simmons. 1995b. *Treatment of aqueous solutions contaminated with technetium-99 originating from uranium enrichment activities: Final report*. Oak Ridge National Laboratory. Report No. K/TCD-1120.
- Boulineau, B. J. 1992. *Silver recovery in the SRS photographic laboratory*. Westinghouse Savannah River Company. Report No. WSRC-TR-91-567.
- Burris, D. R., K. Hatfield, and N. L. Wolfe. 1996. Laboratory experiments with heterogeneous reactions in mixed porous media. *J. of Environ. Engr.* 122 (8): 685-691.
- Butler, L. C., D. C. Staiff, G. W. Sovocool, and J. E. Davis. 1981. Field disposal of methyl parathion using acidified powdered zinc. *J. Environ. Sci. Health.* B16 (1): 49-58.
- Cantrell, K. J., D. I. Kaplan, and T. W. Wietsma. 1995. Zero-valent iron for the in situ remediation of selected metals in groundwater. *J. Haz. Mater.* 42 (2): 201-212.
- Chuang, F.-W., R. A. Larson, and M. Scully Wessman. 1995. Zero-valent iron-promoted dechlorination of polychlorinated biphenyls. *Environ. Sci. Technol.* 29 (9): 2460-2463.
- Clausen, J. L., W. L. Richards, N. L. Korte, and L. Liang. 1995. ORNL/MMES research into remedial applications of zero-valence metals: 3) Removal of TCE, cis-1,2-DCE, vinyl chloride, and technetium. *209th National Meeting. Preprint Extended Abstracts, Division of Environmental Chemistry*. Anaheim, CA. Vol. 35, No. 1, pp. 755-758.
- Dzombak, D. A., and F. M. M. Morel. 1990. *Surface Complexation Modeling: Hydrous Ferric Oxide*. John Wiley & Sons, New York.
- Epic, A. G. 1987. *Removal of selenium from subsurface agricultural drainage by an anaerobic bacterial process*. California Department of Water Resources. Report No. B-55712.
- Erickson, M. D., and E. D. Estes. 1978. *Evaluation of chlorinated hydrocarbon catalytic reduction technology*. U.S. Environmental Protection Agency, Research Triangle Park, NC. Task Final Report. Report No. EPA-600/2-78-059.
- Fairweather, V. 1996. When toxics meet metal. *Civil Engineering*, 44: 44-48.
- Focht, M. R. 1994. *Bench-scale treatability testing to evaluate the applicability of metallic Iron for above-ground remediation of 1,2,3-trichloropropane contaminated groundwater*. M.S. Thesis, University of Waterloo.
- Gillham, R. W. 1995. Resurgence in research concerning organic transformations enhanced by zero-valent metals and potential application in remediation of contaminated groundwater. *209th National Meeting. Anaheim, CA. Preprint Extended Abstracts, Division of Environmental Chemistry*. Vol. 35, No. 1, pp. 691-694.
- Gillham, R. W., D. W. Blowes, C. J. Ptacek, and S. O'Hannesin. 1994. Use of zero-valent metals for in situ remediation of contaminated ground water. *Proceedings of the 33rd Hanford Symposium on Health & the Environment—In Situ Remediation:*

Scientific Basis for Current and Future Technologies. Pasco, WA. Vol. 2, pp. 913-930.

- Gillham, R. W., and S. F. O'Hannesin. 1992. Metal-catalysed abiotic degradation of halogenated organic compounds. *IAH Conference, Modern Trends in Hydrogeology*. Hamilton, Ontario, Canada. pp. 94-103.
- Gillham, R. W., and S. F. O'Hannesin. 1994. Enhanced degradation of halogenated aliphatics by zero-valent iron. *Ground Water*. 32 (6): 958-967.
- Gillham, R. W., S. F. O'Hannesin, and W. S. Orth. 1993. Metal enhanced abiotic degradation of halogenated aliphatics: Laboratory tests and field trials. *Proceedings of the 6th Annual Environmental Management and Technical Conference/HazMat Central Conference*, Rosemont, IL. pp. 440-461.
- Gould, J. P. 1982. The kinetics of hexavalent chromium reduction by metallic iron. *Water Res.* 16 : 871-877.
- Gould, J. P., I. B. Escovar, and B. M. Khudenko. 1987. Examination of the zinc cementation of cadmium in aqueous solutions. *Water Science and Technology*. 19 (3/4): 333-344.
- Gould, J. P., M. Y. Masingale, and M. Miller. 1984. Recovery of silver and mercury from COD samples by iron cementation. *J. Water Pollut. Control Fed.* 56 (3): 280-286.
- Grau, J. M., and J. M. Bisang. 1995. Removal and recovery of mercury from chloride solutions by contact deposition on iron felt. *Chemical Biotechnology*. 65 : 153-158.
- Grittini, C., M. Malcomson, Q. Fernando, and N. Korte. 1995. Rapid dechlorination of polychlorinated biphenyls on the surface of a Pd/Fe bimetallic system. *Environ. Sci. Technol.* 29 (11): 2898-2900.
- Hansen, H. C. B., O. K. Borggaard, and J. Sørensen. 1994. Evaluation of the free energy of formation of Fe(II)-Fe(III)hydroxide-sulphate (green rust) and its reduction of nitrite. *Geochim. Cosmochim. Acta.* 58 (12): 2599-2608.
- Hardy, L., I., and R. W. Gillham. 1996. Formation of hydrocarbons from the reduction of aqueous CO₂ by zero-valent iron. *Environ. Sci. Technol.* 30 (1): 57-65.
- Hassan, S. M., and N. L. Wolfe. 1995. Reaction mechanisms involved in the reduction of halogenated hydrocarbons with sulfated iron. *209th National Meeting ACS. Preprint Extended Abstracts, Division of Environmental Chemistry*. Anaheim, CA. Vol. 35, No. 1, pp. 735-737.
- Helland, B. R., P. J. J. Alvarez, and J. L. Schnoor. 1995. Reductive dechlorination of carbon tetrachloride with elemental iron. *J. Haz. Mater.* 41 (2-3): 205-216.
- Ho, S. V., P. W. Sheridan, C. J. Athmer, M. A. Heitkamp, J. M. Brackin, D. Weber, and P. H. Brodsky. 1995. Integrated in situ soil remediation technology: The Lasagna process. *Environ. Sci. Technol.* 29 (10): 2528-2534.
- Iverson, W. P. 1987. Microbial corrosion of metals. *Adv. Appl. Microbiol.* 32 : 1-36.

- James, B. R. 1996. The challenge of remediating chromium-containing soil. *Environ. Sci. Technol.* 30 (6): 248A-251A.
- James, B. R., M. C. Rabenhorst, and G. A. Frigon. 1992. Phosphorus sorption by peat and sand amended with iron oxides or steel wool. *Wat. Environ. Res.* 64 (5): 699-705.
- Johnson, T. L., W. Fish, Y. A. Gorby, and P. G. Tratnyek. 1996a. Degradation of carbon tetrachloride by iron metal: Complexation effects on the oxide surface. *J. Contam. Hydr.* in press.
- Johnson, T. L., M. M. Scherer, and P. G. Tratnyek. 1996b. Kinetics of halogenated organic compound degradation by iron metal. *Environ. Sci. Technol.* 30 (8): 2634-2640.
- Johnson, T. L., and P. G. Tratnyek. 1994. A column study of carbon tetrachloride dehalogenation by iron metal. *Proceedings of the 33rd Hanford Symposium on Health & the Environment—In Situ Remediation: Scientific Basis for Current and Future Technologies.* Pasco, WA. Vol. 2, pp. 931-947.
- Johnson, T. L., and P. G. Tratnyek. 1995. Dechlorination of carbon tetrachloride by iron metal: The role of competing corrosion reactions. *209th National Meeting ACS. Preprint Extended Abstracts, Division of Environmental Chemistry.* Anaheim, CA. Vol. 35, No. 1, pp. 699-701.
- Kaplan, D. I., K. J. Cantrell, and T. W. Wietsma. 1994. Formation of a barrier to groundwater contaminants by the injection of zero-valent iron colloids: Suspension properties. *Proceedings of the 33rd Hanford Symposium on Health & the Environment—In Situ Remediation: Scientific Basis for Current and Future Technologies.* Pasco, WA. Vol. 2, pp. 821-837.
- Kaplan, D. I., K. J. Cantrell, T. W. Wietsma, and M. A. Potter. 1996. Retention of zero-valent iron colloids by sand columns: Application to chemical barrier Formation. *J. Environ. Qual.* 25 (5): 1086-1094.
- Khudenko, B. M., and J. P. Gould. 1991. Specifics of cementation processes for metals removal. *Water Science and Technology.* 24 (7): 235-246.
- Kimball, B. A., R. E. Broshears, K. E. Bencala, and D. M. McKnight. 1994. Coupling of hydrologic transport and chemical reactions in a stream affected by acid mine drainage. *Environ. Sci. Technol.* 28 (12): 2065-2073.
- Korte, N. L., R. Muftikian, J. Clausen, and L. Liang. 1995. ORNL/MMES Research into remedial applications of zero-valence metals. 2: Bimetallic enhancements. *209th National Meeting ACS. Preprint Extended Abstracts, Division of Environmental Chemistry.* Anaheim, CA. Vol. 35, No. 1, pp. 752-753.
- Kovalick, W. W. 1995. *In Situ Remediation Technology Status Report: Treatment Walls.* USEPA, Solid Waste and Emergency Response, Technology Innovation Office. Report No. EPA542-K-94-004.
- Kriegman-King, M. R., and M. Reinhard. 1992. Transformation of Carbon Tetrachloride in the Presence of Sulfide, Biotite, and Vermiculite. *Environ. Sci. Technol.* 26 (11): 2198-2206.

- Kriegman-King, M. R., and M. Reinhard. 1994. Transformation of carbon tetrachloride by pyrite in aqueous solution. *Environ. Sci. Technol.* 28 (4): 692-700.
- Liang, L., and J. D. Goodlaxson. 1995. Kinetics and byproducts of reductive dechlorination of ground water: TCE with zero-valence iron. *Emerging Technologies in Hazardous Waste Management VII, Extended Abstracts for the Special Symposium*. Atlanta, GA. pp. 46-49.
- Liang, L., B. Gu, and X. Yin. 1996a. Removal of technium-99 from contaminated groundwater with sorbents and reductive materials. *Separations Technology*. 6 : 111-122.
- Liang, L., O. R. West, N. L. Korte, J. D. Goodlaxson, F. D. Anderson, C. A. Welch, and M. Pelfry. 1996b. *Interim report on the X-749/X-120 groundwater treatment facility a field scale test of trichloroethylene dechlorination using iron filings*. Oak Ridge National Laboratory. Submitted to DOE, Piketon, OH.
- Lipczynska-Kochany, E., S. Harms, R. Milburn, G. Sprah, and N. Nadarajah. 1994. Degradation of carbon tetrachloride in the presence of iron and sulphur containing compounds. *Chemosphere*. 29 (7): 1477-1489.
- Lorowitz, W. H., D. P. J. Nagle, and R. S. Tanner. 1992. Anaerobic oxidation of elemental metals coupled to methanogenesis by *Methanobacterium thermoautotrophicum*. *Environ. Sci. Technol.* 26 (8): 1606-1610.
- Mackay, D. M., and J. A. Cherry. 1989. Groundwater contamination: Pump-and-treat remediaton. *Environ. Sci. Technol.* 23 (6): 630-636.
- Mackenzie, P. D., S. S. Baghel, G. R. Eykholt, D. P. Horney, J. J. Salvo, and T. M. Sivavec. 1995a. Pilot-scale demonstration of chlorinated ethene reduction by iron metal: Factors affecting lifetime. *Emerging Technologies in Hazardous Waste Management VII, Extended Abstracts for the Special Symposium*. Atlanta, GA. pp. 59-62.
- Mackenzie, P. D., S. S. Baghel, G. R. Eykholt, D. P. Horney, J. J. Salvo, and T. M. Sivavec. 1995b. Pilot-scale demonstration of reductive dechlorination of chlorinated ethenes by iron metal. *209th National Meeting ACS. Preprint Extended Abstracts, Division of Environmental Chemistry*. Anaheim, CA. Vol. 35, No. 1, pp. 796-799.
- Matheson, L. J. 1994. *Abiotic and Biotic Reductive Dehalogenation of Halogenated Methanes*. Ph.D. Dissertation, Oregon Graduate Institute.
- Matheson, L. J., and P. G. Tratnyek. 1994. Reductive dehalogenation of chlorinated methanes by iron metal. *Environ. Sci. Technol.* 28 (12): 2045-2053.
- Milburn, R., S. Harms, E. Lipczynska-Kochany, C. Ravary, and G. Sprah. 1995. Iron (Fe(0)) induced dehalogenation of polychlorinated aliphatic compounds. *209th National Meeting ACS. Preprint Extended Abstracts, Division of Environmental Chemistry*. Anaheim, CA. Vol. 35, No. 1, pp. 822-824.
- Morrison, S., and R. Spangler. 1995. *Research on Permeable Barriers*. Minutes of EPA Research Technology Development Forum: Permeable Barriers Working Group. Wilmington, DE.

- Muftikian, R., Q. Fernando, and N. Korte. 1995. A method for the rapid dechlorination of low molecular weight chlorinated hydrocarbons in water. *Wat. Res.* 29 (10): 2434-2439.
- Nyer, E. K., and S. Suthersan. 1996. In situ reactive zones. *Ground Water Monitoring & Remediation*. Summer : 70-75.
- O'Hannesin, S., and R. W. Gillham. 1993. In situ degradation of halogenated organics by permeable reaction wall. *EPA Groundwater Currents*. : March.
- O'Hannesin, S. F. 1993. *A Field Demonstration of a Permeable Reaction Wall for the In Situ Abiotic Degradation of Halogenated Aliphatic Organic Compounds*. M.S. Thesis, University of Waterloo, Ontario.
- Pankow, J. F., and J. A. Cherry. 1996. *Dense Chlorinated Solvents and Other DNAPLs in Groundwater: History, Behavior, and Remediation*. Waterloo Press, Portland, OR.
- Powell, R. M., R. W. Puls, and C. J. Paul. 1994. Chromate reduction and remediation utilizing the thermodynamic instability of zero-valence iron. *Water Environment Federation Specialty Conference Series, Innovative Solutions for Contaminated Site Management*. Miami, Florida.
- Pulgarin, C., J. P. Schwitzguebel, P. Peringer, G. M. Pajonk, J. Bandara, and J. Kiwi. 1995. Abiotic degradation of atrazine on zero-valent iron activated by visible light. *209th National Meeting ACS. Preprint Extended Abstracts, Division of Environmental Chemistry*. Anaheim, CA. Vol. 35, No. 1, pp. 767-770.
- Puls, R. W., R. M. Powell, and C. J. Paul. 1995. In situ remediation of ground water contaminated with chromate and chlorinated solvents using zero-valent iron: A field study. *209th National Meeting ACS. Preprint Extended Abstracts, Division of Environmental Chemistry*. Anaheim, CA. Vol. 35, No. 1, pp. 788-791.
- Ravary, C., and Lipczynska-Kochany. 1995. Abiotic aspects of zero-valent iron induced degradation of aqueous pentachlorophenol. *209th National Meeting ACS. Preprint Extended Abstracts, Division of Environmental Chemistry*. Anaheim, CA. Vol. 35, No. 1, pp. 738-740.
- Reynolds, G. W., J. T. Hoff, and R. W. Gillham. 1990. Sampling bias caused by materials used to monitor halocarbons in groundwater. *Environ. Sci. Technol.* 24 (1): 135-142.
- Scherer, M. M., and P. G. Tratnyek. 1995. Dechlorination of carbon tetrachloride by iron metal: Effect of reactant concentrations. *209th National Meeting ACS. Preprint Extended Abstracts, Division of Environmental Chemistry*. Anaheim, CA. Vol. 35, No. 1, pp. 805-806.
- Schreier, C. G., and M. Reinhard. 1995. Transformation of chlorinated ethylenes by iron powder in 4-(2-Hydroxyethyl)-1-Piperazineethanesulfonic Acid (HEPES) buffer. *209th National Meeting ACS. Preprint Extended Abstracts, Division of Environmental Chemistry*. Anaheim, CA. Vol. 35, No. 1, pp. 833-835.

- Senzaki, T. 1991. Removal of chlorinated organic compounds from wastewater by reduction process. III. Treatment of trichloroethylene with iron powder. *Kogyo Yosui*. 391 : 29-35.
- Senzaki, T., and K. Yasuo. 1988. Removal of chlorinated organic compounds from wastewater by reduction process. I. Treatment of trichloroethylene with iron powder. *Kogyo Yosui*. 357: 2-7.
- Senzaki, T., and K. Yasuo. 1989. Removal of chlorinated organic compounds from wastewater by reduction process. II. Treatment of trichloroethylene with iron powder. *Kogyo Yosui*. 369: 19-25.
- Shapiro, A. P., and R. F. Probst. 1993. Removal of contaminants from saturated clay by electroosmosis. *Environ. Sci. Technol.* 27 (2): 283-291.
- Shelp, G. S., W. Chesworth, and G. Spiers. 1995. The amelioration of acid mine drainage by an in situ electrochemical method—I. Employing scrap iron as the sacrificial anode. *Appl. Geochem.* 10 : 705-713.
- Siantar, D. P., C. G. Schreier, and M. Reinhard. 1995. Transformation of the pesticide 1,2-dibromo-3-chloropropane (DBCP) and nitrate by iron powder and by $H_2/Pd/Al_2O_3$. *209th National Meeting ACS. Preprint Extended Abstracts, Division of Environmental Chemistry*. Anaheim, CA. Vol. 35, No. 1, pp. 745-748.
- Sivavec, T. M., and D. P. Horney. 1995. Reductive dechlorination of chlorinated ethenes by iron metal. *209th National Meeting ACS. Preprint Extended Abstracts, Division of Environmental Chemistry*. Anaheim, CA. Vol. 35, No. 1, pp. 695-698.
- Smith, E. H. 1995. Cadmium removal by a granular iron adsorbant. *Emerging Technologies in Hazardous Waste Management VII, Extended Abstracts for the Special Symposium*, Atlanta, GA. pp. 1205-1208.
- Somlev, V., and S. Tishkov. 1994. Anaerobic corrosion and bacterial sulfate reduction: Application for the purification of industrial wastewater. *Geomicrobiology Journal*. 12 (1): 53-60.
- Star, R. C., and J. A. Cherry. 1994. In situ remediation of contaminated ground water: the funnel and gate system. *Ground Water*. 32 (3): 465-476.
- Sweeny, K. H. 1979. Reductive degradation treatment of industrial and municipal wastewaters. *Water Reuse Symposium*. Washington, DC. Vol. 2, pp. 1487-1497.
- Sweeny, K. H. 1981. The reductive treatment of industrial wastewaters. II. Process applications. *AIChE Symposium Ser.* 77 (209): 72-78.
- Sweeny, K. H., and J. R. Fischer. 1973. Decomposition of halogenated organic compounds using metallic couples. *U.S. Patent No. 3,737,384*.
- Thomas, A. O., D. M. Drury, G. Norris, S. F. O'Hannesin, and J. L. Vogan. 1995. The *in-situ* treatment of trichloroethylene-contaminated groundwater using a reactive barrier—Results of laboratory feasibility studies and preliminary design considerations. *In* : W. J. von den Brink, R. Bosman, and F. Arendt (ed.), *Contaminated Soil '95*. Kluwer, The Netherlands, pp. 1083-1091.

- Tratnyek, P. G. 1996. Putting corrosion to use: Remediation of contaminated groundwater with zero-valent metals. *Chemistry & Industry*. 13: 499-503.
- Vidic, R. D., and F. G. Pohland. 1996. *Remediation Technology Status Report: Treatment Walls*. Ground Water Remediation Technologies Analysis Center. Pittsburgh, PA. Report No. EPA542-K-94-004.
- Vogan, J. 1996. In-Situ Reactive Iron: Capital Costs. *Environment News Magazine*.
- Vogan, J. L., R. W. Gillham, S. F. O'Hannesin, and W. H. Matulewicz. 1995. Site specific degradation of VOCs in groundwater using zero valent iron. *209th National Meeting ACS. Preprint Extended Abstracts, Division of Environmental Chemistry*. Anaheim, CA. Vol. 35, No. 1, pp. 800-804.
- Weathers, L. J., G. F. Parkin, P. J. Novak, and P. J. J. Alvarez. 1995. Methanogens couple anaerobic Fe(0) oxidation and CHCl₃ reduction. *209th National Meeting ACS. Preprint Extended Abstracts, Division of Environmental Chemistry*. Anaheim, CA. Vol. 35, No. 1, pp. 829-832.
- Weber, E., J. 1995. Iron-mediated reductive transformations: Investigation of reaction mechanism. *209th National Meeting ACS. Preprint Extended Abstracts, Division of Environmental Chemistry*. Anaheim, CA. Vol. 35, No. 1, pp. 702-705.
- Weber, E. J. 1996. Iron-mediated reductive transformations: Investigation of reaction mechanism. *Environ. Sci. Technol.* 30 (2): pp.716-719.
- Weber, E. J., and R. L. Adams. 1995. Chemical- and sediment mediated reduction of the azo dye disperse blue 79. *Environ. Sci. Technol.* 29 (5): 1163-1170.
- West, O. R., L. Liang, W. L. Holden, N. E. Korte, Q. Fernando, and J. L. Clausen. 1996. *Degradation of polychlorinated biphenyls (PCBs) using palladized iron*. Report No. ORNL/TM-13217.
- Wilson, E. K. 1995. Zero-valent metals provide possible solution to groundwater problems. *Chemical & Engineering News*. 73 (27): 19-23.
- Yamane, C. L., S. D. Warner, J. D. Gallinatti, F. S. Szerdy, T. A. Delfino, D. A. Hankins, and J. L. Vogan. 1995. Installation of a subsurface groundwater treatment wall composed of granular zero-valent iron. *209th National Meeting ACS. Preprint Extended Abstracts, Division of Environmental Chemistry*. Anaheim, CA. Vol. 35, No. 1, pp. 792-795.

Chapter 2

A Column Study of Geochemical Factors Affecting Reductive Dechlorination of Chlorinated Solvents by Zero-Valent Iron¹

2.1 ABSTRACT

Laboratory and field studies have shown that filings of metal that are predominantly Fe⁰ can rapidly dehalogenate a variety of chlorinated solvents, and several technologies have recently been proposed to use this reaction in remediation of contaminated groundwater. This report describes results from a laboratory column designed to model the spatial distribution of chemical conditions where iron is applied as part of an in situ permeable reactive barrier. The column contains a zone of granular iron located between up-gradient and down-gradient zones of sand, and has been in continuous operation for over six months. Aerobic corrosion results in complete consumption of dissolved oxygen and precipitation of ferric hydroxides at the interface where water enters the iron-bearing zone. Within the iron-bearing zone, corrosion continues due to oxidation of iron by water and carbon tetrachloride, resulting in increased pH and concentration of dissolved iron in the pore water. At the down-gradient interface, pH decreased and precipitates, including siderite, were formed. Carbon tetrachloride (up to 1.6 mM) was fully dehalogenated at the first sample port within the iron-bearing zone. The chloroform produced was further dechlorinated to dichloromethane, but more slowly. First-order disappearance kinetics for chloroform applied across the zone of iron and k_{obs} has changed little over several months. No evidence has been found so far for unusual reactivity of the chlorinated solvents at either the up-gradient or down-gradient interfaces.

¹Johnson, T. L., and P. G. Tratnyek. 1994. A column study of carbon tetrachloride dehalogenation by iron metal. Proceedings of the 33rd Hanford Symposium on Health & the Environment—In Situ Remediation: Scientific Basis for Current and Future Technologies. Pasco, WA. Vol. 2, pp 931-947.

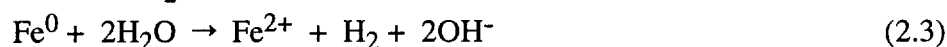
2.2 INTRODUCTION

Gillham and coworkers (Gillham and O'Hannesin, 1992; Gillham and O'Hannesin, 1994; Gillham *et al.*, 1993) have recently shown that fine granular iron metal can rapidly dechlorinate a variety of chlorinated solvents, and concluded that this process may be useful in remediating contaminated groundwater. So far, two means of applying this process have been demonstrated in the field (Gillham *et al.*, 1994). One involves placing a permeable zone of granular iron across the path of a contaminant plume that effects remediation by acting as a reactive barrier. The other approach involves circulating waste streams or water from pump-and-treat systems through above-ground reactors packed with a mixture of granular iron and other materials. The success of these demonstrations suggests that they may lead to novel alternatives to existing techniques for remediating plumes of chlorinated solvents in groundwater.

The further development of iron-based remediation technologies will be facilitated by a detailed process-level understanding of the interactions between the metal, the contaminants to be degraded, and the surrounding porous medium. A recent study of chlorinated methane dehalogenation in $\text{Fe}^0\text{-H}_2\text{O}$ model systems has contributed to this understanding by demonstrating the importance of access to, and concentration of, clean iron metal surfaces (Matheson and Tratnyek, 1994). Clearly, reactions on metal surfaces will be affected by precipitation of iron (oxy)hydroxides, carbonates, or sulfides. The possible effects of these solid phases on halocarbon reduction by iron metal are currently under investigation by several groups using mixed-batch and homogeneous-column systems. One aspect of the field situation that has not been incorporated in laboratory studies reported to date, is the development of steep chemical gradients within the iron-bearing zone, at the interfaces between the iron-bearing zone and the surrounding material, and down-gradient where the plume of treated water interacts with the native aquifer material. This study attempts to characterize these effects with a physical model consisting of a column packed with consecutive zones of sand, iron, and sand. The primary goals are to (1) characterize the spatial variation in chemistry along the flow path through a zone containing iron metal, (2) determine the effect this variation has on dehalogenation, and (3) observe how the chemical processes taking place within the column evolve during extended operation. The results reported here are for a column that has been in continuous operation for over six months.

2.2.1 Chemical Background. Zero-valent iron metal, Fe^0 , is readily oxidized to ferrous iron, Fe^{2+} , by many substances. This accounts for the utility of iron as a reductant in organic synthesis (House, 1972; Hudlicky, 1984; Smith, 1968), the improved cutting

and grinding of metals where halocarbons are used as extreme pressure lubricants (Smentkowski *et al.*, 1990), and the ubiquitous problem of metal corrosion (Jones, 1992). The primary reaction responsible for corrosion of Fe⁰ in aerobic aqueous systems is represented by equation 2.1. Available O₂ is further consumed by oxidation of Fe²⁺ to Fe³⁺ (equation 2.2). Where conditions are anoxic, and where there are no other strong oxidants available, corrosion in aqueous systems proceeds slowly by reaction with water (equation 2.3).



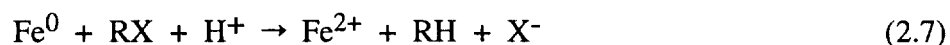
Factors that affect the rates of these reactions have been studied extensively (Shoesmith, 1987). Low pH and the presence of strong oxidants favor faster rates of iron corrosion until the products of reaction begin to passivate the metal by coating its surface with a protective layer. The passivating layer may consist of precipitates, such as ferric oxides (rust) under aerobic conditions. Under anaerobic conditions, the passivating layer may consist of a surface film of H₂ that is generated according to equation 2.3.

In the field applications of iron to remediation, the formation of precipitates is likely to be important, both in the presence of corroding iron, as well as down-gradient in the resulting plume of treated water. A stability diagram for the Fe-H₂O-CO₂ system under conditions used in this study shows the solid phases that are expected to form (Figure 2.1). Where aerobic corrosion takes place, precipitation of amorphous Fe(OH)₃ is expected (equation 2.4), which can eventually crystallize to ferric oxides such as hematite. Under reducing conditions, dissolution of iron metal to Fe²⁺ should lead to Fe(CO)₃ at near-neutral pH (equation 2.5), and Fe(OH)₂ above pH 8.5 (equation 2.6).



The possible effects of these precipitates include: (1) decreased reduction rates by inhibiting access of substrates to the metal surface; (2) reduced hydraulic conductivity due to filling of pore space; or (3) increased reaction due to the formation of new sites for adsorption, reaction, or catalysis. Precipitation as colloids, instead of coating existing grains, could also result in facilitated transport of adsorbed species.

Most halogenated aliphatic hydrocarbons, RX, can be reduced by iron metal. The overall reaction (equation 2.7) results in dehalogenation of RX and oxidative dissolution of Fe⁰. Three general pathways by which this process may occur have been proposed (Matheson and Tratnyek, 1994). The first involves direct reaction at the metal surface, in which case equation 2.7 alone adequately represents the pathway of reduction. The other two possible pathways do not involve the metal surface directly. Instead, Fe²⁺ and H₂, which are products of corrosion by water, serve as the reductants that are directly responsible dehalogenation of RX (equations 2.8 and 2.9).



Corrosion of chlorinated solvents by iron (equation 2.7) has been studied extensively due to its importance in industrial applications (Archer and Harter, 1978; Archer and Simpson, 1977; Rhodes and Carty, 1925), and is apparently the dominant dechlorination pathway in simple aqueous systems containing high-purity iron (Matheson and Tratnyek, 1994). Conditions within the column used in this study are more variable, however, so the results should help reveal what other processes have the greatest effect on field performance of iron-based remediation technologies.

2.3 EXPERIMENTAL SECTION

2.3.1 Chemicals. Chlorinated solvents were obtained in high purity and used without further purification. These included carbon tetrachloride, HPLC grade (Aldrich); chloroform, LC grade, preserved with 1% (v/v) ethanol (Burdick & Jackson); and dichloromethane, 99+%, anhydrous (Aldrich). Saturated aqueous stock solutions of these halocarbons were prepared by allowing roughly 1 mL of organic phase to equilibrate with 40 mL of water in glass vials capped with Teflon Mininert valves. Aqueous standard solutions were made by diluting the saturated stock solutions with deionized water (18 MΩ-cm NANOpure).

“Degreased” iron filings were obtained from EM Science. The material is nominally >99% pure with <0.05% of any impurity, and was used as received without pretreatment. The sand used in the column was a well sorted fine-grained crushed silica that was washed 3 times with deionized water before use.

2.3.2 Column Design. The column was constructed from a 15 cm diameter Plexiglas pipe 90 cm in length. Holes were drilled in a spiral pattern every 2.5 cm over the first 40 cm and at 5 cm intervals over the remaining length of the column. Nylon Swagelok fittings were used to hold sampling tubes consisting of 0.32-cm OD Teflon tubing. The tubes were terminated near the center of the column with plugs of glass wool to prevent leakage of the sand. The column was assembled to simulate an up-gradient, iron-bearing zone, and down-gradient cross-section of an in situ permeable iron barrier (Figure 2.2). The up-gradient zone was 14 cm in length, and the down-gradient section 51 cm, both containing only crushed quartz sand. The iron bearing zone was 25 cm in length and was composed of the same sand mixed with iron filings to give 24% by weight iron (total iron content 1575 gr). The column was packed dry and flushed with CO₂ before being saturated from the bottom up. The column experiment was conducted in a temperature controlled chamber at 15°C, and in the dark except for room lighting during sampling. Two HPLC pumps (Gilson) were used to supply solvent saturated and deionized water which was mixed with an HPLC dynamic mixer before introduction to the column. Flow rates and feed concentrations were varied from 0.5 to 2.5 cm/hr and 0.13 to 1.6 mM CCl₄ respectively. Water was introduced to the column on 2 August 1993 and carbon tetrachloride was introduced on 31 October 1993.

2.3.3 Analyses. Samples of column pore water (1-mL) were collected from sample ports with a gas-tight syringe and dispensed into 2-mL autosampler vials, which were immediately crimp-sealed in the 15°C room. Halocarbon concentrations were determined by gas chromatography with direct aqueous injection (HP 5890 Series II). An autosampler was used with an on-column inlet at 92 °C. A 2.5-m x 0.53-mm ID precolumn was used, followed by 30-m x 0.53-mm ID DB 624 analytical column (J&W) in an oven heated to 104 °C. Satisfactory results were obtained with detection by FID. Peaks were identified by comparison with the retention times of standard compounds. All standards were handled in the same manner as the column sample, so no headspace corrections were needed. Concentrations of halocarbons were determined from peak areas using the external standard method of the Chemstation software (Hewlett Packard).

Iron concentrations were determined colorimetrically with ferrozine (Stookey, 1970). Samples were not filtered before analysis. Determination of speciation was accomplished by substituting DI water for reductant in the ferrozine method. In-situ measurements of pH were made by inserting an 18-gauge needle-form combination electrode (Microelectrodes, Inc.) into the center of the column through the sample port tubing. To insure that these measurements were representative, 0.25 mL of water was allowed to leak from the port. Chloride was measured with a rapid flow analyzer

(Perstorp) using the mercuric cyanide method. Dissolved oxygen was measured colorimetrically with CHEMets self-filling ampoules (CHEMetrics).

Mineralogical samples were collected from selected ports after removing the glass wool plug. The grains of iron and sand were allowed to flow into 5 mL-beakers, and were immediately washed with acetone, filtered, and washed repeatedly with additional acetone to dry the sample as quickly as possible. This method appears to minimize formation of oxides due to oxidation or other precipitates due to residues after drying. The dried samples were analyzed by scanning electron microscopy (SEM, Zeiss DSM-960) with energy dispersive X-ray spectroscopy (EDS). SEM images were obtained at an accelerating voltage of 10kV using a lanthanum hexaboride source and a beryllium window with a working distance of 16 mm. EDS was performed at a working distance of 31 mm.

2.4 RESULTS AND DISCUSSION

2.4.1 Chemistry of the Fe-H₂O-Sand System. Before CCl₄ was added to the system, the column feed consisted of deionized water in equilibrium with the atmosphere at 15 °C. The feed water typically had a pH≈6. As a result of iron reaction with corroding iron (equations 2.1 and 2.2), dissolved O₂ decreased upon entering the iron-bearing zone, to 10 ppb at the first sampling port within the zone, and below detection at the second port. Formation of ferric iron precipitates at the up-gradient interface was evidenced by the development of a narrow band of orange-black precipitate that was visible through the side of the Plexiglas column. Dissolved O₂ concentrations throughout the remainder of the column remained below detection (MDL ≈ 5 ppb).

Oxidation of Fe⁰ by O₂ (equations 2.1 and 2.2), H₂O (equation 2.3), and halocarbons (equations 2.7 and 2.8) all should cause an increase in the system pH. In our column, the measured values of pH increased sharply across the up-gradient interface and continued to increase throughout the zone of active corrosion due to dechlorination (Figure 2.3). Beyond the down-gradient interface, pH declined sharply and reached approximately up-gradient values after about 45 cm. Two zones of precipitation were visible down-gradient. At the immediate interface, a narrow gray band formed which transitioned to a zone down-gradient where the sand acquired a brown color after several months of column operation. The gray zone appears to be due to the formation of FeCO₃(s) according to equation 2.5 (see below), and the brown zone suggests precipitation of Fe(OH)₂ or perhaps ferric hydroxides (equations 2.4 and 2.6).

The concentration of iron in the pore water rises steeply at the up-gradient

interface of the wall and then more slowly across the remainder of the iron-bearing zone (Figure 2.4). The highest concentration of 1.2 mM was found just beyond the down-gradient interface, during a period when the column feed included 1.6 mM CCl_4 . These results are consistent with equations 2.1, 2.3, and 2.7, which suggest high concentrations of dissolved iron should result from oxidative dissolution of the metal. In the anoxic regions of the column, high concentrations of a strongly oxidizing halocarbon like CCl_4 apparently result in equation 2.7 being the dominant corrosion process. A preliminary attempt to determine the speciation of this iron with the ferrozine method suggests that it was primarily Fe^{2+} . In the region beyond the down-gradient interface, the concentration of iron in solution decreased, as expected, due to precipitation of $\text{Fe}(\text{CO})_3$, $\text{Fe}(\text{OH})_2$, and $\text{Fe}(\text{OH})_3$.

2.4.2 Iron Surface Analysis. Grains of iron metal taken from the last sampling port before the down-gradient interface were analyzed by scanning electron microscopy (SEM) with energy dispersive X-ray spectroscopy (EDS). The secondary SEM image (Figure 2.5) shows a complex surface structure with pits of clean metal, together with regions covered with precipitate. The well developed hexagonal crystals contain Fe, C, and O as determined by EDS, and are most likely siderite.

2.4.3 Dechlorination of Solvents. In mixed batch systems containing roughly 20 g/L of fine-grained high-purity iron, CCl_4 undergoes sequential dehalogenation, via CHCl_3 , to CH_2Cl_2 (Matheson and Tratnyek, 1994). Under those conditions, both reduction steps were pseudo-first-order, but the dechlorination of CCl_4 was roughly 100-fold faster than that of CHCl_3 . In the column used in this study, the fate of CCl_4 was apparently similar. CCl_4 disappearance was accompanied by appearance of CHCl_3 , which later degraded to CH_2Cl_2 . When high feed concentrations of CCl_4 were used, preliminary evidence suggests that dechlorination may proceed to chloromethane, and, perhaps, even to methane. Within the iron-bearing zone, CCl_4 disappearance is so rapid that rigorous determination of the rate was not possible. However, the available data indicate that the half-life of reduction is no more than 15 minutes at an average linear velocity of 2.5 cm/hr. Since CHCl_3 dechlorinates more slowly, its concentration could be measured throughout the iron-bearing zone. Concentration versus time data for CHCl_3 indicate that the kinetics of conversion to CH_2Cl_2 are pseudo-first-order and roughly constant throughout the iron-bearing zone (Figure 2.6). The rate of CHCl_3 reduction did not change significantly over 4 months of column operation (Table 2.1). However, k_{obs} for dehalogenation of CHCl_3 did vary significantly with the rate of flow in the column, increasing roughly 2-fold with a 5-fold increase in flow velocity. This effect suggests that mass transport contributes to the observed rate of solvent reduction under the conditions

of this column. A similar conclusion was drawn from batch studies done previously with CCl_4 (Matheson and Tratnyek, 1994).

2.5 IMPLICATIONS FOR IN-SITU REMEDIATION

Steep chemical gradients and zones of precipitation like those observed in this column study can certainly be expected when iron metal is employed in canisters for above-ground remediation of field sites, and they may also develop around in situ permeable barriers that contain granular metals. The corrosion of iron will cause water flowing from the treatment zone to be anoxic, alkaline, and high in ferrous iron, but pH and iron concentration will decrease rapidly where precipitation of iron hydroxides and carbonates occurs. Disappearance of chlorinated methanes is due to dechlorination, which is confined to regions where metal is present and actively corroding. Although the formation of precipitates could effect the dechlorination reaction in several ways, data from this column study show remarkable consistent rates of degradation with respect to position within the iron-bearing zone, and with respect to duration of column operation. The dependence of dechlorination rate on flow velocity provides further evidence that the reaction tends to be effected by mass transport of the substrate to reactive sites on the iron surface.

ACKNOWLEDGMENTS AND DISCLAIMER

This study has been supported in part by the University Consortium Solvent-In-Groundwater Research Program, and the U.S. Environmental Protection Agency through Cooperative Agreement CR 82078-01-0 to P. Tratnyek, and an Energy Research Fellowship to T. Johnson from the U.S. Department of Energy. This report has not been subject to review by the U.S. Environmental Protection Agency or the U.S. Department of Energy and therefore does not necessarily reflect the views of these Agencies and no official endorsement should be inferred.

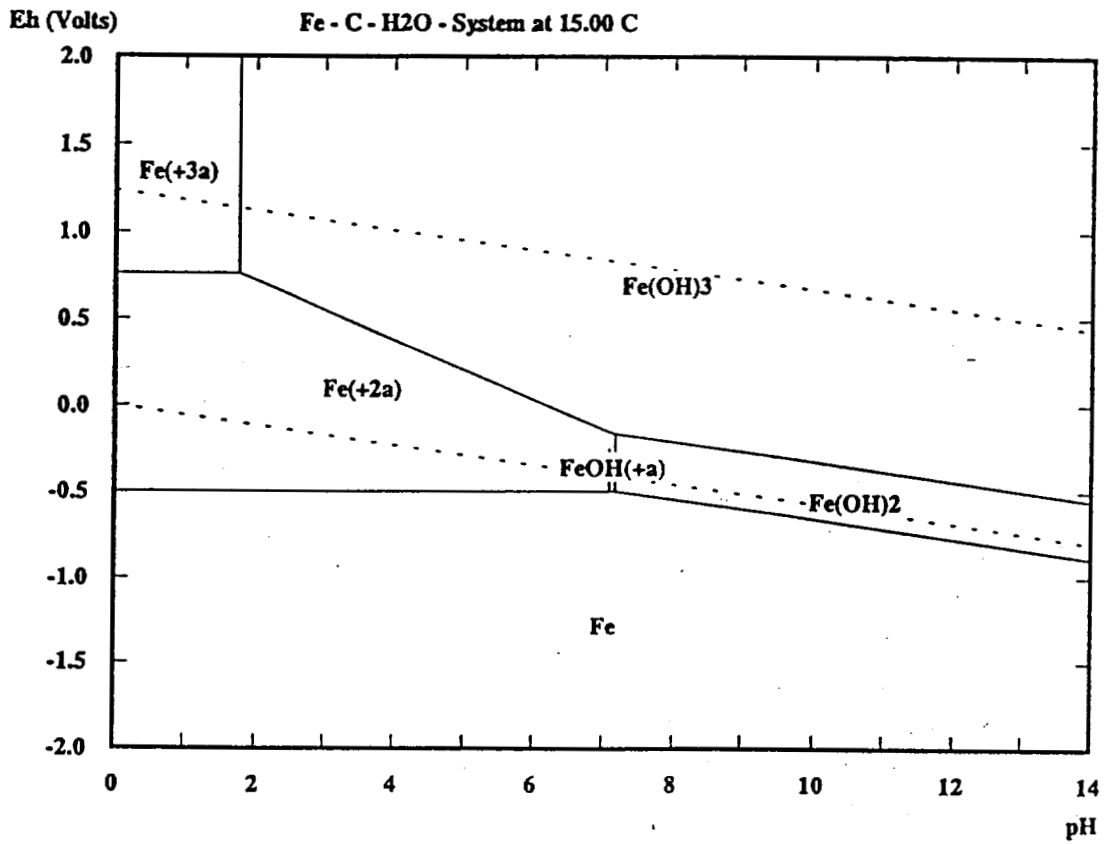


Figure 2.1 Eh-pH diagram for the Fe-H₂O-CO₂ system at equilibrium. Calculated for 1.0×10^{-3} molal CO₂, 2.0×10^{-3} molal Fe, and 15 °C using HSC Chemistry (Outokumpu Research, Finland).

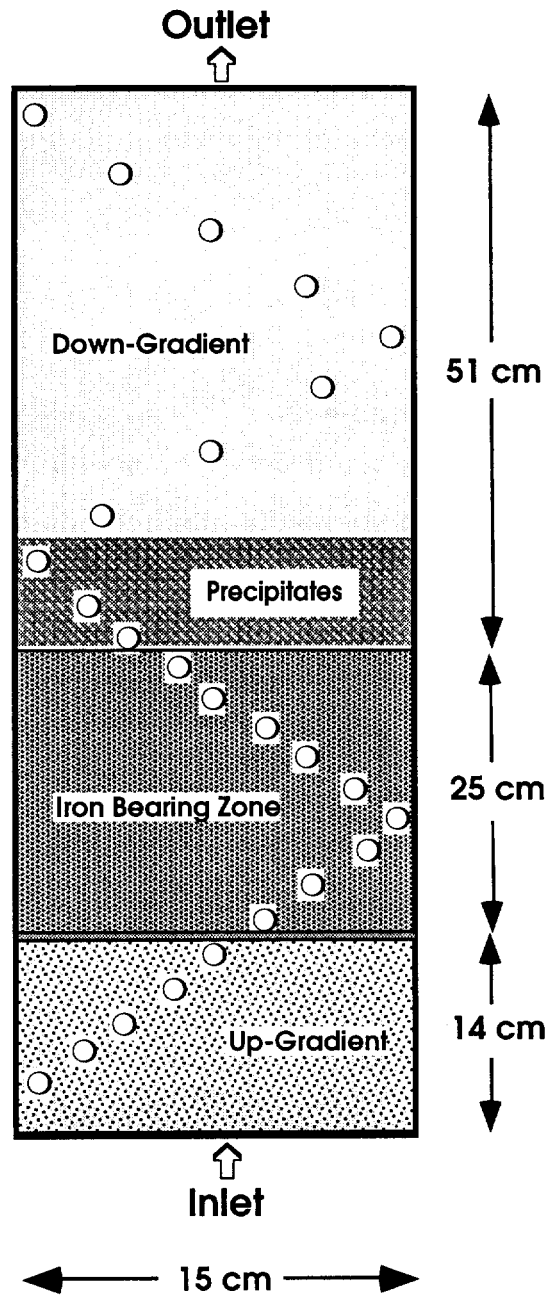


Figure 2.2 Schematic of the column used in this study. The system was run in up-flow mode at 15 °C in the dark, with the up-gradient and down-gradient zones consisting of sand, and the iron-bearing zone containing 24% (w/w) iron filings and sand. A narrow band of red-black precipitation formed at the interface between up-gradient sand and the iron-bearing zone. Two regions of precipitate formed down-gradient from the iron, one gray and the other brown. Flow rate varied from 0.5 to 2.5 cm/hr.

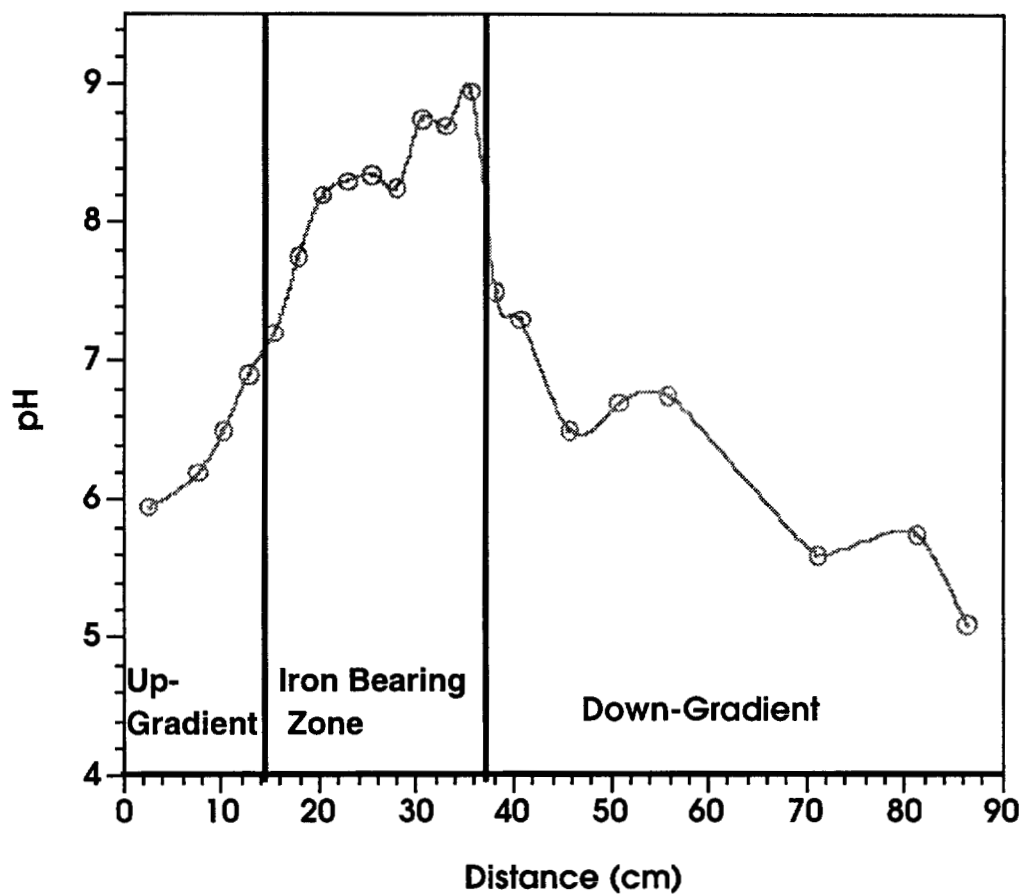


Figure 2.3 pH versus distance along the column flow path. Data represent the average of 6 profiles taken over the first 2 months of column operation. During this period, the flow rate was constant at 1.25 cm/hr and no CCl_4 had been introduced to the column.

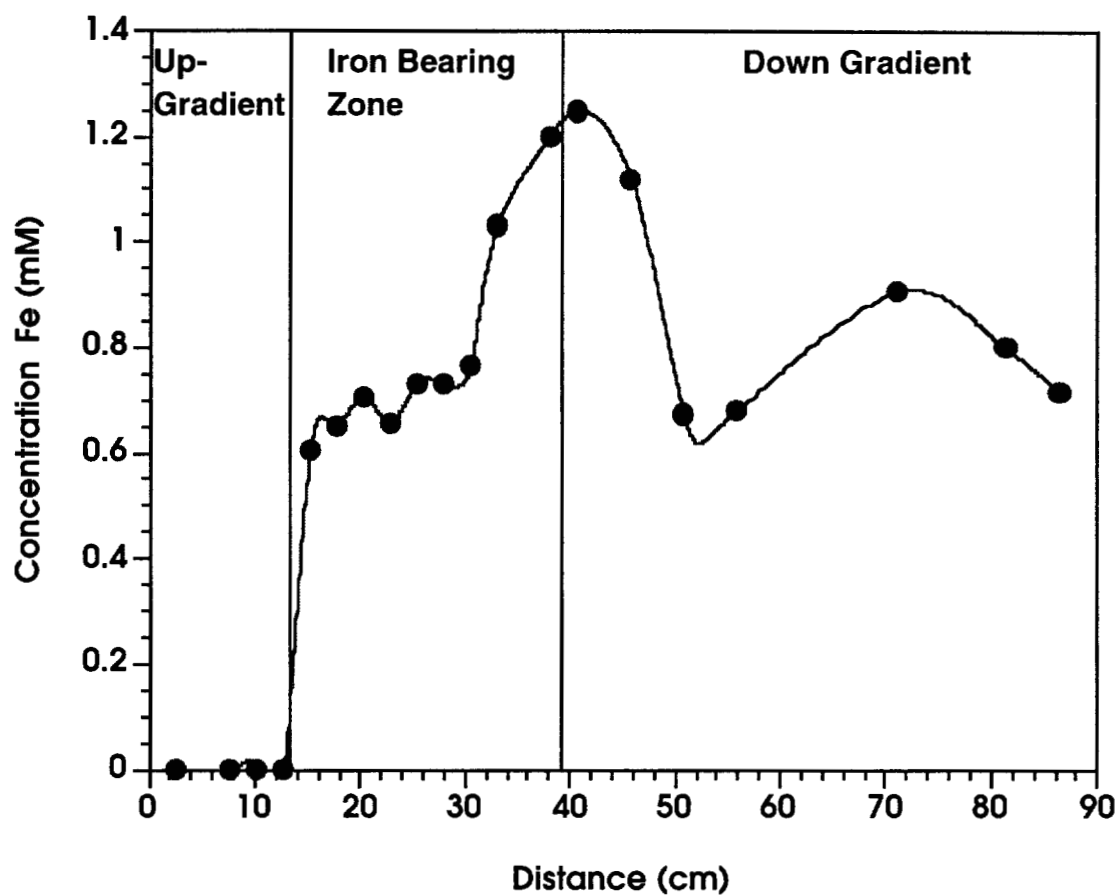


Figure 2.4 Concentration of iron in the pore water versus distance along the column flow path. Data represent the average of 3 profiles taken at about 6 months of column operation. During this period, the flow rate was 2.5 cm/hr and the feed water contained 1.6 mM CCl_4 .



Figure 2.5 Scanning electron micrograph of an iron grain removed from the down-gradient interface after 6 months of continuous column operation. X-ray micro-probe analysis confirmed that the smooth regions are bare iron metal and the hexagonal crystals are siderite. The image shown is a secondary electron image taken at a magnification of 1500.

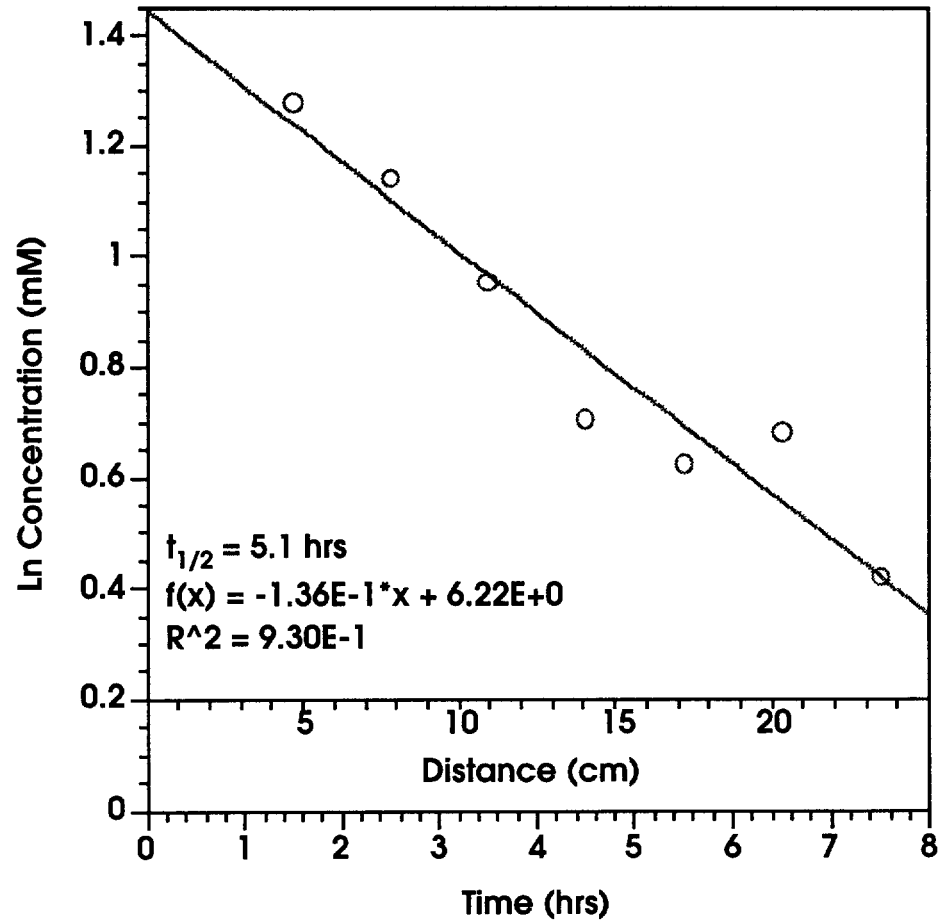


Figure 2.6 Natural logarithm of CHCl_3 concentration from within the iron-bearing zone, versus time calculated from distance along the column and the average linear flow velocity. Rates were similar for initial CCl_4 concentrations ranging from 0.13-1.6 mM, for flow rates of 0.5-2.5 cm/hr, and time of column operation from 2-6 months.

TABLE 2.1 PSEUDO-FIRST-ORDER RATES OF CHLOROFORM DISAPPEARANCE IN THE COLUMN IRON-BEARING ZONE.

Date	V, cm/hr	k_{obs} , 1/hr	r^2	$t_{1/2}$, hr
2/9/94	2.5	0.171	0.76	4.0
2/10		0.194	0.74	3.6
2/18		0.114	0.93	5.1
2/21		0.150	0.90	4.6
Average		0.182	0.83	4.3
2/24/94	2.0	0.141	0.86	4.1
2/26		0.107	0.76	6.5
Average		0.124	0.81	5.3
11/1/93	1.25	0.122	0.95	5.7
11/3		0.130	0.72	5.3
11/4		0.105	0.77	6.6
11/5		0.123	0.80	5.6
11/7		0.066	0.52	10.5
11/9		0.086	0.63	8.1
11/12		0.105	0.73	6.6
11/15		0.109	0.62	6.4
Average		0.098	0.72	6.8
11/17/93		0.5	0.081	0.83
11/19	0.071		0.83	9.8
11/22	0.086		0.85	8.1
Average	0.079		0.84	8.7

Chloroform resulted from input of 0.13 to 1.6 mM Carbon Tetrachloride.

2.6 REFERENCES

- Archer, W. L., and M. K. Harter. 1978. Reactivity of carbon tetrachloride with a series of metals. *Corrosion* 34(5): 159-162.
- Archer, W. L., and E. L. Simpson. 1977. Chemical profile of polychloroethanes and polychloroalkenes. *Ind. Eng. Chem. Prod. Res. Dev.* 16(2): 158-162.
- Gillham, R. W., D. W. Blowes, C. J. Ptacek, and S. O'Hannesin. 1994. Use of zero-valent metals for in situ remediation of contaminated groundwater. *Proceedings of the 33rd Hanford Symposium on Health & the Environment—In Situ Remediation: Scientific Basis for Current and Future Technologies*. Pasco, WA. Vol. 2, pp. 913-930.
- Gillham, R. W., and S. F. O'Hannesin. 1992. Metal-catalysed abiotic degradation of halogenated organic compounds. *IAH Conference, Modern Trends in Hydrogeology*. Hamilton, Ontario, Canada. pp. 94-103.
- Gillham, R. W., and S. F. O'Hannesin. 1994. Enhanced degradation of halogenated aliphatics by zero-valent iron. *Ground Water* 32(6): 958-967.
- Gillham, R. W., S. F. O'Hannesin, and W. S. Orth. 1993. Metal enhanced abiotic degradation of halogenated aliphatics: Laboratory tests and field trials. *Proceedings of the 6th Annual Environmental Management and Technical Conference/HazMat Central Conference*, Rosemont, IL. pp. 440-461.
- House, H. O. 1972. *Modern Synthetic Reactions*. W. A. Benjamin, Menlo Park, CA.
- Hudlicky, M. 1984. *Reductions in Organic Chemistry*. Ellis Horwood, Chichester.
- Jones, D. A. 1992. *Principles and Prevention of Corrosion*. Macmillan, New York.
- Matheson, L. J., and P. G. Tratnyek. 1994. Reductive dehalogenation of chlorinated methanes by iron metal. *Environ. Sci. Technol.* 28(12): 2045-2053.
- Rhodes, F. H., and J. T. Carty. 1925. The corrosion of certain metals by carbon tetrachloride. *Ind. Eng. Chem.* 17: 909-911.
- Shoosmith, D. W. 1987. Kinetics of aqueous corrosion. L. J. Korb and D. L. Olson (ed.), *Metals Handbook*. 9th ed. ASM, Metals Park, OH, Vol. 13, pp. 45-49.
- Smentkowski, V. S., C. C. Cheng, and J. T. J. Yates. 1990. The interaction of carbon tetrachloride with Fe(110): A system of tribological importance. *Langmuir* 6(1): 147-158.
- Smith, M. 1968. Dissolving metal reductions. In : R. L. Augustine (ed.), *Reduction. Techniques and Applications in Organic Synthesis*. Marcell Dekker, New York, NY, pp. 95-169.
- Stookey, L. L. 1970. Ferrozine—A new spectrophotometric reagent for iron. *Anal. Chem.* 42(7): 779-781.

Chapter 3

Kinetics of Halogenated Organic Compound Degradation by Iron Metal¹

3.1 ABSTRACT

A combination of new and previously reported data on the kinetics of dehalogenation by zero-valent iron (Fe^0) has been subjected to an analysis of factors effecting contaminant degradation rates. First-order rate constants (k_{obs}) from both batch and column studies vary widely and without meaningful correlation. However, normalization of these data to iron surface area concentration yields a specific rate constant (k_{SA}) that varies by only 1 order of magnitude for individual halocarbons. Correlation analysis using k_{SA} reveals that dechlorination is generally more rapid at saturated carbon centers than unsaturated carbons and high degrees of halogenation favor rapid reduction. However, new data and additional analysis will be necessary to obtain reliable quantitative-structure activity relationships. Further generalization of our kinetic model has been obtained by accounting for the concentration and saturation of reactive surface sites, but k_{SA} is still the most appropriate starting point for design calculations. Representative values of k_{SA} have been provided for the common chlorinated solvents.

¹Reprinted with permission from Johnson, T. L., M. M. Scherer, and P. G. Tratnyek. 1996. Kinetics of halogenated organic compound degradation by iron metal. *Environmental Science & Technology* 30(8): 2634-2640. Copyright 1996 American Chemical Society.

Studies of halocarbon degradation by zero-valent iron metal (Fe^0) often report contaminant disappearance rates as the primary measure of potential remediation performance. With the abundance of kinetic data that are now available for many compounds, the range of reported degradation rates has grown, giving the impression that these values are highly variable and very sensitive to operating conditions. Much of this variability is due to the effect of experimental factors (such as pH, metal surface area concentration, and mixing rate) that have been described with quantitative models in previous studies (Agrawal and Tratnyek, 1996; Gillham and O'Hannesin, 1994; Matheson and Tratnyek, 1994; Sivavec and Horney, 1995). However, the generality of these models has not been tested, so quantitative corrections are not commonly being made. In the absence of quantitative corrections for important experimental parameters, direct comparisons between data from independent sources have not been very successful, and only qualitative conclusions have been drawn from this type of analysis (Gillham, 1996).

The purpose of this study is to improve our understanding of degradation kinetics involving Fe^0 by evaluating the full range of available data using a consistent model. Published data from batch and column studies have been assembled and analyzed to assess the most important sources of variability in degradation rates over the range of realistic field conditions. New data have also been included to describe effects that have not been thoroughly investigated previously. The analysis shows that most variability in observed degradation rates for particular compounds is attributable to the effects of iron surface area concentration. Although incorporating the influence of other factors into the kinetic model provides mechanistic insight, the magnitude of these effects is relatively modest over the range of environmentally realistic conditions. Thus, initial first-order degradation rate constants normalized to the concentration of iron surface area (k_{SA}) appear to offer the most practical, general descriptor of contaminant degradation kinetics. A comparison of these data for the various halocarbons confirms that there is a wide range of reactivities with Fe^0 . Perhalogenated substances are reduced more rapidly than their less highly chlorinated congeners, and dechlorination is more rapid at saturated carbon centers (e.g., carbon tetrachloride and hexachloroethane) than unsaturated carbons (e.g., perchloroethene or trichloroethene). Although the data currently available are barely adequate to begin developing quantitative structure-activity relationships, they have been used to calculate average values of k_{SA} , which should provide improved input parameters for design of full-scale remediation operations.

3.3 METHODS

New data for CCl_4 disappearance kinetics came from batch tests performed in a manner similar to methods described previously (Matheson and Tratnyek, 1994; Scherer and Tratnyek, 1995). Experiments were conducted with electrolytically-produced 100-mesh iron powder (Fisher certified grade) in N_2 -purged unbuffered water, and 20-32 mesh iron turnings (Fluka, puriss. grade) in carbonate buffered medium. In contrast to our previous work, the iron was used without treatment to clean or activate the metal surface. Specific surface area determinations were done by Micromeritics (Norcross, GA) using BET gas adsorption with N_2 . New values include $0.019 \text{ m}^2 \text{ g}^{-1}$ for Fluka turnings, $0.061 \text{ m}^2 \text{ g}^{-1}$ for Fisher electrolytic iron as received, and $0.057 \text{ m}^2 \text{ g}^{-1}$ after removing fines <325 mesh. Mixing was achieved by rotation at 36 rpm, in the dark, and at room temperature ($23 \pm 1 \text{ }^\circ\text{C}$). CCl_4 disappearance kinetics were determined by periodic sampling of the aqueous phase from a single bottle and analysis by gas chromatography with direct aqueous injection (Matheson and Tratnyek, 1994).

Previously reported kinetic data for dehalogenation of alkanes and alkenes by zero-valent iron were gathered from all citeable sources available as of November 1995. With the addition of a few critical parameters obtained by personal communications, adequate experimental detail to allow meaningful comparisons between research groups were available for 18 studies. Experimental conditions from these studies are summarized in Table 3.1. The results of each study and our subsequent analyses are summarized in tables provided as supporting information. The scope of our analysis does not include experiments performed with halogenated aromatic compounds, zero-valent metals other than Fe^0 , "bimetallic" reductants, or non-aqueous systems.

Several studies report kinetic data on the effects of experimental variables from otherwise replicate experiments. These often include a number of rate constants determined over a wider range of conditions than is expected in most contaminated groundwaters. Incorporation of all these original data as if they were independent and equally relevant would bias our analysis of variability between research groups. In such cases, we have represented the series with data from the one experiment that most closely approximated realistic groundwater conditions (15°C , 1 ft d^{-1} linear velocity, and 1 mg L^{-1} initial substrate concentration). Normalization for Fe^0 surface area concentration was made if the necessary data were reported in the original reference, or if the data could be reliably assigned using information from other sources.

3.4.1 Pseudo-First-Order Rate Data. Experimental conditions for the 18 kinetic studies included in this analysis are summarized in Table 3.1. The conditions vary widely, providing a broad basis for comparison between the work of independent investigators. Most studies have found that disappearance of the primary substrate (the contaminant) proceeds by kinetics that are first-order with respect to contaminant concentration. Therefore, first-order rate constants (k_{obs}) should be characteristic of a particular contaminant and set of conditions irrespective of contaminant concentration. Half-lives ($t_{1/2}$) derived from k_{obs} values offer similar advantages of generality. We have used the reported values of k_{obs} or $t_{1/2}$ as primary data for subsequent analysis.

The kinetic data from batch and column experiments are summarized in graphical form in Figure 3.1. The range in reported disappearance rates for *batch* experiments corresponds to $t_{1/2}$ values from 10 min to 30 d, with a typical value of roughly 15 hr. The scatter in k_{obs} for individual halocarbons is best determined from the chlorinated alkenes, where $n \geq 4$ in all cases. For these data, the mean relative standard deviation of reported k_{obs} values is 84%. The range in rate data from *column* studies corresponds to $t_{1/2}$ values from 30 sec to 30 hr, with a typical value of roughly 1.5 hr. Thus, rate constants from column studies tend to be greater than those from batch studies by about 1 order of magnitude, but the variability in both types of experiments is similar (about 3 orders of magnitude). Except for the notably high k_{obs} values for perhalogenated alkanes (carbon tetrachloride and hexachloroethane), the k_{obs} data do not exhibit any clear trend in reactivity between halocarbons. This is consistent with the widely held impression that raw kinetic data for dechlorination by iron metal are highly variable. In the following discussion we develop a kinetic model that accounts for the experimental factors that contribute most to variability in k_{obs} .

3.4.2 Surface Area Normalized Kinetics. Previous studies have shown that the rate of contaminant reduction by iron metal is not only first order in contaminant concentration, but that it appears to be first order with respect to the amount of metal available to serve as reductant. To describe this, the pseudo-first-order kinetic model used to determine k_{obs} can be expanded to

$$-\frac{d[P]}{dt} = k_{SA} a_s \rho_m [P] \quad (3.1)$$

or

$$-\frac{d[P]}{dt} = k_{SA}\rho_a[P] \quad (3.2)$$

where k_{SA} is the specific reaction rate constant ($L\ hr^{-1}\ m^{-2}$), a_s is the specific surface area of Fe^0 ($m^2\ g^{-1}$), ρ_m is the mass concentration of Fe^0 ($g\ L^{-1}$ of solution), ρ_a is the surface area concentration of Fe^0 ($m^2\ L^{-1}$ of solution), and P represents the reacting halocarbon. Since $k_{obs} = k_{SA}\rho_a$ where $\rho_a = a_s\rho_m$, the model suggests straight-line plots should be obtained from k_{obs} versus ρ_a , a_s , or ρ_m . Linear relationships of this sort have been observed using CCl_4 (Matheson and Tratnyek, 1994), TCE (Gillham and O'Hannesin, 1994; Sivavec and Horney, 1995), nitrobenzene (Agrawal and Tratnyek, 1996), and chromate (Gould, 1982) by varying ρ_m of a particular type of iron (constant a_s), and for TCE by varying a_s (different types of iron at constant ρ_m) (Sivavec and Horney, 1995).

Regression of data where k_{obs} versus ρ_a are linear, gives a slope equal to the specific reaction rate constant k_{SA} (i.e., $k_{SA} = k_{obs}$ normalized to ρ_a). Reduction rates characterized in these terms should be independent of the mass and specific surface area of the metal, and the volume of the reaction system. For single experiments, dividing k_{obs} by the corresponding value of ρ_a gives a point estimate of k_{SA} that lacks the statistical power that comes from regressing larger quantities of data. However, Figure 3.2 shows that the values of k_{SA} obtained by the two methods generally overlap, and therefore give equivalent expected values. The only outlier corresponds to very early data on TCE disappearance versus Fe^0 surface concentration reported by Gillham and O'Hannesin (Gillham and O'Hannesin, 1994). For most individual compounds the range in k_{SA} is about 1 order of magnitude, which represents significantly less scatter than is exhibited by the original k_{obs} data (cf. Figures 3.1 and 3.2) and by the range of reactivities of all halocarbons in Figure 3.2 (roughly 4 orders of magnitude). Clearly, k_{SA} is a more general descriptor of reactivity with Fe^0 than k_{obs} , and therefore is more appropriate for remediation design calculations and other inter-system comparisons.

3.4.3 Factors Effecting k_{SA} . The data in Figure 3.2 indicate that about 1 order of magnitude variability in disappearance rates for any particular halocarbon remains unexplained by normalization with ρ_a . Undoubtedly, some of the variability is due to the values of a_s used to calculate ρ_a (which in turn are used to calculate k_{SA}). The degree of uncertainty in a_s determined by BET gas adsorption is illustrated for three types of reagent grade iron (Fig. 3.3). Analytical error should be <0.5 % relative standard deviation for replicates done on a particular sample and instrument and <5% between laboratories using best methods on a particular surface area standard material (Everett *et al.*, 1974; Rothenberg *et al.*, 1987). This degree of variability is negligible on the scale used in Figure 3.3. There

is no pattern in the data attributable to the use of Kr over N₂ as the adsorption gas, or any other methodological factor. Therefore, the major source of variability in a_s for a particular type of iron must derive from the treatment and handling of samples. Acid washing clearly increases ρ_a , but by highly variable degrees: ranging from an order of magnitude (0.005 to 0.038 m²/g) for Fluka turnings (Agrawal and Tratnyek, 1996) to a 10% increase (0.9 to 1.0 m²/g) in surface area for Fisher filings (Burriss *et al.*, 1995). The remaining variability is probably dominated by differences in grain size distribution (deliberately due to sieving and inadvertently due to biased sampling).

A more profound source of variability in k_{SA} is due to the difference between *physical* surface area as measured by standard techniques such as gas adsorption, and *reactive* surface area, which contributes directly to contaminant transformation (White and Peterson, 1990). An empirical kinetic model to quantify the effect of variation in the specific reactivity of the metal surface can be formulated in terms of reactive surface sites

$$-\frac{d[P]}{dt} = k_2 \Gamma \rho_a [P] \quad (3.3)$$

where k_2 is the second-order rate constant for reduction at a particular type of site (L hr⁻¹ mol⁻¹) and Γ is the surface concentration of reactive sites (mol m⁻² of Fe⁰). This formulation is most appropriate if contaminant degradation occurs preferentially at distinct sites; such as impurities, pits, kinks, steps, other surface defects, or crystal faces. The importance of high energy sites in mineral dissolution is well documented (Hochella, 1990), and corrosion of metals has also been interpreted in these terms (Young and Hulett,). As written, eq 3.3 implies a single type of reactive site with a characteristic reactivity (k_2) and site density (Γ), with all other surface area having negligible effect. A model postulating more than one type of discrete site can be accommodated simply by formulating the sum, or integral, of k_2 and Γ terms over all types of sites that contribute to transformation.

Although the data are not yet available to quantify Γ (surface concentration of reactive sites), it is still useful to differentiate k_{SA} into the product of k_2 and Γ in order to clarify the factors that cause reduction rates to vary. This is illustrated by comparing the three k_{obs} versus ρ_a plots for CCl₄ shown in Figure 3.4. Slopes of the three lines obtained by regression reveal that k_{SA} for Fluka Fe⁰ is approximately three times greater than the two values for Fisher Fe⁰. This may be due to the relative lack of oxide precipitates on the Fluka material (Agrawal and Tratnyek, 1996), which would increase k_{SA} through a higher Γ of reactive metal sites. The presence of carbonate buffer in the experiment may also influence k_{SA} , most likely through the indirect effects of pH, ionic strength, or carbonate-

mediated corrosion (Agrawal and Tratnyek, 1996). With Fisher Fe^0 , k_{SA} was 20% faster at 36 rpm than at 15 rpm. More aggressive mixing presumably increases the second-order rate constant (k_2) by increasing the rate of association with the surface (k_f). However, previous work has shown that a two-fold increase in mixing rate should increase k_{SA} by about 60% (Matheson and Tratnyek, 1994). It is likely that the effect of mixing rate is smaller than expected because the 15 rpm experiment was done with acid-washed Fe^0 . In addition to increasing ρ_a , (Figure 3.3), pretreatment by acid-washing apparently increases k_{SA} , presumably by removing older crystalline oxides and leaving a fresh amorphous iron hydroxide film that is more reactive. This amounts to a higher Γ of sites with larger k_2 .

3.4.4 Apparent Deviations from the Kinetic Model. The most prevalent type of deviation from the proposed kinetic model occurs when long exposure to an aqueous environment results in changes in reactivity of the metal surface due to contaminant degradation or other surface reactions. This interpretation has been used by several groups to rationalize tailing in semi-logarithmic disappearance plots from batch experiments. In most cases the resulting nonlinearity in log concentration versus time plots has been addressed by assessing *initial* rates before secondary reactions begin to have a discernible effect on contaminant disappearance kinetics (Agrawal and Tratnyek, 1996; Lipczynska-Kochany *et al.*, 1994). Gillham and O'Hannesin, however, interpreted tailing in their data by reporting values of t_{50} (the time required to reach 50% of initial halocarbon concentration) in addition to $t_{1/2}$ values calculated from full disappearance curves (Gillham and O'Hannesin, 1994). Under these circumstances, the reported t_{50} values give a better approximation of initial first-order disappearance rates, and are therefore preferred. Systems with pyrite added to buffer pH appear to exhibit rapid initial disappearance of PCE due to adsorption (Burriss *et al.*, 1995). Thus, proper characterization of *degradation* at the surfaces found in this system may require correction for initial loss to non-reactive sites.

Another type of deviation becomes apparent when we compare "first-order" rate constants for CCl_4 disappearance over a wide range of initial contaminant concentrations ($[\text{P}]_0$). As illustrated in Figure 3.5, the rate of degradation rises as $[\text{P}]_0$ increases from low to moderate levels, and only appears to approach a constant value at high $[\text{P}]_0$. Behavior of this type is often observed in heterogeneous systems and is usually interpreted as evidence that association with the surface (either through mass transport or surface complexation) and reaction once a surface complex is formed, both influence the reaction rate (Scherer and Tratnyek, 1995; Zepp and Wolfe, 1987). For a steady-state concentration of the surface complex, the kinetic model (eq 3.3) can be elaborated to take the kinetics of surface association and effect of site saturation into account

$$-\frac{d[P]}{dt} = \frac{V_m[P]}{K_{1/2} + [P]} \quad (3.4)$$

where $V_m = k_r \Gamma \rho_a$, $K_{1/2} = (k_b + k_r)/k_f$, k_r is the rate constant for reduction of the surface complex, and k_f and k_b are rate constants for forward association with the surface (diffusion, adsorption, or surface complexation) and backward disassociation from the surface (diffusion or desorption). By analogy to familiar forms of the Michaelis-Menton equation, V_m can be interpreted as the maximum reaction rate for a particular type and amount of iron metal, and $K_{1/2}$ (the concentration of P at $V_m/2$) as a measure of the affinity of surface sites for the substrate. Nonlinear regression on the data in Figure 3.5 gives $V_m = 0.026 \pm 0.006 \mu\text{M s}^{-1}$ and $K_{1/2} = 184 \pm 149 \mu\text{M}$ for CCl_4 degradation by $\rho_a = 1.02 \text{ m}^2 \text{ L}^{-1}$ of electrolytically-produced 100-mesh Fisher iron powder (Fig. 3.4). It is important to recognize that this analysis is based on initial rates that were first-order over the duration of each individual experiment, and is not the same as tailing observed in individual experiments over long exposure times due to gradual changes in metal surface composition.

3.4.5 Relating Batch to Column Kinetics. The second-order kinetic model should apply to both batch and column reactors, but several differences must be considered before quantitative comparisons can be made. First, most linear relationships between k_{obs} and ρ_a have been determined on batch systems where the range of surface area concentrations has been limited ($5\text{-}30 \text{ m}^2 \text{ L}^{-1}$). It would be convenient if such correlations could be extrapolated from loadings typical of batch experiments to column or field conditions where ρ_a may be greater by several orders of magnitude. Such linear extrapolations have been made in a few studies (Gillham and O'Hannesin, 1994; Sivavec and Horney, 1995), but there are many reasons to expect they will not be reliable in general.

The most likely reason for nonlinearity in the k_{obs} versus ρ_a relationship, and for differences between batch and column results in general, is the role of mass transport in determining degradation kinetics. Batch experiments have shown that the rate of nitrobenzene reduction increases linearly with the square root of rpm (Agrawal and Tratnyek, 1996), and k_{obs} data for CCl_4 (Matheson and Tratnyek, 1994) also conform to this relationship. However, the slope of these lines are both about 1%, suggesting that only a modest amount of the scatter in k_{SA} data (Figure 3.2) can be attributed to the effect of mixing. However, the linearity of k_{obs} versus $\text{rpm}^{0.5}$ plots is still evidence that reduction by Fe^0 under batch conditions is influenced by mass transport processes. A similar conclusion has been drawn for chromate reduction by Fe^0 in a stirred batch reactor (Gould, 1982).

In column studies, the effect of mass transport has been studied by varying flow rate and determining k_{obs} after establishing steady-state conditions. The results indicate a modest increase in k_{obs} for CCl_4 with flow rate increasing from 0.4 to 2.0 ft d^{-1} (Johnson and Tratnyek, 1994) and for TCE from 10 to 40 ft d^{-1} (Mackenzie *et al.*, 1995b). However, the latter study found k_{obs} leveled off at flow rates $>40 \text{ ft d}^{-1}$, and another study produced no discernible effect on k_{obs} for TCE from 2 to 8 ft d^{-1} (Gillham *et al.*, 1993). Such modest effects on k_{obs} over wide ranges in velocity suggest that degradation kinetics in column systems may be controlled primarily by reaction rather than mass transport (Gillham and O'Hannesin, 1994; Orth, 1993). Thus, it appears that rates of halocarbon degradation by Fe^0 may be controlled by reaction and/or diffusion, depending on experimental conditions. In the absence of data for which the two processes have been isolated, ambiguous results are inevitable. This is illustrated by Figure 3.6 where the available k_{SA} data have been superimposed for batch and column studies. Despite expected differences between the two types of experiments, the reported results do not show distinguishable distributions.

3.4.6 Indirect Effects on the Second-Order Model. The kinetic model represented by eqs 1-3 is adequate to describe the primary effects of substrate and metal on the rate of halocarbon degradation. In addition, degradation kinetics are influenced by other factors including: dissolved oxygen (Helland *et al.*, 1995; Siantar *et al.*, 1995; Tratnyek *et al.*, 1995), chloride (Reardon, 1995; Siantar *et al.*, 1995), solution pH (Agrawal and Tratnyek, 1996; Gillham and O'Hannesin, 1994; Matheson and Tratnyek, 1994; Siantar *et al.*, 1995), carbonate alkalinity (Agrawal and Tratnyek, 1996; Mackenzie *et al.*, 1995b; Reardon, 1995), and sulfur added as sulfide, pyrite, or organic buffer (Lipczynska-Kochany *et al.*, 1994; Reardon, 1995). In all cases, it is likely that these factors exert their influences indirectly through changes in the interfacial region. For example, the rate enhancements reported from addition of sulfide (Lipczynska-Kochany *et al.*, 1994) are likely to be due to precipitation of iron sulfide on the Fe^0 surface, thereby changing k_{SA} via k_2 and/or Γ . The effects of carbonate also appear to be indirect: accelerating degradation at low alkalinity and short exposure times by minimizing pH (Figure 3.4), or inhibiting degradation due to precipitation of siderite on the Fe^0 surface at higher carbonate concentrations and longer exposure times (Agrawal and Tratnyek, 1996; Mackenzie *et al.*, 1995a). Additional examples include the effect of dissolved oxygen, which modifies the reactive surface by favoring the formation of passivating films of iron oxyhydroxides; and chloride, which depassivates the iron oxyhydroxide surface film. Sufficient data are not yet available to make quantitative corrections for these variables other than their individual contributions to k_{SA} .

3.4.7 Correlating Representative Rate Constants. The overlap of k_{SA} values from individual batch experiments with those determined from regression of k_{obs} versus ρ_a plots (Fig. 3.2) and k_{SA} data from column experiments (Fig. 3.6), suggests combining all three types of data to get average reaction rates. This calculation was done by weighting the three types of data equally and the results are presented in Table 3.2. The standard deviations are large, reflecting the collective impact of all the experimental variables that are not accounted for by k_{SA} . However, the mean values still indicate significant differences in reactivity between the various halocarbons. Because the data included in this calculation represent a wide range of batch and column conditions, they provide a robust starting point for future design of feasibility studies or full-scale remediation applications.

Although the perspective provided by Figures 3.2 and 3.6 allows qualitative conclusions to be drawn about the relative rates of halocarbon degradation by Fe^0 , it is desirable to have a quantitative structure-activity relationship (QSAR) for comparing and predicting values of k_{SA} . Unfortunately, this exercise is limited by the lack of published data for appropriate descriptor variables over the full range of environmentally significant halocarbons. The most satisfactory correlation we found with currently available descriptors uses estimated values of the two-electron reduction potential for hydrogenolysis (Vogel *et al.*, 1987). The average k_{SA} values define a nonlinear but smooth increase in rate with increasing reduction potential, with the exception of four values that appear to be anomalously high (Fig. 3.7). The outliers include the k_{SA} value for TCE that was identified as anomalous in Figure 3.2, and the data for 1,1,1,2-tetrachloroethane, 1,1,2,2-tetrachloroethane, and 1,1,1-trichloroethane reported by Gillham and O'Hannesin (Gillham and O'Hannesin, 1994). When the latter three values were first reported, they were included in a QSAR that was based on estimated potentials for complete hydrogenolysis (i.e., from substrate to the corresponding unhalogenated alkane or alkene). However, a correlation plot of this type using the full set of published kinetic data (not shown), gives a relationship that is even more complex than Figure 3.7. Other modifications that did not improve on Figure 3.7 include (i) separating compounds likely to be reduced by other mechanisms (Roberts *et al.*, 1996), (ii) correlating to potentials for other types of half-reactions, and (iii) correlating to descriptors of physico-chemical properties such as partition coefficients. Thus, it appears that the kinetic data currently available do not provide a sufficient basis for detailed QSAR analysis of dehalogenation rates by iron. The average rate data in Table 3.2 provide a data set that is more robust in a statistical sense, but probably reflects a mixture of rate-limiting mechanisms for loss of halocarbon from solution. Before fully satisfactory QSARs can be achieved, these factors will have to be

resolved by using a rate constant more fundamental than k_{SA} , or using data sets determined under highly controlled conditions specifically for correlation analysis. 62

ACKNOWLEDGMENTS

The authors acknowledge A. Agrawal and L. Matheson for early contributions to the analysis and review of the manuscript. P. Mackenzie, S. O'Hannesin, and J. Vogan also contributed to the analysis. This study was supported in part by the University Consortium Solvents-In-Groundwater Research Program, the National Science Foundation through Award BCS-9212059, and the Petroleum Research Fund through award 29995-AC5.

3.5 LIST OF SYMBOLS

ρ_m	mass concentration (g L^{-1})
ρ_a	surface area concentration ($\text{m}^2 \text{L}^{-1}$)
Γ	surface concentration of reactive sites (mol m^{-2})
a_s	specific surface area ($\text{m}^2 \text{g}^{-1}$)
V_m	maximum reaction rate ($\text{mol L}^{-1} \text{s}^{-1}$)
k_2	second-order reaction rate constant ($\text{L mol}^{-1} \text{hr}^{-1}$)
k_b	backward reaction rate constant (hr^{-1})
k_f	forward reaction rate constant ($\text{L mol}^{-1} \text{hr}^{-1}$)
k_r	reduction reaction rate constant (hr^{-1})
k_{SA}	observed reaction rate (k_{obs}) normalized to surface area ($\text{L m}^{-2} \text{hr}^{-1}$)
k_{obs}	observed pseudo-first-order disappearance rate constant (hr^{-1})
$K_{1/2}$	concentration of P at $V_m/2$ (mol L^{-1})
[P]	molar concentration of substrate (mol L^{-1})

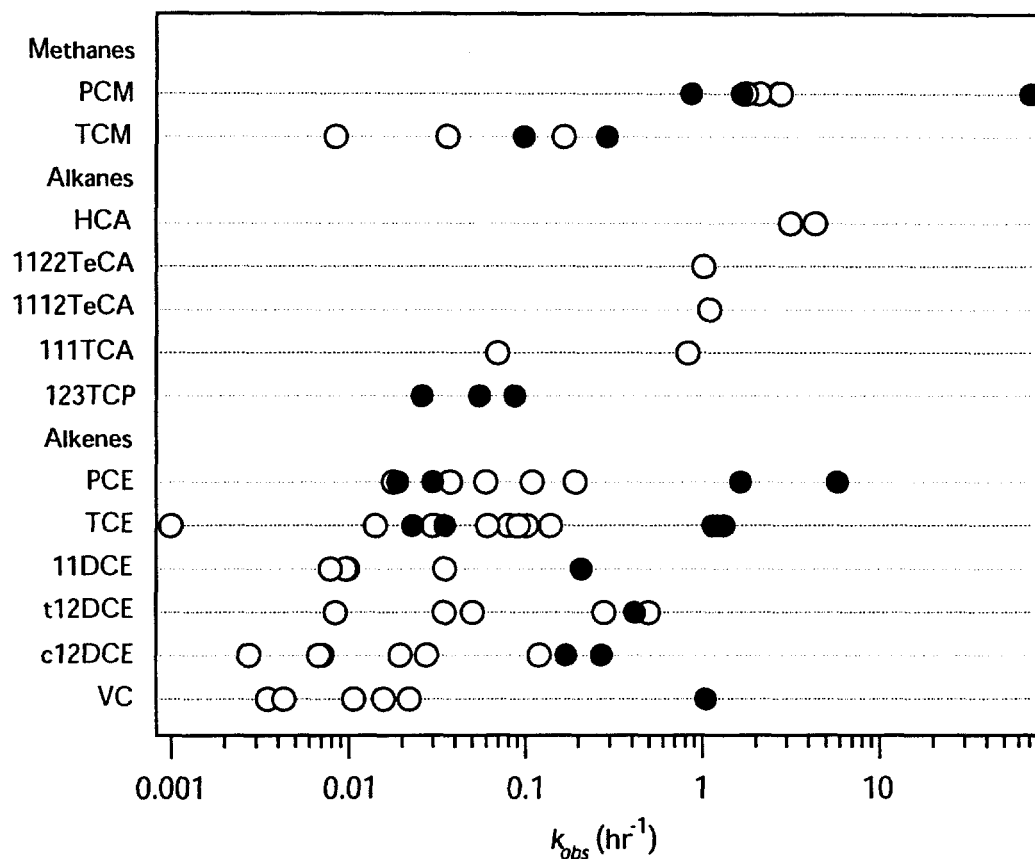


Figure 3.1 Distribution of k_{obs} data from literature data for batch tests (open circles) and column experiments (solid circles). Most values are pseudo-first-order rate constants for halocarbon disappearance from solution. Some values of k_{obs} (Gillham and O'Hannesin, 1994) were derived using t_{50} data (instead of $t_{1/2}$) because they better reflect initial rates. Abbreviations are defined in Table 3.2, and original data are tabulated as Supplemental Material (Tables 3.S1-3.S4).

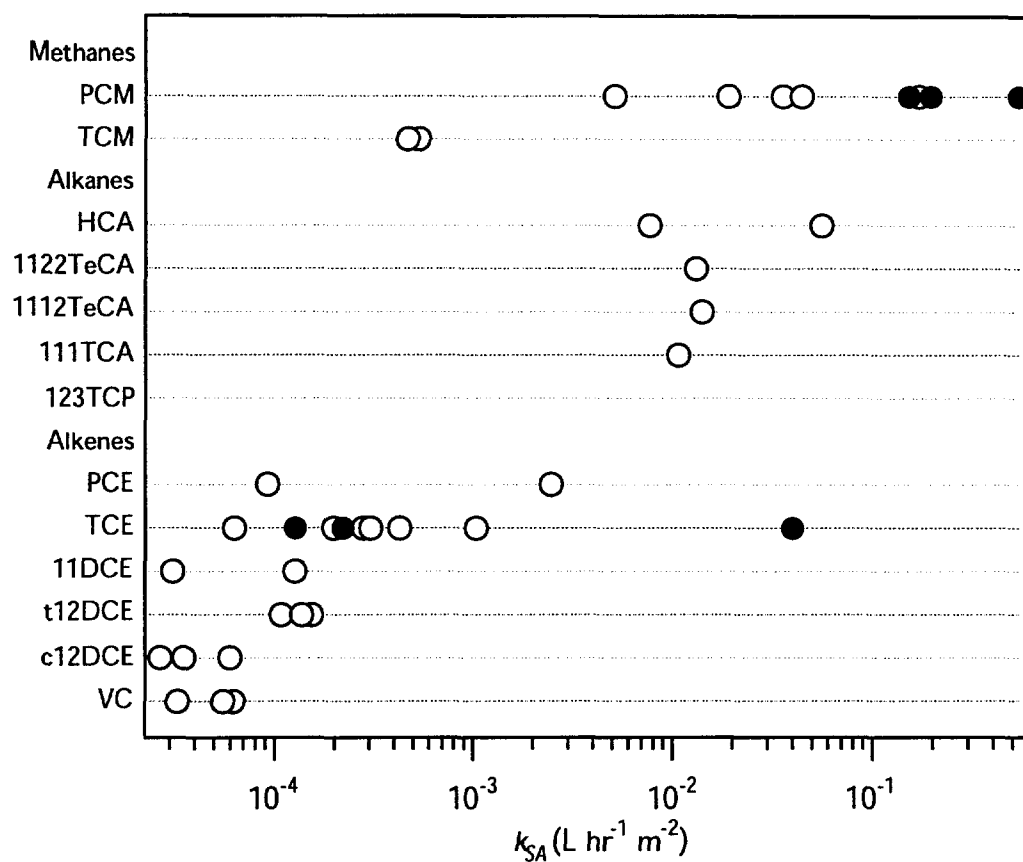


Figure 3.2 Distribution of k_{SA} values derived from literature data. Open circles are for single values of k_{obs} normalized to ρ_a , whereas the solid symbols show values of k_{SA} derived by linear regression on k_{obs} versus $m^2\ L^{-1}\ Fe^0$ (from Figure 3.4 and data in (Gillham and O'Hannesin, 1994; Matheson and Tratnyek, 1994; Sivavec and Horney, 1995)). The outlier among TCE data is from (Gillham and O'Hannesin, 1994). Note that some data shown in Figure 3.1 do not appear in this figure because the necessary information was not available to calculate ρ_a .

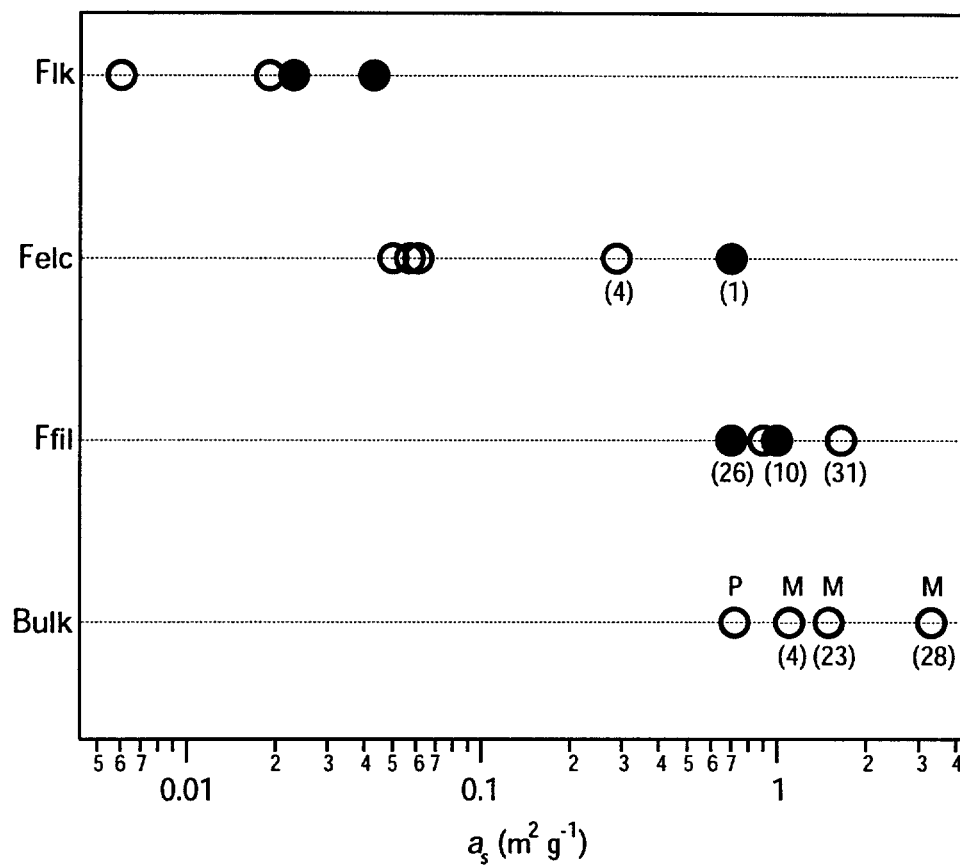


Figure 3.3 Range of specific surface areas, ρ_a , measured by BET gas adsorption. Solid symbols indicate samples that were acid-washed. Numbers refer to references for values taken from the literature, and unnumbered values are from this study. Two types of high-volume commercial grade irons are included under "bulk": M indicates Master Builder, and P indicates Peerless Iron (Detroit, MI, -8 to +16 mesh, surface area of $0.7215 \text{ m}^2 \text{ g}^{-1}$). For other abbreviations, see Table 3.1.

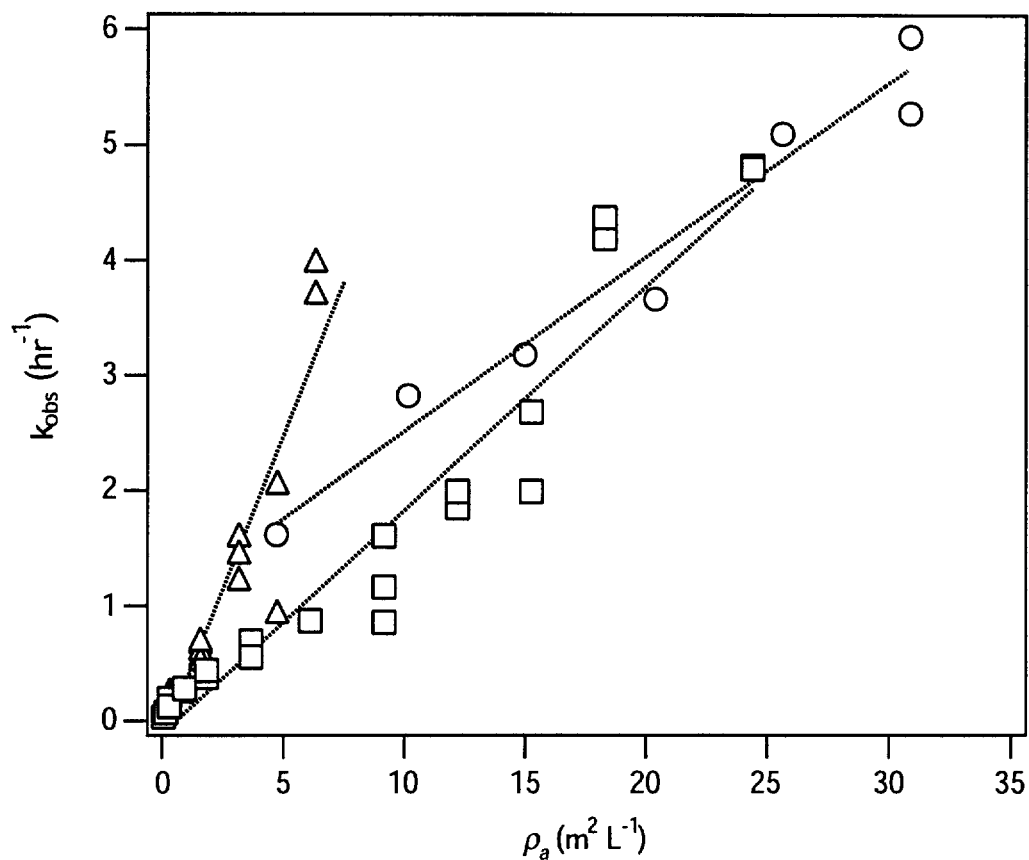


Figure 3.4 Effect of metal pretreatment and medium composition on k_{obs} versus ρ_a data from three batch experiments. (triangles) Untreated Fluka iron, $a_s = 0.019 \text{ m}^2 \text{ g}^{-1}$, carbonate buffer at pH 5.8, $[\text{CCl}_4]_0 = 85 \text{ } \mu\text{M}$, 36 rpm, $k_{SA} = 0.53 \pm 0.06 \text{ L hr}^{-1} \text{ m}^{-2}$. (circles) Acid-washed Fisher iron, $0.7 \text{ m}^2 \text{ g}^{-1}$, unbuffered water, $[\text{CCl}_4]_0 = 170 \text{ } \mu\text{M}$, 15 rpm, $0.15 \pm 0.01 \text{ L hr}^{-1} \text{ m}^{-2}$ (Matheson and Tratnyek, 1994). (squares) Untreated Fisher iron, $0.061 \text{ m}^2 \text{ g}^{-1}$, unbuffered water, $[\text{CCl}_4]_0 = 85 \text{ } \mu\text{M}$, 36 rpm, $0.19 \pm 0.01 \text{ L hr}^{-1} \text{ m}^{-2}$.

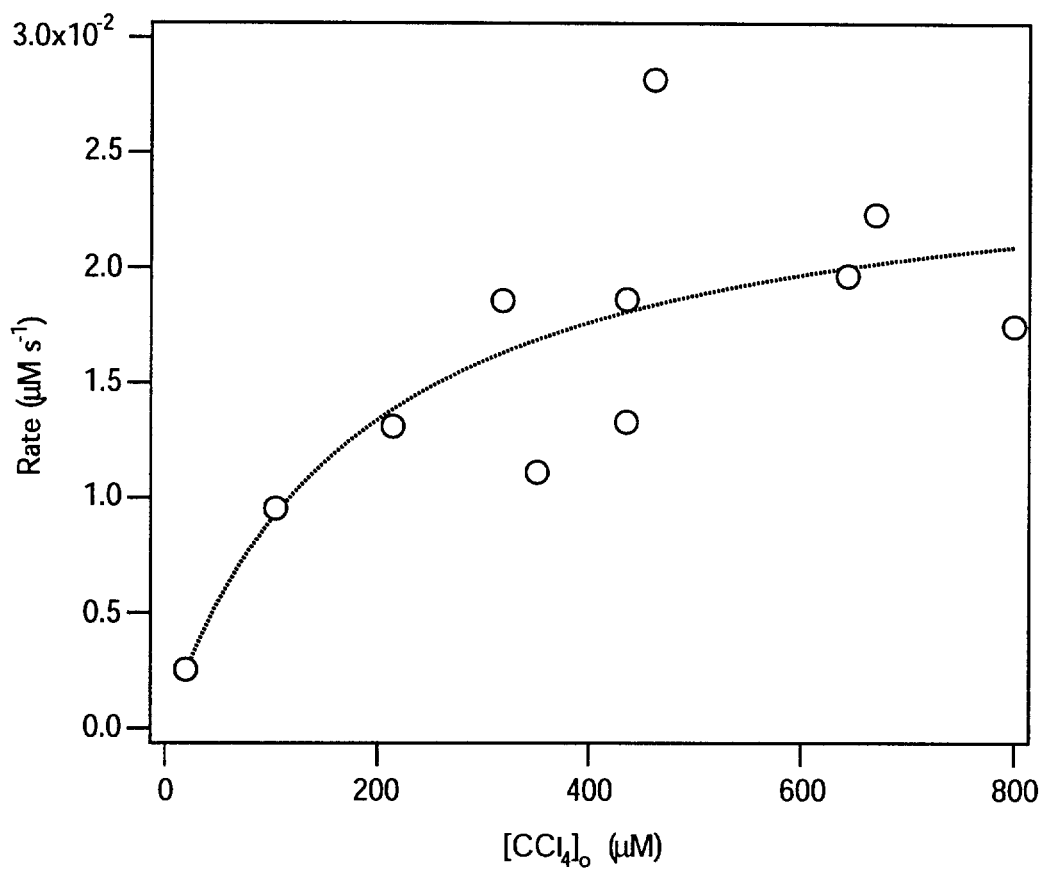


Figure 3.5 Effect of initial CCl_4 concentration on k_{obs} for dechlorination. All experiments were performed in batch systems using Fisher iron (untreated, $\rho_a = 1.02 \text{ m}^2 \text{ L}^{-1}$) in unbuffered medium. Mixing was achieved by rotation at 36 rpm. Curve is fit to eq 3.4 with parameters given in the text.

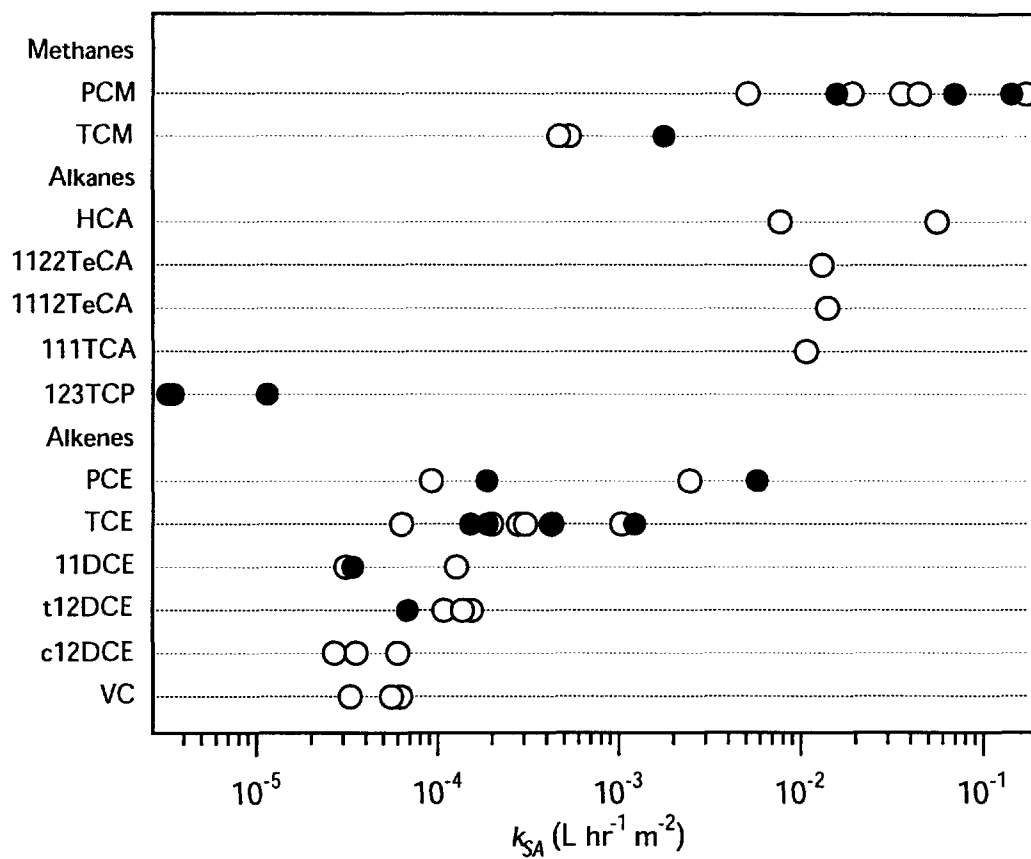


Figure 3.6 Comparison of k_{SA} data obtained from batch tests (open circles) and column studies (solid circles). Batch data are identical to those in Fig. 3.2. Original column data are tabulated as Supplemental Material (Tables 3.S1-3.S4).

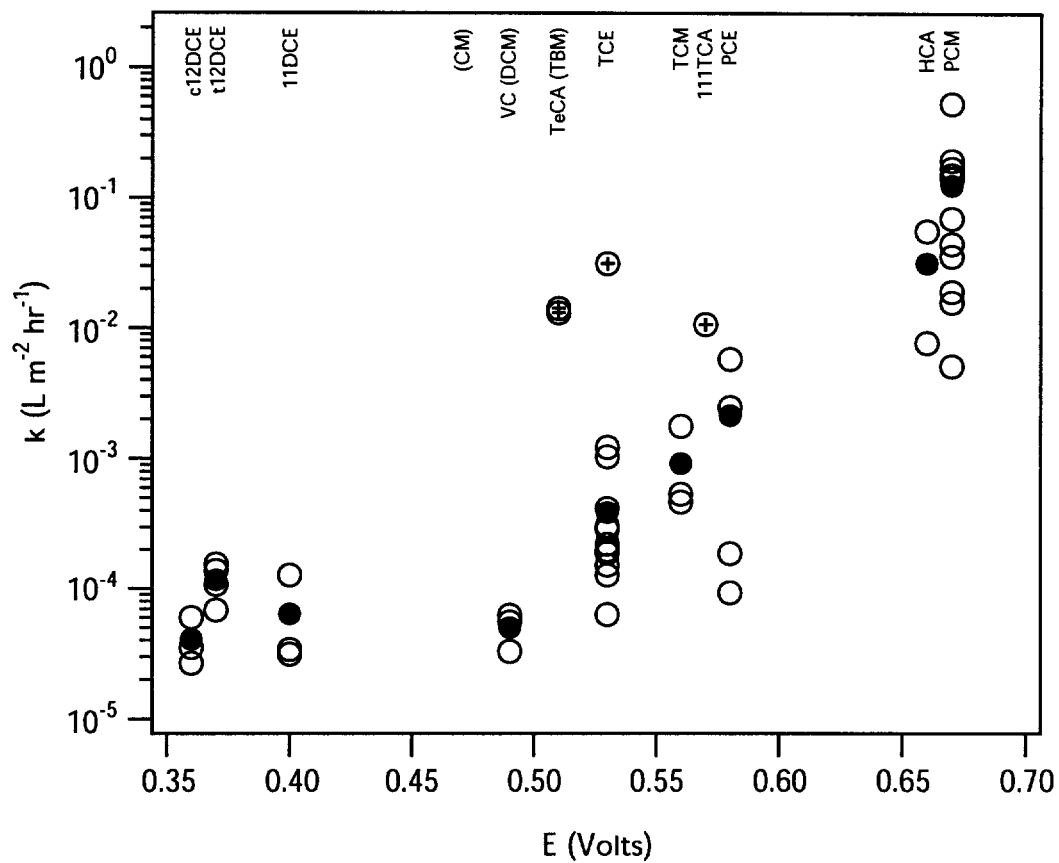


Figure 3.7 Correlation between k_{SA} and two-electron reduction potentials for hydrogenolysis (Perlinger, 1994). Open circles represent individual data, and solid circles indicate the average k_{SA} values reported in Table 3.1. Labels in parenthesis are for halocarbons discussed in the text, but for which data do not appear on the plot.

TABLE 3.1 EXPERIMENTAL CONDITIONS

Source of Iron	Grain Size (mm)	Surface Area m ² /g	Mixing	Initial Condition	pH	Reference
Master Builder (MBcs)	0.43	--	--	aerobic	6.2-9.2	(Clausen <i>et al.</i> , 1995)
Master Builder (MBfn)	0.23	3.3	150 cm/d	aerobic	--	(Focht, 1994)
Fisher filings (Ffil)	0.15	--	2 rpm	aerobic	constant ¹	(Gillham and O'Hannesin, 1992)
Fisher Electrolytic (Felc)	0.15	0.287	2 rpm	aerobic	7.2-9.2 ¹	(Gillham and O'Hannesin, 1994)
Aldrich (Ald1)	0.10	2.4	mag stir	aer/anaer	7.7 ²	(Helland <i>et al.</i> , 1995)
EM Science (EMS)	0.15	0.14	30 cm/d	anaerobic	7-9 ²	(Johnson and Tratnyek, 1994)
Felc	0.15	0.0567	30 cm/d	anaerobic	5-9 ²	Johnson, unpublished
Ffil	0.43	1.635	--	--	6.5 ¹	(Liang and Goodlaxson, 1995)
Felc	<0.1 ₅	--	170 spm ⁴	aerobic	6-12 ⁵	(Lipczynska-Kochany <i>et al.</i> , 1994)
VWR	--	--	6500 cm/d	aerobic	7-8 ¹	(Mackenzie <i>et al.</i> , 1995b)
Felc	0.15	0.70	15 rpm	anaerobic	5-8 ^{2,3}	(Matheson and Tratnyek, 1994)
Electrolytic	<0.1 ₅	--	--	aerobic	7-10.5	(Milburn <i>et al.</i> , 1995)
Kanmet Casting (KC)	--	--	2 rpm	aerobic	7.1-9.0	(O'Hannesin, 1993)
Felc	0.15	0.20	36 rpm	anaerobic	6-9	(Scherer and Tratnyek, 1995)
Johnson Matthey (JM)	0.10	--	--	anaerobic	7.2-8.5 ³	(Schreier and Reinhard, 1995)
Kishida Elec (Kelc)	0.075	--	--	anaerobic	--	(Senzaki and Yasuo, 1989)
VWR	--	1.24	--	aer/anaer	init 7	(Sivavec and Horney, 1995)
MBcs	0.43	--	47 cm/d	aerobic	--	(Vogan <i>et al.</i> , 1995)

¹carbonate buffer²deionized water³Goods Buffers⁴shakes per minute⁵sulfur bearing compounds

TABLE 3.2 REPRESENTATIVE KINETIC DATA FOR DEHALOGENATION BY IRON METAL

Halocarbon	Abbreviation	k_{SA} (L m ⁻² hr ⁻¹)	n (batch/ regression/ column) ¹
Tetrachloromethane	PCM	(1.2±1.5) x 10 ⁻¹	5/3/3
Trichloromethane	TCM	(9.2±7.3) x 10 ⁻⁴	2/0/1
Tribromomethane	TBM	1.7 x 10 ⁻²	1/0/0
Hexachloroethane	HCA	(3.1±3.3) x 10 ⁻²	2/0/0
1,1,2,2-Tetrachloroethane	1122TeCA	1.3 x 10 ⁻²	1/0/0
1,1,1,2-Tetrachloroethane	1112TeCA	1.4 x 10 ⁻²	1/0/0
1,1,1-Trichloroethane	111TCA	1.1 x 10 ⁻²	1/0/0
1,2,3-Trichloropropane	123TCP	(6.1±4.7) x 10 ⁻⁶	0/0/3
Tetrachloroethene	PCE	(2.1±2.7) x 10 ⁻³	2/0/2
Trichloroethene	TCE	(3.9±3.6) x 10 ⁻⁴	6/2/4
1,1-Dichloroethene	11DCE	(6.4±5.5) x 10 ⁻⁵	2/0/1
t-1,2-Dichloroethene	t12DCE	(1.2±0.4) x 10 ⁻⁴	3/0/1
c-1,2-Dichloroethene	c12DCE	(4.1±1.7) x 10 ⁻⁵	3/0/0
Vinyl Chloride	VC	(5.0±1.5) x 10 ⁻⁵	3/0/0

¹Number of data points included in the average k_{SA} value. Batch data and column data are from individual concentration versus time profiles, whereas regression data refer to slopes from k_{obs} versus ρ_a plots. All were weighted equally.

TABLE 3.S1 BATCH DATA FOR HALOGENATED ALKANE REDUCTION

Haloalkane	Source Fe ⁰	Fe ⁰ (m ² /L)	C ₀ (mg/L)	k _{obs} (1/hr)	Half-Life (hr)	Reference
PCM	Felc	15.9	23.254	2.70	0.26	(Matheson and Tratnyek, 1994)
	Felc	78	1.631	2.77	0.25	(Gillham and O'Hannesin, 1994)
	Elc	--	--	1.73	0.40	(Milburn <i>et al.</i> , 1995)
	Ald1	90.5	0.5	1.72	0.40	(Helland <i>et al.</i> , 1995)
	Felc	17	65	0.15	4.62	(Scherer and Tratnyek, 1995)
	Ffil	410	1.630	2.10	0.33	(Gillham and O'Hannesin, 1992)
	Felc	40	1.108	1.77	0.39	(Lipczynska-Kochany <i>et al.</i> , 1994)
TCM	Felc	15.9	12.680	0.0085	81.9	(Matheson and Tratnyek, 1994)
	Felc	78	2.013	0.036	19.1*	(Gillham and O'Hannesin, 1994)
	KC	--	2.845	0.165	4.2	(O'Hannesin, 1993)
DCM	Felc	15.9	4.400	no deg	--	(Matheson and Tratnyek, 1994)
	Felc	78	2.751	no deg	--	(Gillham and O'Hannesin, 1994)
TBM	Felc	78	2.120	1.33	0.52*	(Gillham and O'Hannesin, 1994)
HCA	Felc	78	3.621	4.33	0.16*	(Gillham and O'Hannesin, 1994)
	Ffil	410	3.620	3.15	0.22	(Gillham and O'Hannesin, 1992)
1122TeCA	Felc	78	2.513	1.02	0.68*	(Gillham and O'Hannesin, 1994)
1112TeCA	Felc	78	2.334	1.1	0.63*	(Gillham and O'Hannesin, 1994)
111TCA	Felc	78	0.68	0.835	0.83*	(Gillham and O'Hannesin, 1994)
	JM	--	1.334	0.07	10	(Schreier and Reinhard, 1994)

TABLE 3.S2 BATCH DATA FOR HALOGENATED ALKENE REDUCTION

Haloalkene	Source Fe ⁰	Fe ⁰ (m ² /L)	C ₀ (mg/L)	k _{obs} (1/hr)	Half-Life (hr)	Reference
PCE	Felc	78	2.246	0.192	3.6*	(Gillham and O'Hannesin, 1994)
	Ffil	410	2.25	0.038	18.3	(Gillham and O'Hannesin, 1992)
	JM	--	1.658	0.018	38	(Schreier and Reinhard, 1994)
	JM	--	1.658	0.0379	18.3	(Schreier and Reinhard, 1995)
	KC	--	1.981	0.060	11.5	(O'Hannesin, 1993)
TCE	Kelc	--	0.065	0.11	6.3	(Senzaki and Yasuo, 1989)
	Felc	78	1.555	0.0806	8.6*	(Gillham and O'Hannesin, 1994)
	Felc	15.9	--	0.001	840	(Matheson and Tratnyek, 1994)
	KC	--	2.350	0.102	6.8	(O'Hannesin, 1993)
	Ffil	327	10.25	0.139	5.0	(Liang <i>et al.</i> , 1995)
	Ffil	327	3.5	0.0931	7.41	(Liang and Goodlaxson, 1995)
	VWR	310	25.5	0.0613	11.3	(Sivavec and Horney, 1995)
	VWR	100	25.5	0.0304	22.8	(Sivavec and Horney, 1995)
	JM	--	1.31	0.0142	48.8	(Schreier and Reinhard, 1995)
	MB	--	3.25	0.030	23	(Clausen <i>et al.</i> , 1995)
11DCE	Felc	78	2.333	0.010	70*	(Gillham and O'Hannesin, 1994)
	JM	--	0.97	0.035	20	(Schreier and Reinhard, 1994)
	JM	--	0.97	0.0096	72.2	(Schreier and Reinhard, 1995)
	VWR	254	22.2	0.0079	87.7	(Sivavec and Horney, 1995)

TABLE 3.S2 CONT. BATCH DATA FOR HALOGENATED ALKENE REDUCTION

Halo-alkene	Source Fe ⁰	Fe ⁰ (m ² /L)	C ₀ (mg/L)	k _{obs} (1/hr)	Half-Life (hr)	Reference
t12DCE	Felc	78	1.774	0.008	82*	(Gillham and O'Hannesin, 1994)
	Ffil	327	2.6	0.0504	13.7	(Liang and Goodlaxson, 1995)
	JM	--	0.97	0.0208	33.3	(Schreier and Reinhard, 1995)
	Elec	--	--	0.28	2.5	(Milburn <i>et al.</i> , 1995)
	VWR	254	21.8	0.0349	19.8	(Sivavec and Horney, 1995)
c12DCE	Felc	78	1.949	0.0028	252*	(Gillham and O'Hannesin, 1994)
	Ffil	327	2.8	0.0196	35.2	(Liang and Goodlaxson, 1995)
	JM	--	0.97	0.0071	97.6	(Schreier and Reinhard, 1995)
	MB	--	3.25	0.0277	25.0	(Clausen <i>et al.</i> , 1995)
	elec	--	--	0.12	6.0	(Milburn <i>et al.</i> , 1995)
	VWR	254	22.4	0.0068	101.5	(Sivavec and Horney, 1995)
VC	VWR	254	22.0	0.0158	43.9	(Sivavec and Horney, 1995)
	Ffil	327	1.56	0.0107	64.7	(Liang and Goodlaxson, 1995)
	MB	--	3.25	0.0035	>200	(Clausen <i>et al.</i> , 1995)
	JM	--	0.62	0.0221	31.4	(Schreier and Reinhard, 1995)
	Felc	78	3.663	0.0043	160.6*	(Gillham and O'Hannesin, 1994)

TABLE 3.S3 COLUMN DATA FOR HALOGENATED ALKANE REDUCTION

Haloalkane	Source Fe ⁰	Fe ⁰ (m ² /L)	C ₀ (mg/L)	Avg v (cm/d)	k _{obs} (1/hr)	Half-Life (hr)	Reference
PCM	EMS	55.4	200	30	0.87	<0.8	(Johnson and Tratnyek, 1994)
	Felc	1000	--	1019	69.3	<.01*	(Gillham and O'Hannesin, 1994)
	Felc	11.8	258	30	1.67	0.42	Johnson, unpublished
TCM	KC	--	45	32	0.29	2.4	(O'Hannesin, 1993)
	EMS	55.4	200	30	0.098	6.8	(Johnson and Tratnyek, 1994)
	Felc	11.8	50	30	no deg	--	Johnson, unpublished
DCM	EMS	55.4	30	30	no deg	--	(Johnson and Tratnyek, 1994)
123TCP	MB	8000	48	30	0.026	26.8	(Focht, 1994)
	MB	7580	54	60	0.087	8.0	(Focht, 1994)
	MB-fine	15750	54	50	0.055	12.6	(Focht, 1994)

TABLE 3.S4 COLUMN DATA FOR HALOGENATED ALKENE REDUCTION

Halo-alkene	Source Fe ⁰	Fe ⁰ (m ² /L)	C ₀ (mg/L)	Avg v (cm/d)	k _{obs} (1/hr)	Half-Life (hr)	Reference
PCE	KC	--	16.3	32	0.030	23.5	(O'Hannesin, 1993)
	KC	--	16.0	19	0.019	37	(O'Hannesin, 1993)
	Felec	1000	--	--	5.78	0.12*	(Gillham and O'Hannesin, 1994)
	MB	8800	4.4	47	1.65	0.42	(Gillham and O'Hannesin, 1994)
TCE	EMS	55.4	8.0	30	0.023	30.1	(Johnson and Tratnyek, 1994)
	KC	--	24.58	32	0.035	19.7	(O'Hannesin, 1993)
	MB	8800	9.00	47	1.33	0.52	(Gillham and O'Hannesin, 1994)
	VWR	6121	7.1	1158	1.15	0.60	(Mackenzie <i>et al.</i> , 1995b)
	Felc	1000	--	--	1.22	0.57*	(Gillham and O'Hannesin, 1994)
11DCE	VWR	6121	2.2	1158	0.208	3.33	(Mackenzie <i>et al.</i> , 1995b)
t12DCE	VWR	6121	1.9	1158	0.417	1.66	(Mackenzie <i>et al.</i> , 1995b)
c12DCE	VWR	--	1.0	30.5	0.17	4.0	(Mackenzie <i>et al.</i> , 1995a)
	MBcs	--	0.450	47	0.27	2.6	(Vogan <i>et al.</i> , 1995)
VC	MBcs	--	0.014	47	0.66	1.05	(Vogan <i>et al.</i> , 1995)

3.6 REFERENCES

- Agrawal, A., and P. G. Tratnyek. 1996. Reduction of nitro aromatic compounds by zero-valent iron metal. *Environ. Sci. Technol.* 30(1): 153-160.
- Burris, D. R., T. J. Campbell, and V. S. Manoranjan. 1995. Sorption of trichloroethylene and tetrachloroethylene in a batch reactive metallic iron-water system. *Environ. Sci. Technol.* 29(11): 2850-2855.
- Clausen, J. L., W. L. Richards, N. L. Korte, and L. Liang. 1995. ORNL/MMES research into remedial applications of zero-valence metals: 3) Removal of TCE, cis-1,2-DCE, vinyl chloride, and technetium. *209th National Meeting ACS. Preprint Extended Abstracts, Division of Environmental Chemistry*. Anaheim, CA. Vol. 35, No. 1, pp 755-758.
- Everett, D. H., G. D. Parfitt, K. S. W. Sing, and R. Wilson. 1974. The SCI/IUPAC/NPL project on surface area standards. *J. App. Chem. and Biotechnol.* 24: 199-219.
- Focht, M. R. 1994. *Bench-scale treatability testing to evaluate the applicability of metallic Iron for above-ground remediation of 1,2,3-trichloropropane contaminated groundwater*. M.S. Thesis, University of Waterloo.
- Gillham, R. W. 1996. In situ treatment of groundwater: Metal-enhanced degradation of chlorinated organic contaminants. *Recent Advances in Ground-Water Pollution Control and Remediation*, A NATO Advanced Study Institute. Kemer, Antalya, Turkey. pp 249-274.
- Gillham, R. W., and S. F. O'Hannesin. 1992. Metal-catalysed abiotic degradation of halogenated organic compounds. *IAH Conference, Modern Trends in Hydrogeology*. Hamilton, Ontario, Canada. pp 94-103.
- Gillham, R. W., and S. F. O'Hannesin. 1994. Enhanced degradation of halogenated aliphatics by zero-valent iron. *Ground Water* 32(6): 958-967.
- Gillham, R. W., S. F. O'Hannesin, and W. S. Orth. 1993. Metal enhanced abiotic degradation of halogenated aliphatics: Laboratory tests and field trials. *Proceedings of the 6th Annual Environmental Management and Technical Conference/HazMat Central Conference*, Rosemont, IL. pp. 440-461.
- Gould, J. P. 1982. The kinetics of hexavalent chromium reduction by metallic iron. *Water Res.* 16: 871-877.
- Helland, B. R., P. J. J. Alvarez, and J. L. Schnoor. 1995. Reductive dechlorination of carbon tetrachloride with elemental iron. *J. Haz. Mat.* 41(2-3): 205-216.
- Hochella, M. F., Jr. 1990. Atomic structure, microtopography, composition, and reactivity of mineral surfaces. In : M. F. Hochella, Jr. and A. F. White (ed.), *Mineral-Water Interface Geochemistry. Reviews in Mineralogy*, Mineralogical Society of America, Washington, DC, Vol. 23, pp 87-132.

- Johnson, T. L., and P. G. Tratnyek. 1994. A column study of carbon tetrachloride dehalogenation by iron metal. *Proceedings of the 33rd Hanford Symposium on Health & the Environment—In Situ Remediation: Scientific Basis for Current and Future Technologies*. Pasco, WA. Vol. 2, pp 931-947.
- Liang, L., and J. D. Goodlaxson. 1995. Kinetics and byproducts of reductive dechlorination of ground water TCE with zero-valence iron. *Emerging Technologies in Hazardous Waste Management VII, Extended Abstracts for the Special Symposium*. Atlanta, GA. pp 46-49.
- Liang, L., J. D. Goodlaxson, N. E. Korte, J. L. Clausen, and D. T. Davenport. 1995. ORNL/MMES research into remedial applications of zero-valence metals. 1: Laboratory analysis of reductive dechlorination of trichloroethene. *209th National Meeting ACS. Preprint Extended Abstracts, Division of Environmental Chemistry*. Anaheim, CA. Vol. 35, No. 1, pp 728-731.
- Lipczynska-Kochany, E., S. Harms, R. Milburn, G. Sprah, and N. Nadarajah. 1994. Degradation of carbon tetrachloride in the presence of iron and sulphur containing compounds. *Chemosphere* 29(7): 1477-1489.
- Mackenzie, P. D., S. S. Baghel, G. R. Eykholt, D. P. Horney, J. J. Salvo, and T. M. Sivavec. 1995a. Pilot-scale demonstration of chlorinated ethene reduction by iron metal: Factors affecting lifetime. *Emerging Technologies in Hazardous Waste Management VII, Extended Abstracts for the Special Symposium*. Atlanta, GA. pp 59-62.
- Mackenzie, P. D., S. S. Baghel, G. R. Eykholt, D. P. Horney, J. J. Salvo, and T. M. Sivavec. 1995b. Pilot-scale demonstration of reductive dechlorination of chlorinated ethenes by iron metal. *209th National Meeting ACS. Preprint Extended Abstracts, Division of Environmental Chemistry*. Anaheim, CA. Vol. 35, No. 1, pp 796-799.
- Matheson, L. J., and P. G. Tratnyek. 1994. Reductive dehalogenation of chlorinated methanes by iron metal. *Environ. Sci. Technol.* 28(12): 2045-2053.
- Milburn, R., S. Harms, E. Lipczynska-Kochany, C. Ravary, and G. Sprah. 1995. Iron (Fe(0)) induced dehalogenation of polychlorinated aliphatic compounds. *209th National Meeting ACS. Preprint Extended Abstracts, Division of Environmental Chemistry*. Anaheim, CA. Vol. 35, No. 1, pp 822-824.
- O'Hannesin, S. F. 1993. *A Field Demonstration of a Permeable Reaction Wall for the In Situ Abiotic Degradation of Halogenated Aliphatic Organic Compounds*. M.S. Thesis, University of Waterloo, Ontario.
- Orth, W. S. 1993. *Mass Balance of the Degradation of Trichloroethylene in the Presence of Iron Filings*. M.S. Thesis, University of Waterloo, Ontario.
- Perlinger, J. A. 1994. *Reduction of Polyhalogenated Alkanes by Electron Transfer Mediators in Aqueous Solution*. Ph.D. Dissertation, Swiss Federal Institute of Technology Zürich.
- Reardon, E. J. 1995. Anaerobic corrosion of granular iron: Measurement and interpretation of hydrogen evolution rates. *Environ. Sci. Technol.* 29(12): 2936-2945.
- Roberts, A. L., L. A. Totten, W. A. Arnold, D. R. Burris, and T. J. Campbell. 1996.

- Reductive elimination of chlorinated ethylenes by zero-valent metals. *Environ. Sci. Technol.* 30(8): 2654-2659.
- Rothenberg, S. J., D. K. Flynn, A. F. Eidson, J. A. Mewhinney, and G. J. Newton. 1987. Determination of specific surface area by krypton adsorption, comparison of three different methods of determining surface area, and evaluation of different surface area standards. *J. Colloid and Interface Sci.* 116: 541-554.
- Scherer, M. M., and P. G. Tratnyek. 1995. Dechlorination of carbon tetrachloride by iron metal: Effect of reactant concentrations. *209th National Meeting ACS. Preprint Extended Abstracts, Division of Environmental Chemistry.* Anaheim, CA. Vol. 35, No. 1, pp 805-806.
- Schreier, C. G., and M. Reinhard. 1994. Transformation of chlorinated organic compounds by iron and manganese powders in buffered water and in landfill leachate. *Chemosphere* 29(8): 1743-1753.
- Schreier, C. G., and M. Reinhard. 1995. Transformation of chlorinated ethylenes by iron powder in 4-(2-Hydroxyethyl)-1-Piperazineethanesulfonic Acid (HEPES) buffer. *209th National Meeting ACS. Preprint Extended Abstracts, Division of Environmental Chemistry.* Anaheim, CA. Vol. 35, No. 1, pp 833-835.
- Senzaki, T., and K. Yasuo. 1989. Removal of chlorinated organic compounds from wastewater by reduction process. II. Treatment of trichloroethylene with iron powder. *Kogyo Yosui* 369: 19-25.
- Siantar, D. P., C. G. Schreier, and M. Reinhard. 1995. Transformation of the pesticide 1,2-dibromo-3-chloropropane (DBCP) and nitrate by iron powder and by $H_2/Pd/Al_2O_3$. *209th National Meeting ACS. Preprint Extended Abstracts, Division of Environmental Chemistry.* Anaheim, CA. Vol. 35, No. 1, pp 745-748.
- Sivavec, T. M., and D. P. Horney. 1995. Reductive dechlorination of chlorinated ethenes by iron metal. *209th National Meeting ACS. Preprint Extended Abstracts, Division of Environmental Chemistry.* Anaheim, CA. Vol. 35, No. 1, pp 695-698.
- Tratnyek, P. G., T. L. Johnson, and A. Schattauer. 1995. Interfacial phenomena affecting contaminant remediation with zero-valent iron metal. *Emerging Technologies in Hazardous Waste Management VII.* Atlanta, GA. pp 589-592.
- Vogan, J. L., R. W. Gillham, S. F. O'Hannesin, and W. H. Matulewicz. 1995. Site specific degradation of VOCs in groundwater using zero valent iron. *209th National Meeting ACS. Preprint Extended Abstracts, Division of Environmental Chemistry.* Anaheim, CA. Vol. 35, No. 1, pp 800-804.
- Vogel, T. M., C. S. Criddle, and P. L. McCarty. 1987. Transformations of halogenated aliphatic compounds. *Environ. Sci. Technol.* 21(8): 722-736.
- White, A. F., and M. L. Peterson. 1990. Role of reactive-surface-area characterization in geochemical kinetic models. In : Melchior (ed.), *Chemical Modeling of Aqueous Systems II.* ACS Symposium Series, American Chemical Society, Washington, DC, pp. 461-475.

- Young, F. W., Jr., and L. D. Hulett. The role of crystal imperfections in the chemical reactivity of copper surfaces. *In* : W. D. Robertson and N. A. Gjostein (ed.), *Metal Surfaces: Structure, Energetics and Kinetics*. American Society for Metals, Metals Park, OH, pp. 375-400.
- Zepp, R. G., and N. L. Wolfe. 1987. Abiotic transformation of organic chemicals at the particle-water interface. *In* : W. Stumm (ed.), *Aquatic Surface Chemistry: Chemical Processes at the Particle-Water Interface*. Wiley, New York, pp. 423-455.

Chapter 4

Degradation of Carbon Tetrachloride by Iron Metal: Complexation Effects on the Oxide Surface¹

4.1 ABSTRACT

Dehalogenation of chlorinated aliphatic contaminants at the surface of zero-valent iron metal (Fe^0) is mediated by the thin film of iron (hydr)oxides found on Fe^0 under environmental conditions. To evaluate the role this oxide film plays in the reduction of chlorinated methanes, carbon tetrachloride (CCl_4) degradation by Fe^0 was studied under the influence of various anions, ligands, and initial CCl_4 concentrations ($[\text{P}]_0$). Over the range of conditions examined in these batch experiments, the reaction kinetics could be characterized by surface-area-normalized rate constants that were pseudo-first order for CCl_4 disappearance (k_{CCl_4}), and zero order for the appearance of dissolved Fe^{2+} ($k_{\text{Fe}^{2+}}$). The rate of dechlorination exhibits saturation kinetics with respect to $[\text{P}]_0$, suggesting that CCl_4 is transformed at a limited number of reactive surface sites. Because oxidation of Fe^0 by CCl_4 is the major corrosion reaction in these systems, $k_{\text{Fe}^{2+}}$ also approaches a limiting value at high CCl_4 concentrations. The adsorption of borate strongly inhibited reduction of CCl_4 , but a concomitant addition of chloride partially offset this effect by destabilizing the film. Redox active ligands (catechol and ascorbate), and those that are not redox active (EDTA and acetate), all decreased k_{CCl_4} (and $k_{\text{Fe}^{2+}}$). Thus, it appears that the relatively strong complexation of these ligands at the oxide-electrolyte interface blocks the sites where weak interactions with the metal oxide lead to dehalogenation of chlorinated aliphatic compounds.

¹Johnson, T. L., W. Fish, Y. A. Gorby, and P. G. Tratnyek. 1997. Degradation of carbon tetrachloride by iron metal: Complexation effects on the oxide surface. *Journal of Contaminant Hydrology*. In press.

4.2 INTRODUCTION

In the subsurface environment, heterogeneous chemical reactions characteristically depend on properties of the particle-water interface. One reaction of this type—of current interest in groundwater remediation—is the dehalogenation of chlorinated aliphatic contaminants by treatment with zero-valent iron metal (Fe^0) (Gillham, 1996; Tratnyek, 1996). The reaction involves corrosion of the metal coupled to the dechlorination of organic contaminant, as illustrated in Figure 4.1. Corrosion of Fe^0 involves both oxidation-reduction reactions (where $\text{Fe}^0 \rightarrow \text{Fe}^{2+} + 2\text{e}^-$ is the primary anodic half-reaction) and coordination processes (such as hydration and dissolution of Fe^{2+}) (Sato, 1989). The reduction of chlorinated solvents by Fe^0 provides a favorable cathodic reaction (e.g., $\text{CCl}_4 + \text{H}^+ + 2\text{e}^- \rightarrow \text{CHCl}_3 + \text{Cl}^-$) which drives the overall process and results in contaminant degradation. Thus, much of what has been learned about metal corrosion rates as part of efforts to limit material damage (Shoesmith, 1987) applies in the present context where dehalogenation of contaminants is the desired effect of corrosion.

An important factor influencing corrosion of Fe^0 is the oxide film that forms on the metal surface. Since iron (hydr)oxides will be ubiquitous on Fe^0 under subsurface conditions, it has been suggested that they may play a role in mediating dechlorination (Johnson and Tratnyek, 1995; Klausen et al., 1995; Sivavec and Horney, 1997; Sivavec et al., 1995). This hypothesis is represented in Figure 4.1 for reductive dechlorination of CCl_4 . The structure and mineralogy of the (hydr)oxide film can be complex and variable (Graham et al., 1990; Ho and Ord, 1973; Oblonsky and Devine, 1995; Uhlig, 1979), but its presence generally inhibits corrosion (i.e., passivates the metal). Eventually, a steady state may be reached in which the thickness of the passive film is governed by a balance of film dissolution and corrosion of Fe^0 to form new (hydr)oxide. Dissolution of iron (hydr)oxides on Fe^0 is analogous to that of other iron oxides in geological systems and should be subject to similar controls (Sinniger, 1992; Stumm et al., 1990).

One of the most successful explanations of the factors controlling metal oxide dissolution is the surface complexation model (SCM) of ligand attachment to metal oxide surfaces (Blesa et al., 1994; Dzombak and Morel, 1990; Stumm, 1992). The SCM describes ionic adsorption as the formation of complexes between solution ions and surface sites. Cations coordinate to surface (hydr)oxide ligands and anions exchange with surface (hydr)oxide ligands to coordinate with oxide-matrix metal ions. A finite density of coordination sites is presumed to exist on the oxide, so site saturation is approached asymptotically with increasing concentration of adsorbate in the system. Stumm and coworkers (Furrer and Stumm, 1986; Wieland et al., 1988; Zinder et al., 1986) have

shown that metal-oxide dissolution rates depend on the chemical speciation of the oxide surface, which in turn, can be predicted from the solution composition. For example, some adsorbed ligands promote the dissolution of metal oxides, while other ligands are “non-promoting” and block dissolution. A quantitative SCM can be used to calculate the relative fraction of surface sites bound to each type of ligand when appropriate equilibrium constants are available. The rate of dissolution is directly proportional to the fraction of sites occupied by dissolution-promoting ligands. In addition to its geochemical applications, the SCM can be used to relate solution composition to the dissolution rate of passive films coating Fe^0 or other corroding metals (Blesa et al., 1994; Sinniger, 1992; Stumm et al., 1990).

In this study, we have applied insights derived from the SCM to further our understanding of contaminant dechlorination at the oxide film on iron metal surfaces under conditions of groundwater remediation. The kinetics of CCl_4 reduction and Fe^{2+} production have been used to probe various surface complexation effects, ranging from the weak interactions of chlorinated solvents with the oxide surface, to the effects of strong ligands such as EDTA. The observed effects of solute complexation indicate that the oxide film mediates contaminant reduction by Fe^0 . The findings improve our understanding of how groundwater solutes may influence treatment zone performance, and clarify the relationship between remediation technologies based on zero-valent metals and those based on other means of generating strongly reducing sites on subsurface materials.

4.3 EXPERIMENTAL INFORMATION

4.3.1 Chemicals and Solutions. Most experiments were buffered at pH 6.2 with 10 mM HEPES (N-(2-hydroxyethyl)-piperazine-N'-(2-ethanesulfonic acid) from Sigma) made with deoxygenated, deionized water. HEPES was selected to minimize complexation reactions involving the buffer (Good and Izawa, 1968). The solution was stored in an anaerobic glove box ($[\text{O}_2] < 1$ ppm, $[\text{H}_2] = 4$ ppm) for at least 24 h before use. CCl_4 (HPLC grade, Aldrich) was used as received. Aqueous CCl_4 stock solutions were prepared by allowing 2 mL of organic phase to equilibrate with 100 mL of 10 mM deoxygenated HEPES solution in an anaerobic chamber. Borate buffer was prepared by titrating a solution of H_3BO_3 with $\text{Na}_2\text{B}_4\text{O}_7$ to pH 8.4. Granular zero-valent iron from Fluka (>99.9%, Cat. No. 44905) was sieved to isolate the 18-40 mesh size and then used without further treatment (i.e., with the existing air-formed oxide film intact). The BET surface area of this material was $0.019 \text{ m}^2 \text{ g}^{-1}$ (Johnson et al., 1996).

4.3.2 Batch Systems. Reaction kinetics were determined in 12 mL serum vials containing 0.500 ± 0.002 g Fe^0 (surface area concentration $\rho_a = 0.79 \text{ m}^2 \text{ L}^{-1}$). In the anaerobic chamber, vials were spiked with 200 μL of CCl_4 -saturated stock solution ($[\text{P}]_0 = 0.085 \text{ mM}$), treated with varying amounts of ligand or other ion stock solutions, filled with HEPES buffer (i.e., no head space), and crimp-sealed using Hycar septa (Pierce). During the reaction, the vials were mixed on a rotating-table shaker at 180 RPM in the dark at 25 °C. Vials were sacrificed periodically by transferring samples of the aqueous phase into hexane for organic extraction or into HCl for Fe(II) analysis. The hexane extracts were vortexed and allowed to equilibrate for 1 h before analysis by gas chromatography.

4.3.3 Analyses. Chlorinated hydrocarbons were analyzed by two methods. The first utilized an HP 5890 Series II gas chromatograph with a Supelco VOLCOL™ capillary column (105 m x 0.53 mm ID with 3.0 μm film thickness) and an electron capture detector. The hexane-extracted samples were injected with an autosampler to a port at 200 °C, with the oven temperature constant at 250 °C for 15 min, ramped at 5 °C for 5 min, then held constant at 300 °C for 5 min. Other chlorinated hydrocarbon analyses were carried out using direct aqueous injection of 2 μL samples from a single bottle with flame ionization detection. Samples for Fe(II) determination were pipetted unfiltered into 40 μL of 5 M HCl, mixed with reagents for the ferrozine method (Roden and Zachara, 1996), allowed to react, and the optical absorbance was measured at 562 nm (Gibbs, 1979).

4.4 RESULTS AND DISCUSSION

4.4.1 Kinetics of Dehalogenation. Under most conditions, rates of dehalogenation by Fe^0 were adequately characterized by pseudo-first-order, initial disappearance rate constants normalized to Fe^0 surface area [designated k_{SA} in (Johnson et al., 1996)]. Throughout the following discussion, k_{SA} for dechlorination of CCl_4 is referred to as k_{CCl_4} , to distinguish it from other surface-area normalized rate constants. Note that deviation from this model due to adsorption without immediate dechlorination (Burriss et al., 1995) is not expected for CCl_4 and was not observed in this study.

First-order kinetics imply that disappearance rates increase linearly with initial substrate concentration, $[\text{P}]_0$. This is true at low $[\text{P}]_0$ for CCl_4 , but a transition to constant (zero-order) kinetics has been observed as $[\text{P}]_0$ approaches 0.8 mM (Johnson et al., 1996; Scherer and Tratnyek, 1995). New data (Figure 4.2) collected over a wider range of $[\text{P}]_0$ (up to 2.0 mM) confirm that dechlorination rates approach a limiting value. Such behavior is commonly observed in heterogeneous reactions and is usually interpreted as evidence for saturation of reactive surface sites (Zepp and Wolfe, 1987). The transition from first-order

to site-limited zero-order kinetics in this system can be described by a simple model (Johnson et al., 1996):

$$-\frac{d[P]}{dt} = \frac{V_m[P]}{K_{1/2} + [P]} \quad (4.1)$$

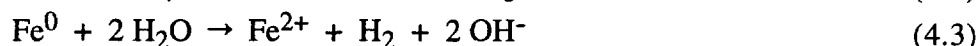
where V_m is the maximum reaction rate for a particular type and amount of iron metal, and $K_{1/2}$ (the concentration of P at $V_m/2$) reflects the affinity of surface sites for the substrate. As defined here, $K_{1/2}$ should not be a function of ρ_a , although it may be affected by changes in the composition of the oxide film.

Previously reported values for Fisher Fe⁰ in unbuffered medium were $V_m = 0.09 \pm 0.02$ mmol hr⁻¹ m⁻² and $K_{1/2} = 0.18 \pm 0.15$ mM (Johnson et al., 1996; Scherer and Tratnyek, 1995). The originally-reported value of V_m was not surface-area normalized, but the value given here has been corrected using $\rho_a = 1.02$ m² L⁻¹. Nonlinear regression on the new surface area normalized data in Figure 4.2 gives $V_m = 0.9 \pm 0.1$ mmol hr⁻¹ m⁻² and $K_{1/2} = 0.19 \pm 0.09$ mM for CCl₄ degradation by Fluka Fe⁰ in HEPES buffer at pH 6.2.

The two sets of fitted parameters can be compared directly, and interpreted in terms of surface site interactions. The values of $K_{1/2}$ are remarkably similar, suggesting there is no difference in surface affinity for CCl₄ despite obvious differences in the two metals used (Fisher filings vs. Fluka turnings). A narrow range in $K_{1/2}$ is consistent with the model in Figure 4.1 if the film that covers the Fe⁰ is a (hydr)oxide that develops in situ. In contrast to the consistency in $K_{1/2}$, there is a 10-fold difference in V_m . This variation suggests the two metals have different concentrations of reactive surface sites (Γ) that are not accounted for by simply normalizing the reaction rate to surface area. Specifically, it appears that Γ for Fluka Fe⁰ is significantly greater than Γ for the Fisher Fe⁰ used previously. There are, however, other differences between the two studies that might contribute to variation in V_m , such as the presence of HEPES buffer in the new experiments and absence of buffer in the earlier work. Factors such as these contribute to the >10-fold variability in reported values of k_{SA} for CCl₄ (Johnson et al., 1996), and could contribute the same degree of variability to V_m . Although a detailed understanding of the factors that control V_m would have practical as well as fundamental utility, further analysis will require more precise estimates of V_m from experimental designs that have been optimized for this purpose.

4.4.2 Kinetics of Iron Dissolution. In addition to CCl₄ disappearance, the appearance of iron in solution was determined in most experiments. We found no evidence for colloidal or dissolved Fe³⁺, so all the iron detected by our colorimetric method was attributed to dissolved Fe²⁺. Despite the simplified speciation of iron, detailed interpretation of these data is difficult because they reflect the net effect of several reactions. In our batch

experiments, Fe^{2+} can be from Fe^0 due to reduction of either CCl_4 (eq 4.2) or H_2O (eq 4.3); assuming further reduction of CHCl_3 is negligible, O_2 was completely removed at set up, and the buffer is not redox active.



Thermodynamically, it is possible that some of the Fe^{2+} produced may be consumed by further oxidation to Fe^{3+} coupled with reduction of CCl_4 (eq 4.4).



The reaction represented by eq 4.4 is slow with aqueous phase Fe^{2+} as the reducing agent (Doong and Wu, 1992), but may be important as a surface process involving Fe^{2+} sites in the oxide film (Section 4.4.8).

Fe^{2+} (and Fe^{3+}) that results from eqs 4.2-4.4 distributes among three states: hydrated or complexed in solution, precipitated as a solid, and adsorbed to the oxide film. In the absence of significant carbonate or sulfide, the precipitate formed is a mixture of iron (hydr)oxides: initially $\text{Fe}(\text{OH})_2$ ($\log K_{\text{sp}} \approx -15$) and $\text{Fe}(\text{OH})_3$ ($\log K_{\text{sp}} \approx -39$), but gradually evolving to Fe_3O_4 and $\gamma\text{-Fe}_2\text{O}_3$ (Graham et al., 1990; Ho and Ord, 1973; Oblonsky and Devine, 1995). Studies performed on pure samples of Fe_3O_4 (Klausen et al., 1995) and $\gamma\text{-Fe}_2\text{O}_3$ (Gorby et al., 1997) suggest that the fraction of Fe^{2+} sorbed at pH 6.2 will be low (Sinniger, 1992). However, it is difficult to estimate how much Fe^{2+} (or Fe^{3+}) is adsorbed to the oxide on Fe^0 , due to the complex and variable composition of the passive film. It is also difficult to measure the quantity of adsorbed Fe^{2+} using conventional selective extraction methods (Amonette et al., 1994a; Heron et al., 1994; Phillips and Lovley, 1987; Ryan and Gschwend, 1991) because the grains of Fe^0 provide a large reservoir of extractable metal ions.

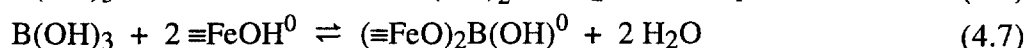
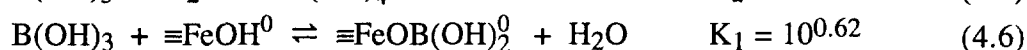
Figure 4.3 shows the aqueous concentration of Fe^{2+} over time, with and without CCl_4 present. Both time series are linear, suggesting that iron dissolution kinetics are zero-order with respect to $[\text{Fe}^{2+}]$ under these conditions. This is typical of dissolution where the rate is limited by dissociation from a steady-state population of a reactive surface complex (Biber et al., 1994).

The slopes of the lines in Figure 4.3 give zero-order rate constants for Fe^{2+} dissolution ($k_{\text{Fe}^{2+}}$) that are $0.32 \pm 0.02 \text{ mM h}^{-1}$ in buffer alone and $0.76 \pm 0.08 \text{ mM h}^{-1}$ in the presence of CCl_4 ($[\text{P}]_0 = 0.085 \text{ mM}$). Thus, it appears that the presence of CCl_4 more than doubled the corrosion rate over the anaerobic aqueous reaction (eq 4.3). Varying the initial CCl_4 concentration up to 2.0 mM (Fig. 4.4), reveals that $k_{\text{Fe}^{2+}}$ exhibits hyperbolic behavior

similar to that found for k_{CCl_4} . Although Figures 4.2 and 4.4 are not directly comparable, their similarity in shape is consistent with other indications that eq 4.2 is the major process occurring over the duration of our experiments (Johnson and Tratnyek, 1995; Scherer and Tratnyek, 1995), and that there is competition for surface sites capable of affecting dechlorination. Further evidence for this conclusion is provided by the direct linear correlation between rates of CCl_4 disappearance ($k_{\text{CCl}_4} \times [\text{P}]_0$) from Figure 4.2 and rates of Fe^{2+} appearance ($k_{\text{Fe}^{2+}}$) from Figure 4.4 (plot not shown, $r^2 = 0.91$, $n = 6$).

4.4.3 Passivation by Borate. To further probe the role of surface-complexation in CCl_4 reduction by Fe^0 , we studied the effect of adding a variety of anionic ligands. Borate is of particular interest because it is a common anion in soils (Biber et al., 1994; Goldberg and Glaubig, 1985; Sims and Bingham, 1968), a minor constituent of some groundwater (Matthess, 1982), and is widely used as a buffer in spectroscopic and electrochemical studies of corrosion (Graham et al., 1990; Gui and Devine, 1991; Pou et al., 1984). The results (Figure 4.5) show that k_{CCl_4} is significantly lower at high concentrations of borate (<0.05 mM), and that essentially complete inhibition of dechlorination occurs above about 0.1 mM.

The major solution species under the conditions of our experiments (pH 8.2) is boric acid, $\text{B}(\text{OH})_3$, with the most commonly invoked surface species on iron oxides being the corresponding mono- (Dzombak and Morel, 1990; Goldberg and Glaubig, 1985; Sims and Bingham, 1968) and bi-nuclear complexes (Biber et al., 1994).



Although boric acid forms weak surface complexes, its inhibition of iron oxide dissolution is well documented (Biber et al., 1994). Much of this effect has been attributed to the formation of uncharged binuclear surface complexes (eq 4.7), which create a large activation energy for simultaneous detachment of two metal centers (Biber et al., 1994; Stumm, 1993). The same effect presumably contributes to the passivation of Fe^0 in borate-buffered media. Extrapolation from this interpretation explains why the addition of borate to the Fe^0 - H_2O - CCl_4 system inhibits dechlorination of CCl_4 as well as dissolution of Fe^{2+} . However, concentrations of borate in groundwater rarely exceed a few μM (Matthess, 1982), so the inhibitory effect probably has no direct influence on remediation under field conditions.

4.4.4 Depassivation by Chloride. Since the results with borate suggest that passivation of Fe^0 slows corrosion by CCl_4 as well as H_2O (i.e., eqs 4.2 and 4.3), we

hypothesized that destabilization of the passive film would accelerate the treatment reaction. The anions of hard bases (such as Cl^- , Br^- , I^- , and S^{2-}) are especially aggressive towards passivating oxides because they diffuse readily into the film and form strong complexes with iron centers (Aramaki et al., 1994; Bockris and Khan, 1993; Janik-Czachor and Kaszczyszyn, 1982; Kruger, 1989; Pou et al., 1984; Yamaguchi et al., 1994). These complexes enhance dissolution of the oxide and often induce pitting. Chloride is of particular interest because it is the most abundant halide in groundwater (Matthess, 1982), and it is a product of dechlorination, so its accumulation has the potential for an autocatalytic effect on the treatment reaction.

As expected, adding chloride (as NaCl) increased k_{CCl_4} (Fig 4.5), presumably by breaking down the oxide film. The increase in k_{CCl_4} was four-fold at 60-100 μM Cl^- , which is approximately the amount of Cl^- that would be produced from complete conversion of CCl_4 to CHCl_3 under conditions typical of this study. Although this suggests that a detectable acceleration in CCl_4 disappearance might result from the Cl^- generated by dechlorination, such an autocatalytic effect has not been observed. The lack of detectable autocatalysis by Cl^- probably reflects the short duration of most batch experiments, compared to the time required for significant degradation of the oxide film by Cl^- derived from dehalogenation.

4.4.5 Modeling Inhibition by Catechol. Ligands that form bidentate-binuclear surface complexes (borate and phosphate) inhibit dissolution of metal oxides, whereas those that form bidentate-mononuclear complexes often enhance dissolution (Stumm et al., 1990). Typical of the latter, are organic ligands with adjacent hydroxyl groups: such as oxalate, salicylate, citrate, and catechol. Under conditions where these ligands promote dissolution of oxides that compose the passive film on metal, corrosion should be accelerated (Stumm et al., 1990). This effect has been reported for oxalate and ascorbate (dos Santos Afonso et al., 1990). In contrast, we have found that increasing concentrations of catechol decreased k_{CCl_4} and $k_{\text{Fe}^{2+}}$ under anaerobic conditions (Fig 4.6). This inhibition is nonetheless consistent with ligand-promoted dissolution of the oxide by catechol under conditions where oxidation by CCl_4 (eq 4.2) is the dominant corrosion reaction rather than oxidation by H_2O (eq 4.3) (Johnson and Tratnyek, 1995; Scherer et al., 1997). Apparently, the strong catechol surface complex (McBride, 1987; Vasudevan and Stone, 1996) interferes with the weaker surface interactions involving CCl_4 , and it is the latter that determine k_{CCl_4} and $k_{\text{Fe}^{2+}}$ via eq 4.2.

A simple kinetic model for ligand-inhibited dechlorination by Fe^0 can be derived, which is analogous to equations that describe inhibition in enzyme kinetics (Huennekens and Chance, 1963) and competitive adsorption of anions on soils (Hingston et al., 1971).

We previously proposed the kinetic model represented by eq 4.1 (Johnson et al., 1996), assuming dechlorination of the substrate, P, involves reversible formation of a precursor complex at the metal surface, P-Fe, followed by rate-limiting charge-transfer to form products of the treatment reaction (eq 4.8). If the interfering ligand, L, also adsorbs reversibly, forming the surface complex, L_n-Fe, then there are competing processes:



where *n* represents the stoichiometry of L per blocked reaction site for P (eq 4.9). Adjusting eq 4.1 to reflect competition for the same surface sites by eq 4.9, yields:

$$-\frac{d[P]}{dt} = \frac{V_m[P]}{K_{1/2}(1 + [L]^n/K_L) + [P]} \quad (4.10)$$

where *V_m* and *K_{1/2}* have the same interpretations as in eq 4.1, and *K_L* = *k₄*/*k₅*. If L interferes by adsorbing to sites other than the surface sites responsible for dechlorination (Huennekens and Chance, 1963), then a slightly different model results, where the correction 1+[L]^{*n*}/*K_L* applies to the whole denominator in eq 4.10, rather than just *K_{1/2}*. However, at low initial concentrations of P, pseudo-first order conditions apply, and both cases simplify to the same expression.

$$k_{CCl_4} = \frac{V_m/K_{1/2}}{1 + [L]^n/K_L} \quad (4.11)$$

In principle, this equation can be expanded to account for multiple (non-interacting) ligands by including additional [L]^{*n*}/*K_L* terms to the denominator.

The steep decline and eventual stabilization of *k_{CCl₄}*

 with increasing catechol concentration was fitted to eq 4.11 by nonlinear regression (Fig 4.6a). The residuals do not vary systematically and standard deviations of the three fitting coefficients (Table 4.1) show that the model is generally well constrained. The parallel behavior exhibited by *k_{Fe²⁺}* (Fig 4.6b) is consistent with the similarity in Figures 4.2 and 4.4. Although additional investigation is needed to further validate this model, the goodness of fit between our current data and eq 4.11 suggests that CCl₄ forms a weak precursor complex at the oxide-water interface prior to dechlorination, and that this initial step is easily blocked by other solutes that complex more strongly to the surface.

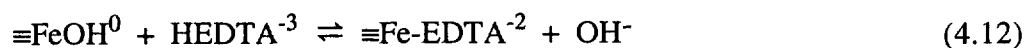
4.4.6 Comparison of Catechol, Ascorbate, and Acetate. Ascorbate and acetate decreased *k_{CCl₄}*

 in a manner similar to that of catechol (Fig 4.7). The data also fit eq

4.11, and the results of nonlinear regression are summarized in Table 4.1. Some interpretation of the fitting parameters is possible even though the model is largely empirical. The ratio $V_m/K_{1/2}$ gives a pseudo-first-order rate constant (i.e., k_{CCl_4}) where the [P] is much greater than $K_{1/2}$ or $K_{1/2}(1+[L]^n/K_L)$, as is the case under most conditions of practical environmental interest. In the control system, $V_m/K_{1/2} = 4.8 \text{ hr}^{-1}$ for k_{CCl_4} (from values fit to Fig 4.2 data), which agrees well with the results obtained by factoring out the effects of catechol and ascorbate (Table 4.1), despite the notable drop in pH (to ~4) caused by the addition of ascorbate. The experiments with acetate give a higher value of $V_m/K_{1/2}$, but no reason for this is apparent. Limited data (not shown) suggest that $k_{Fe^{2+}}$ decreases with acetate concentration in a manner similar to that of catechol, presumably due to a similar inhibition of the primary corrosion reaction (eq 4.11). The effect of ascorbate on $k_{Fe^{2+}}$ was not determined.

The coefficient K_L is not directly comparable to an SCM binding constant, but it is an aggregate measure of affinity between L and the iron oxide surface. As such, K_L may be a useful predictor of inhibitory effects on dehalogenation by Fe^0 when more precise estimates of the parameter become available. The necessary data could be obtained with experimental designs such as those used to characterize specific inhibition mechanisms in enzyme catalyzed reactions (Huennekens and Chance, 1963). The coefficient n was formulated as a stoichiometric factor in eq 4.9, and represents the number of ligand molecules necessary to block a reactive site for CCl_4 . The fitted values of n are all significantly less than unity (Table 4.1), suggesting that adsorption of these organic anions interferes with several sites where CCl_4 might otherwise undergo dechlorination. This difference in n , however, should be treated as an aggregate effect, since CCl_4 undoubtedly forms a very different type of complex with the oxide surface than anionic ligands.

4.4.7 Effect of EDTA. As with all other organic ligands studied, the addition of EDTA to our batch systems decreased k_{CCl_4} (Fig 4.8). However, the resulting profile was linear, rather than the hyperbolic relationship observed for catechol, acetate, and ascorbate. The distinctive effect of EDTA can be explained in terms of its ability to form two types of surface complexes. The mononuclear species (eq 4.12) is not redox active (Norvell, 1991), so it presumably inhibits reduction of CCl_4 in the same way as the corresponding mononuclear complexes of other organic ligands.



However, the solution phase complex of Fe(II)-EDTA (eq 4.13) also adsorbs strongly to the oxide surface (Nowack et al., 1996), and the surface species is likely to retain some

ability to serve as a reduction site for CCl_4 . The effect of competition between these two processes on magnetite dissolution is well documented and was found to vary with the relative abundance of dissolved Fe^{2+} versus EDTA (Blesa et al., 1984; Borghi et al., 1989). When EDTA is in excess, as it was in this study, most dissolved Fe^{2+} is complexed, and some fraction of this species competes with uncomplexed EDTA for sites on the metal surface. Increasing EDTA from 5 to 50 mM favors eq 4.12 over eq 4.13, and proportionally decreases the population of surface sites available to react with CCl_4 . In retrospect, the complexity of this effect confounds our early attempt to isolate the role of Fe^{2+} on the Fe^0 surface by sequestering Fe^{2+} with EDTA (Matheson and Tratnyek, 1994). It is, however, consistent with the complex interactions necessary to explain how EDTA can both clean and passivate steel pipes and boilers (Blesa et al., 1984; Borghi et al., 1989; Frenier and Kennedy, 1986; Joshi et al., 1992).

4.4.8 The Role of Surface-Bound Fe^{2+} . It has long been known that various forms of Fe^{2+} might mediate reduction reactions involving environmental contaminants (Macalady et al., 1986). However, it has only recently become widely recognized that surface-bound Fe^{2+} (Roden and Zachara, 1996; Stucki et al., 1987) can be a much stronger reductant than most ferrous complexes in solution, and this activated form of reduced iron is likely to have the greatest effect on contaminant fate. For example, recent studies have shown that Fe^{2+} adsorbed on a variety of minerals gives enhanced reduction of nitro aromatic compounds (Klausen et al., 1995), chromate (Fendorf and Li, 1996), and pertechnetate (Cui and Eriksen, 1996a; Cui and Eriksen, 1996b). In other studies, Fe^{2+} adsorbed to the surface of iron oxides, such as goethite, hematite, or poorly crystalline ferrihydrite, was shown to give reductive dechlorination of CCl_4 (Fredrickson and Gorby, 1996; Gorby et al., 1997) and trichloroethene (Sivavec and Horney, 1997). The rates and products of dechlorination observed are sufficiently promising that several methods for in situ generation of surface-bound Fe^{2+} are under investigation for use in plume containment or remediation (Amonette et al., 1994b; Fredrickson and Gorby, 1996).

The dechlorinating ability of Fe^{2+} adsorbed on goethite, hematite, and other non-metallic surfaces suggests a close analogy to the role of surface-bound Fe^{2+} in mediating reduction by Fe^0 (Sivavec and Horney, 1997; Sivavec et al., 1995). To assess whether corrosion of underlying Fe^0 is just one way to produce surface-bound Fe^{2+} in the oxide layer, it is instructive to compare the kinetics of reduction with and without Fe^0 (Table 4.2). Normalization of the available rate data to $1 \text{ m}^2 \text{ L}^{-1}$ of solid (BET) surface area suggests that reduction is consistently faster in the presence of Fe^0 . This may mean that (i) Fe^0 produces surface-bound Fe^{2+} at the oxide-water interface more effectively than it can be introduced from solution, (ii) the reactivity of surface-bound Fe^{2+} is influenced by other

electrochemical properties of the oxide film, or (iii) other processes, such as reaction within corrosion pits, contribute to reduction in the presence of Fe^0 . Interpretation of the degradation process at this level, however, will require a more detailed understanding of how reducing equivalents pass to and from the oxide/water interface.

4.5 CONCLUSIONS

Many previous studies have recognized that dehalogenation of chlorinated solvents at the surface of Fe^0 is likely to be mediated by the coating of ferrous (hydr)oxides that is usually present under environmental conditions. However, few of these investigations have tried to articulate the precise role that oxides play in the dehalogenation reaction. Taken together, the results of this study suggest a simple conceptual model that differentiates between the major types of surface interactions (Fig 4.9). All the anions used in this study can form specific bonds with surface hydroxyl groups, resulting in inner-sphere complexes. The number of hydroxyl groups occupied depends on the anion, and the effect on solubilization of the surface oxide will vary accordingly (Stumm et al., 1990). On the other hand, molecules of CCl_4 cannot share exchangeable atoms with the oxide surface, and therefore cannot form inner-sphere complexes. Instead, we assume the precursor required for reduction consists of an outer-sphere complex formed by weak hydrophobic interactions. Stronger complexes prevent formation of the weak precursor complex between surface-bound Fe^{2+} and CCl_4 , and this results in slower dehalogenation and corrosion of the Fe^0 .

Competition by non-reactive adsorbates inhibits the dechlorination reaction by blocking access to reactive surface sites; as was reported here for catechol, ascorbate, acetate, and EDTA, and was suggested previously for polymers of carbohydrate (Bizzigotti et al., 1997). A further implication of this understanding is that the presence of an adsorptive “co-contaminant” such as chromate (Khudenko and Gould, 1991; Powell et al., 1995) may yield slower dehalogenation than would be obtained for an organic contaminant alone. The precursor complexes that lead to reduction of chlorinated solvents are likely to be too weak and non-specific to produce notable intra-substrate competition effects, which is consistent with the few available data on binary mixtures (Burriss et al., 1995).

Dehalogenation by surface-bound Fe^{2+} appears to be faster at the oxide film on Fe^0 , than when the reducing sites are generated in other ways. However, down gradient from an in situ treatment zone, the only major reductant is Fe^{2+} that precipitates on native aquifer surfaces (Johnson and Tratnyek, 1994). It is this down-gradient region where field sites treated with Fe^0 will be most analogous to other situations where adsorbed Fe^{2+}

occurs as a reductant in the environment.

ACKNOWLEDGMENTS

Most experimental work was performed at the Battelle Pacific Northwest National Laboratories, Richland, WA, while T. L. Johnson was supported by an Energy Research Fellowship from the DOE. Other portions were supported by the University Consortium Solvents-In-Groundwater Research Program, the National Science Foundation through Award BCS-9212059, and the Petroleum Research Fund through award 29995-AC5. E. J. Reardon contributed through early discussions and speciation modeling, and J. C. Westall provided additional review of the manuscript.

4.6 LIST OF SYMBOLS

ρ_a	surface area concentration ($\text{m}^2 \text{L}^{-1}$)
Γ	surface concentration of reactive sites (mmol m^{-2})
k_{SA}	observed substrate degradation rate (k_{obs}) normalized to surface area ($\text{hr}^{-1} \text{L m}^{-2}$)
k_{CCl_4}	first-order disappearance rate constant for CCl_4 , surface area normalized ($\text{hr}^{-1} \text{L m}^{-2}$)
$k_{\text{Fe}^{2+}}$	zero-order appearance rate constant for Fe^{2+} , surface area normalized ($\text{mM hr}^{-1} \text{L m}^{-2}$)
[L]	molar concentration of ligand (mmol L^{-1})
n	stoichiometry of L per blocked reaction site for P (unitless)
$K_{1/2}$	concentration of P at $V_m/2$ (mmol L^{-1})
K_L	binding constant for L with the iron oxide surface ($\text{mmol}^{-1} \text{L}$)
[P]	molar concentration of substrate (mmol L^{-1})
[P] ₀	initial molar concentration of substrate (mmol L^{-1})
V_m	maximum reaction rate, surface area normalized ($\text{mmol hr}^{-1} \text{m}^{-2}$)

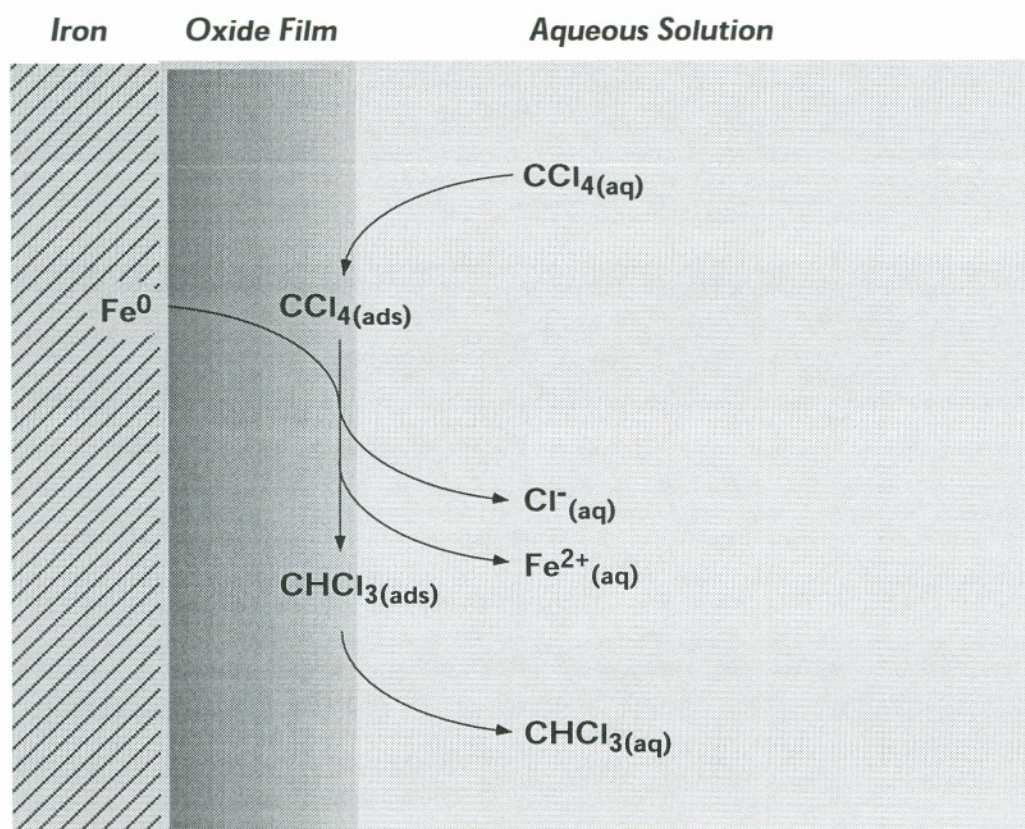


Figure 4.1 Reactions involved in dehalogenation by zero-valent iron metal. Dechlorination takes place at the oxide-electrolyte interface (Stratmann and Müller, 1994). Only reductive dehalogenation of CCl_4 is shown, but additional degradation pathways are possible for other chlorinated solvents (Roberts et al., 1996).

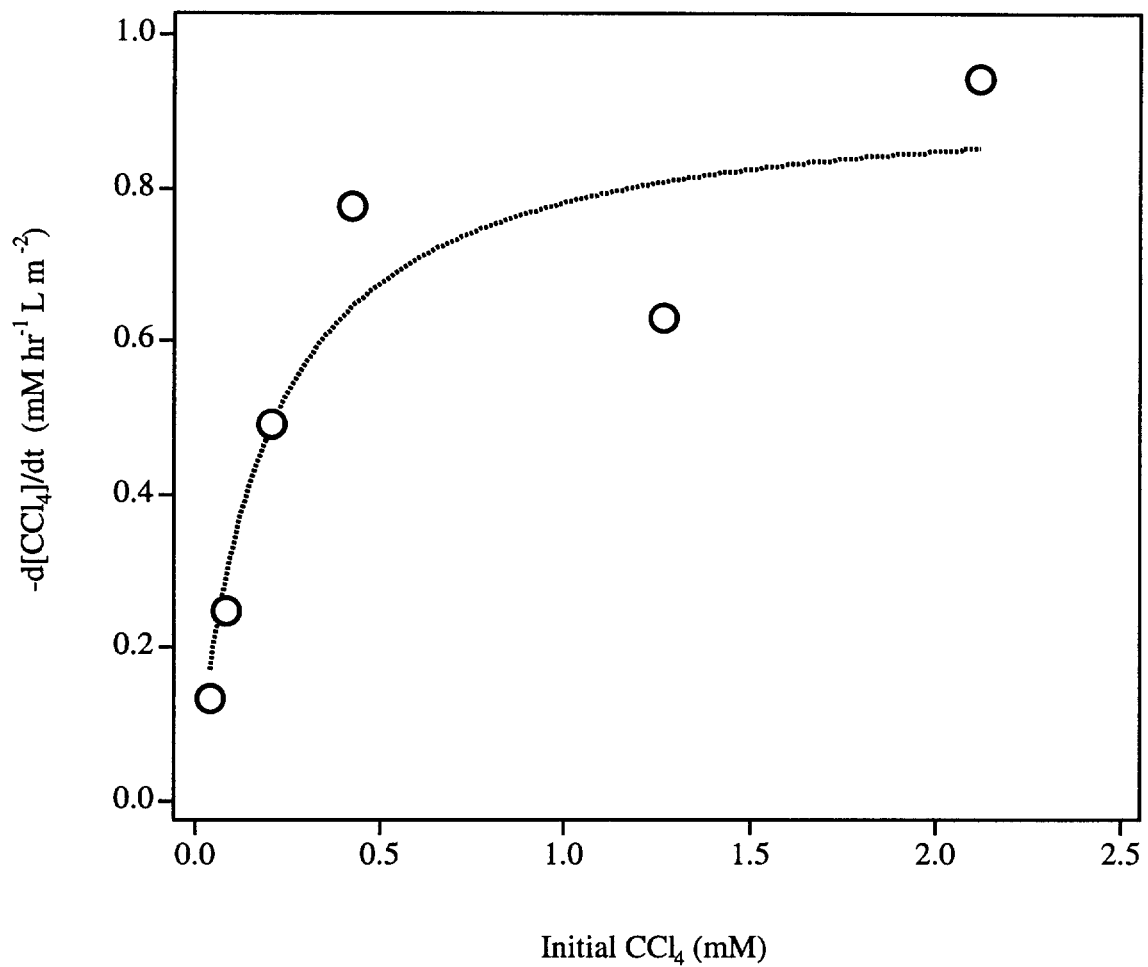


Figure 4.2 Effect of $[P]_o$ on k_{CCl_4} (k_{obs} for CCl_4 disappearance normalized to surface area = $1.0 \text{ m}^2 \text{ L}^{-1}$). Data from well-mixed anaerobic batch experiments containing Fluka Fe^0 and 10 mM HEPES buffer at pH 6.2. Curve is fit to eq 4.1 with coefficients given in the text.

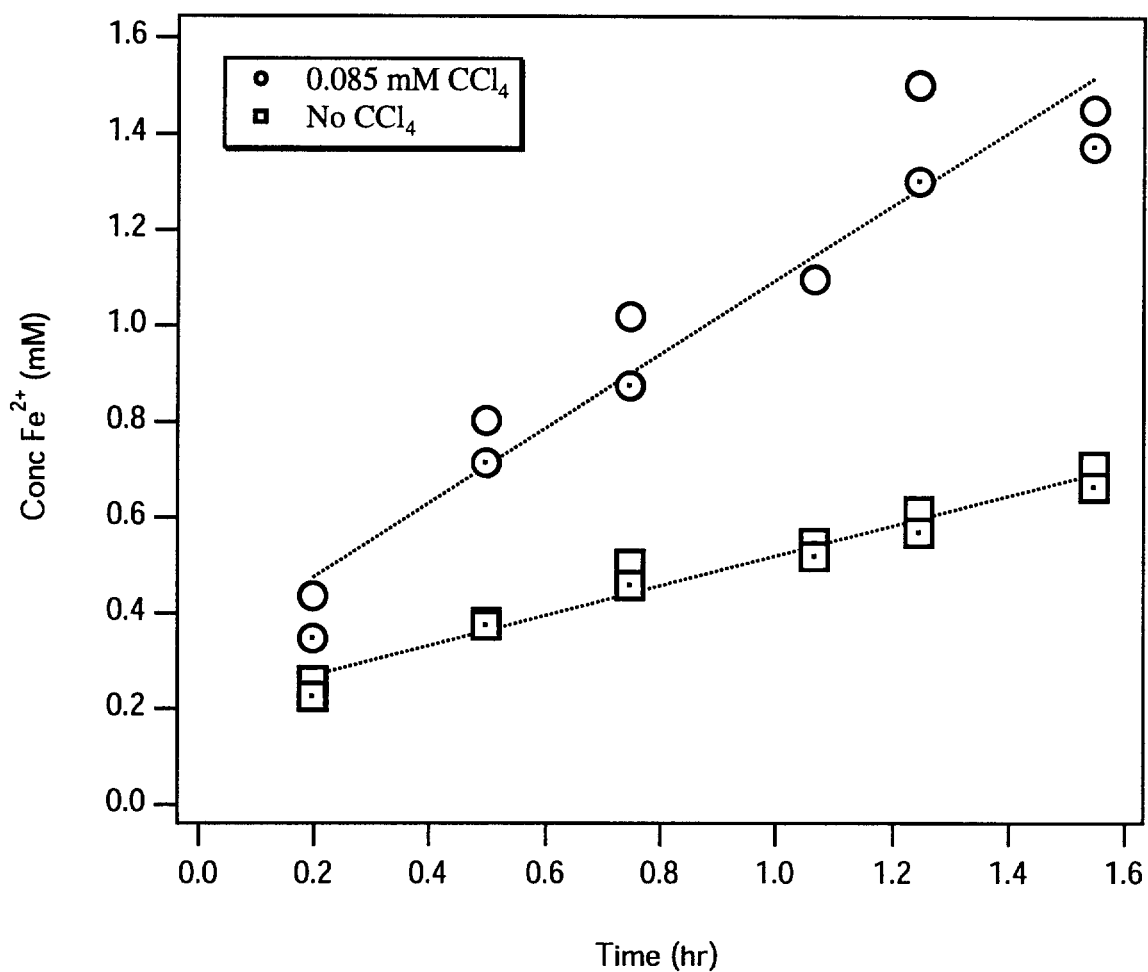


Figure 4.3 Accumulation of Fe²⁺ in solution with time, with and without CCl₄, in an anaerobic, well-mixed batch system containing 0.79 m² L⁻¹ Fluka Fe⁰ and HEPES buffer. Squares represent corrosion from reduction of water only (eq 4.3) and circles represent reduction by water and CCl₄ (eqs 4.2 and 4.3). Pairs of open and filled symbols indicate replicates.

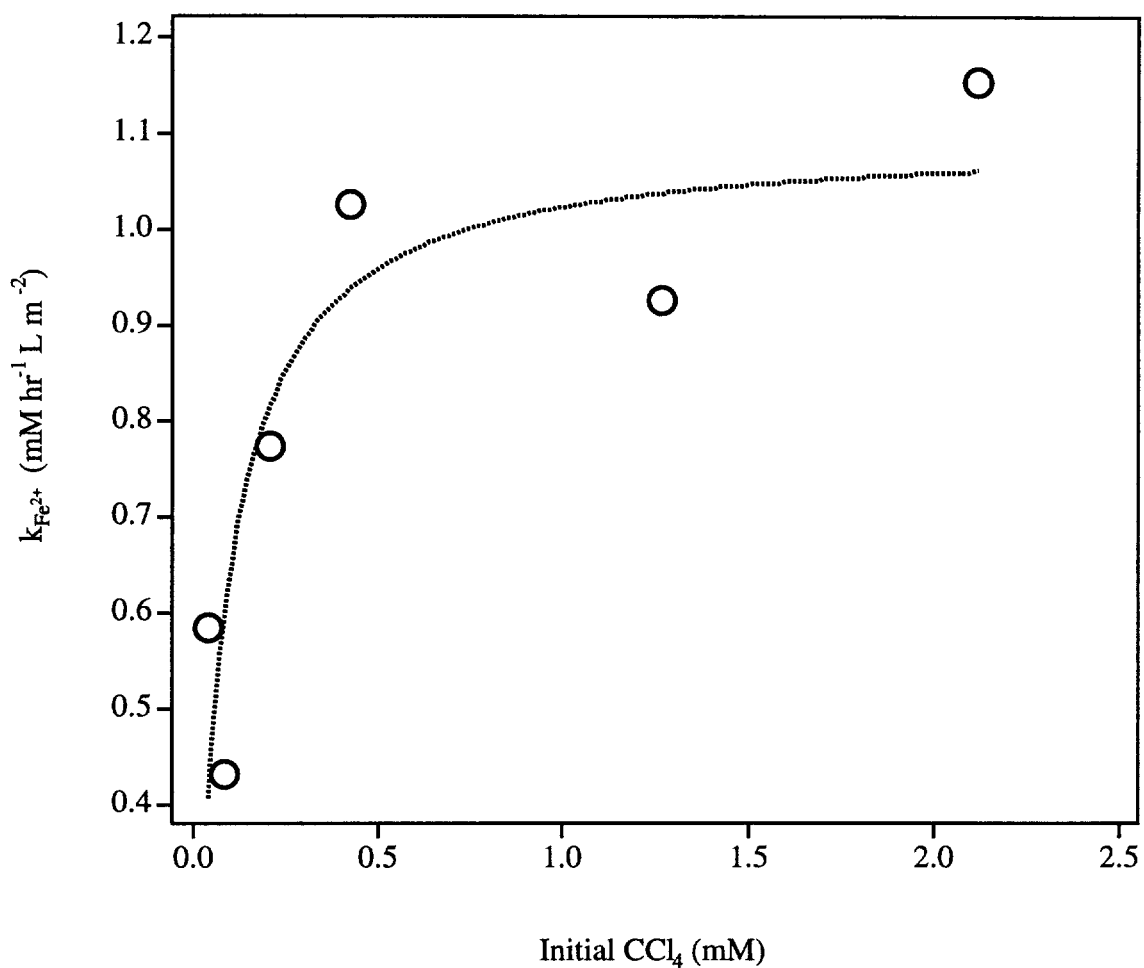


Figure 4.4 Effect of $[P]_0$ on $k_{Fe^{2+}}$ (k_{obs} for Fe^{2+} dissolution normalized to surface area = $1.0\ m^2\ L^{-1}$). Data from well-mixed anaerobic batch experiments containing Fe^0 in HEPES buffer. Curve fit is of the same form as eq 4.1.

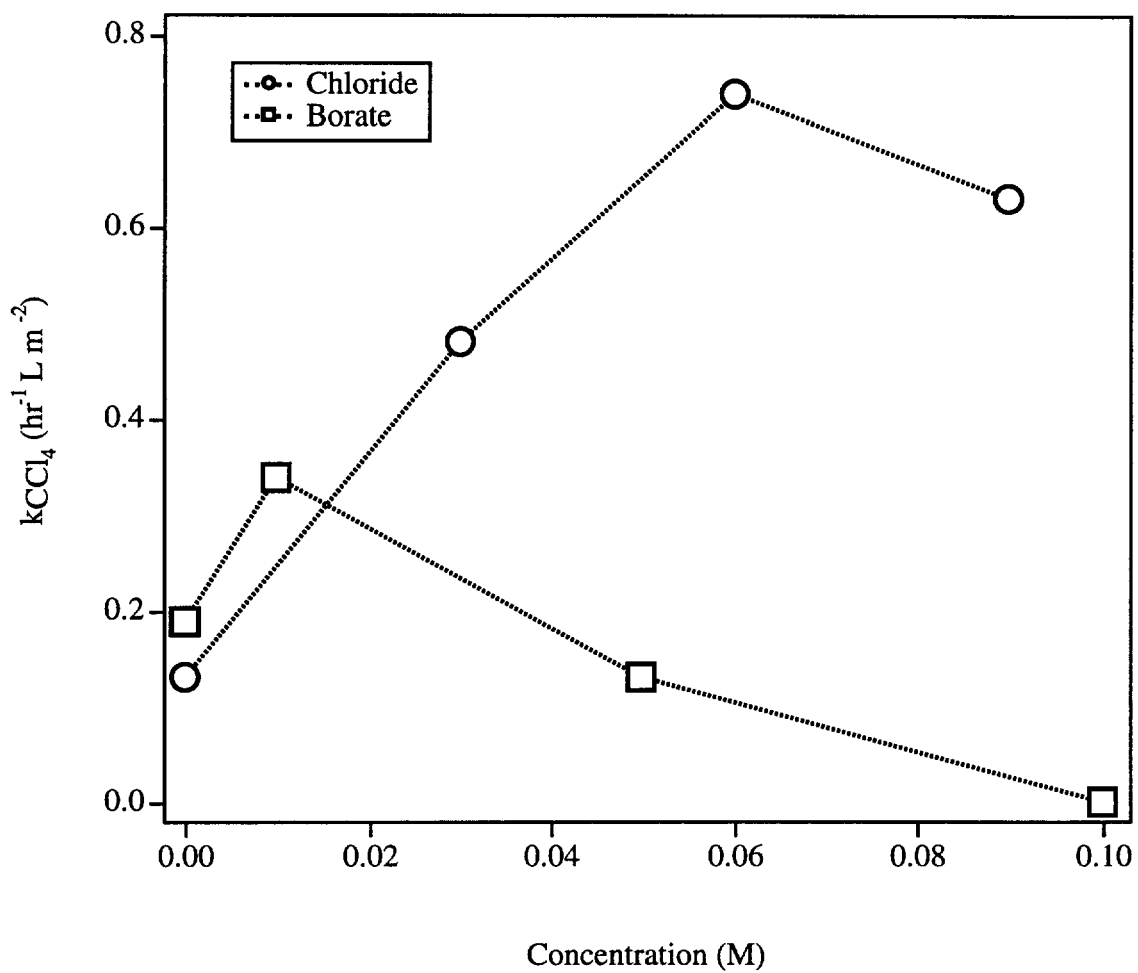


Figure 4.5 Effect of borate and chloride on k_{CCl_4} . Data from well-mixed anaerobic batch experiments containing Fe^0 without added buffer.

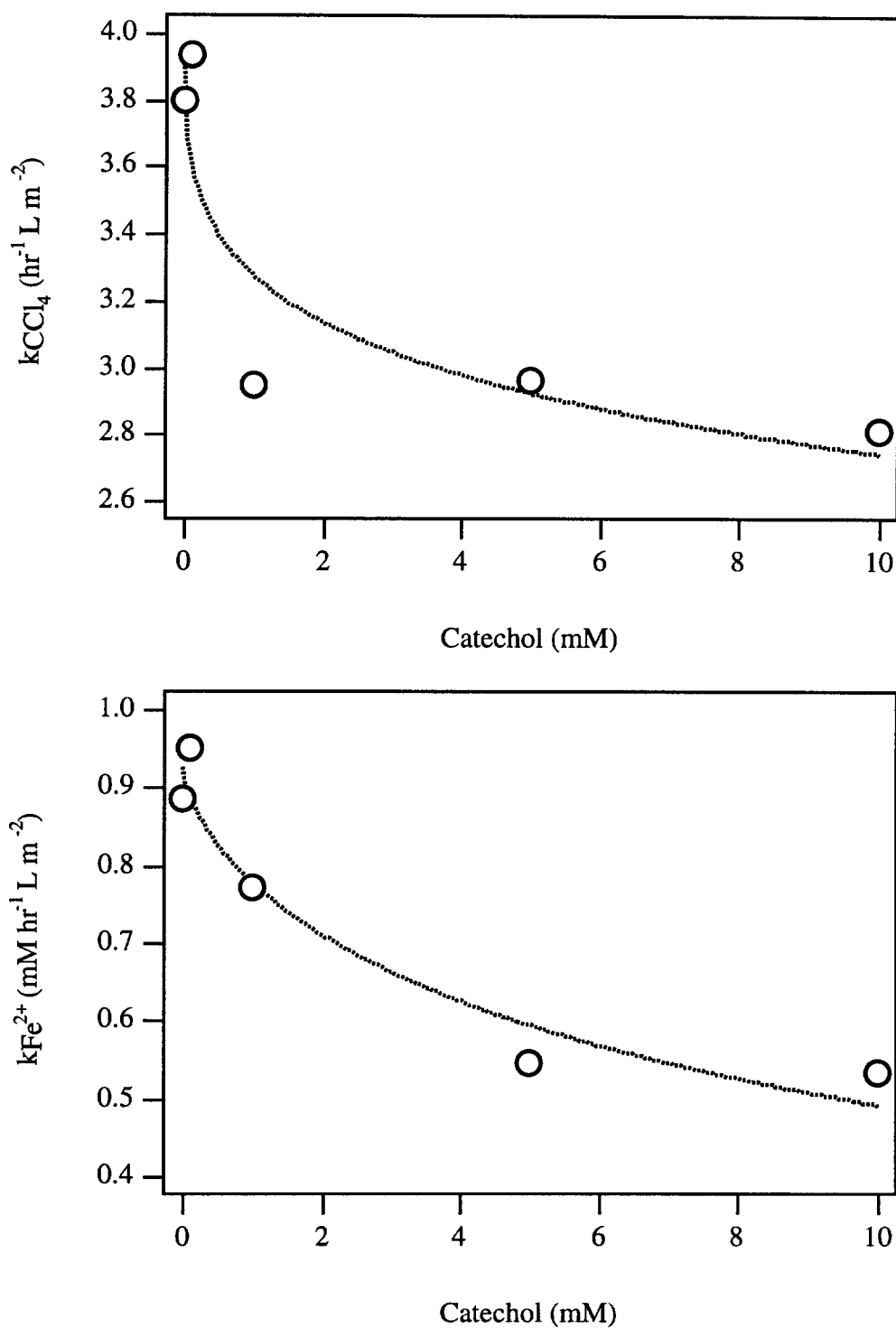


Figure 4.6 Effect of catechol on k_{CCl_4} (a) and $k_{Fe^{2+}}$ (b). Data from well-mixed anaerobic batch experiments containing Fe^0 in HEPES buffer. Curve is a fit to eq 4.11 with coefficients given in Table 4.1.

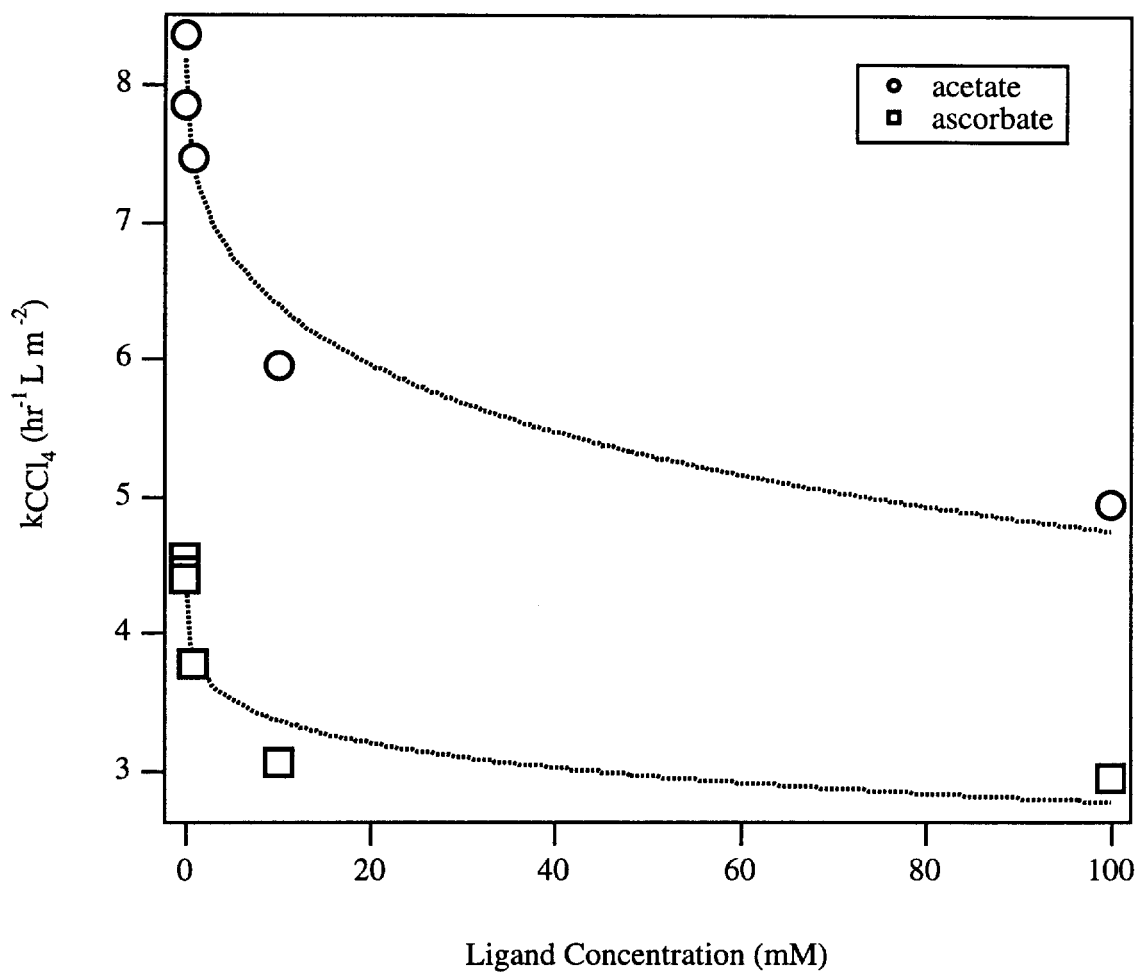


Figure 4.7 Effect of ascorbate and acetate on k_{CCl_4} . Data from well-mixed anaerobic batch experiments containing Fluka Fe^0 in HEPES buffer. Ascorbate pH = 6.2 and acetate pH = 4. Curve are fits to eq 4.11 with coefficients given in Table 4.1.

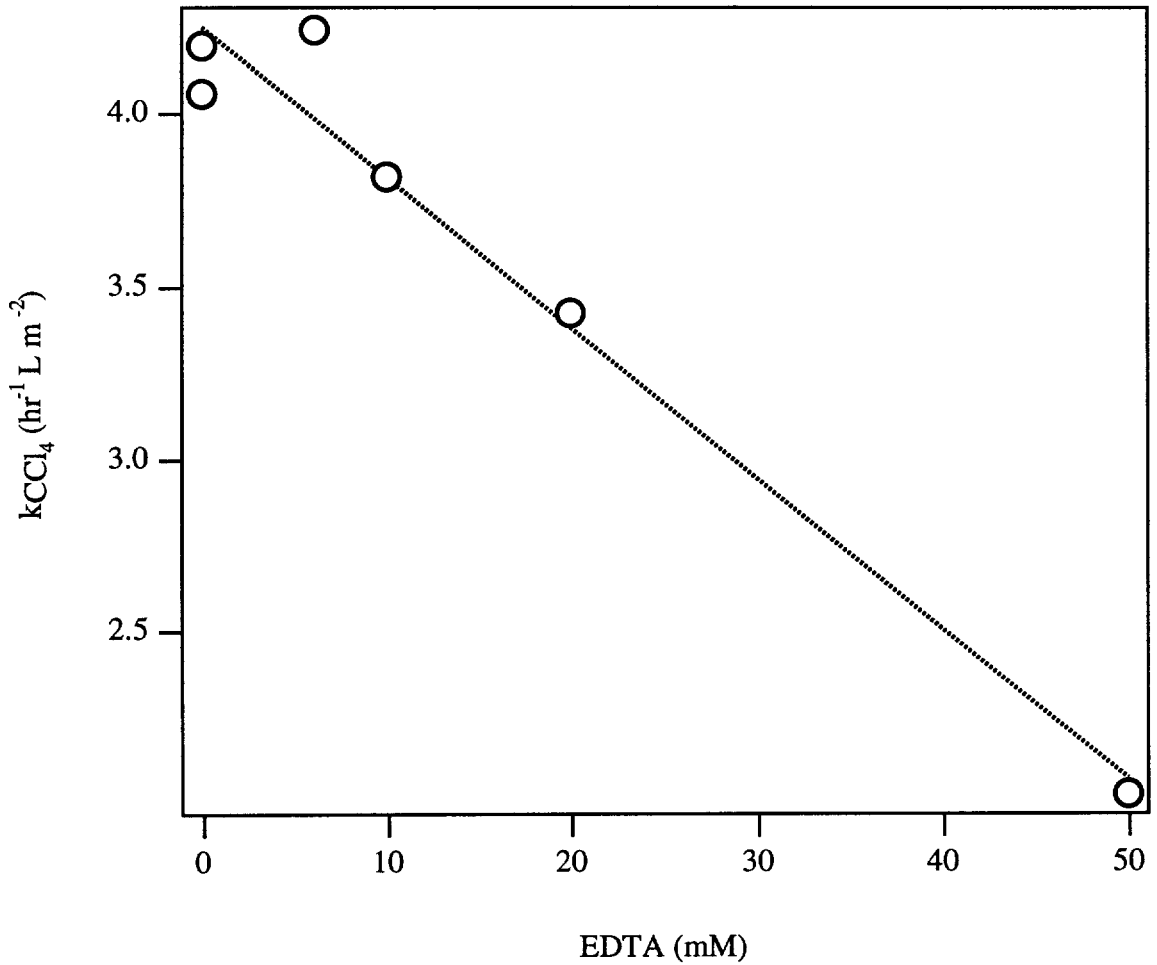


Figure 4.8 Effect of EDTA on k_{CCl_4} . Data from well-mixed anaerobic batch experiments containing Fe^0 in HEPES buffer. The fitted line has intercept = 4.2 ± 0.1 , slope = -0.98 ± 0.001 , and $r^2 = 0.969$.

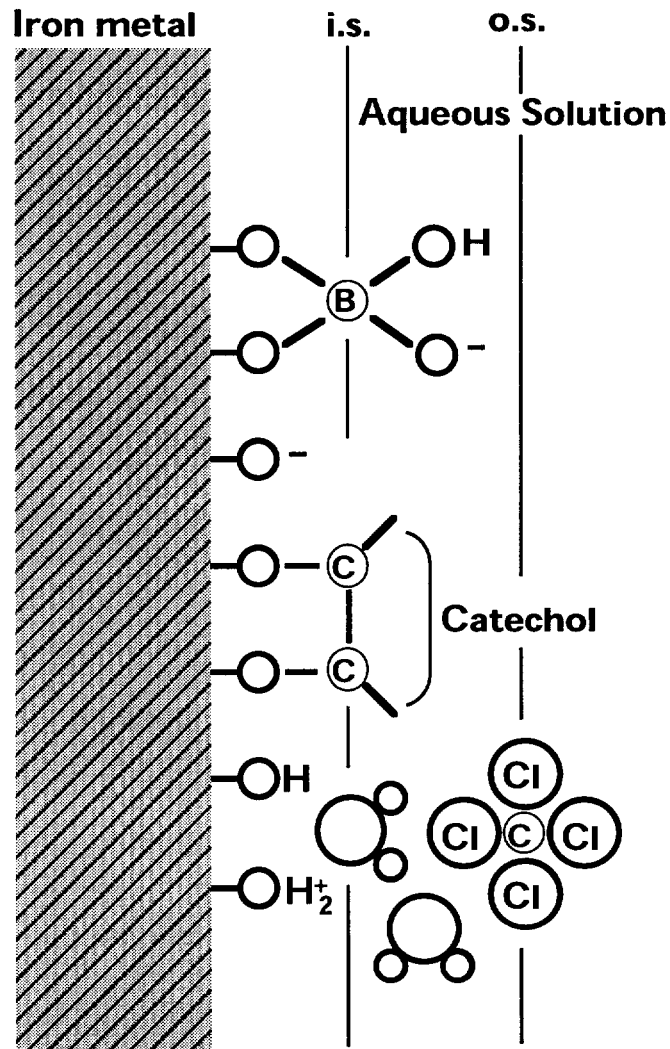


Figure 4.9 Conceptual model contrasting the inner sphere (i.s.) adsorption of ligands such as phosphate and catechol with the relatively weak (presumably outer-sphere, o.s.) precursor complex that precedes reduction of CCl_4 at the oxide-water interface on Fe^0 . Adapted from (Sposito, 1984; Stumm, 1987).

TABLE 4.1. MODEL PARAMETERS FOR INHIBITION OF THE CCL₄ REACTION WITH FE⁰.

Inhibitory Adsorbate	Data	$V_m/K_{1/2}$ (hr ⁻¹)	K_L (mM ⁻¹)	n
k_{CCl_4} vs [Catechol]	Fig 4.6a	4.0±0.6	4.5±4.9	0.3±0.3
k_{CCl_4} vs [Acetate]	Fig 4.7	8.2±0.5	9.2±7.3	0.4±0.2
k_{CCl_4} vs [Ascorbate]	Fig 4.7	4.5±0.2	5.2±2.0	0.3±0.1

TABLE 4.2. COMPARISON OF REDUCTION RATES BY Fe^{2+} WITH AND WITHOUT Fe^0 .

Substrate	Surface	Media	Half-life ⁵	Source
CCl ₄	Fe ⁰	Wide range ¹	5.8 hr	(Johnson et al., 1996)
	goethite	PIPES ^{2,3}	2500 hr	(Gorby et al.,)
TCE	Fe ⁰	Wide range ¹	74 d	(Johnson et al., 1996)
	magnetite	Deionized water	1500 d	(Sivavec and Horney, 1997)
Nitrobenzene	Fe ⁰	pH 7.9 CO ₂ buffer	0.30 hr	(Agrawal and Tratnyek, 1996)
	magnetite	MOPS ^{2,4}	1.0 hr	(Klausen et al., 1995)

¹ Representative of n > 12 previously published batch and column studies; Fe²⁺ adsorbed variable. ² added [Fe²⁺] > 1 mM where $V \approx V_m$. ³ pH = 7 where Fe²⁺ adsorbed ≈ 15%. ⁴ pH = 7 where Fe²⁺ adsorbed ≈ 30%. ⁵ normalized to 1 m² of solid surface area per liter of solution volume.

4.6 REFERENCES

- Agrawal, A. and Tratnyek, P.G., 1996. Reduction of nitro aromatic compounds by zero-valent iron metal. *Environ. Sci. Technol.*, 30(1): 153-160.
- Amonette, J.E., Khan, F.A., Scott, A.D., Gan, H. and Stucki, J.W., 1994a. Quantitative oxidation-state analysis of soils. In: J.E. Amonette and L.W. Zelazny (Editors), *Quantitative Methods in Soil Mineralogy*. Soil Science Society of America, Madison, WI, pp. 83-113.
- Amonette, J.E. et al., 1994b. Abiotic reduction of aquifer materials by dithionite: A promising in-situ remediation technology. *Proceedings of the 33rd Hanford Symposium on Health & the Environment—In Situ Remediation: Scientific Basis for Current and Future Technologies*, Battelle Pacific Northwest Laboratories, Pasco, WA, Vol. 2. pp. 851-881.
- Aramaki, K., Tomihari, M., Furuya, S., Yamaguchi, M. and Nishihara, H., 1994. The inhibitive effect of organic cations on passive film breakdown of iron in a chloride-containing borate buffer solution. *Corr. Sci.*, 36(7): 1133-1141.
- Biber, M.V., Afonso, M.S. and Stumm, W., 1994. The coordination chemistry of weathering: IV. Inhibition of the dissolution of oxide minerals. *Geochim. Cosmochim. Acta*, 58(9): 1999-2010.
- Bizzigotti, G.O., Reynolds, D.A. and Kueper, B.H., 1997. Enhanced solubilization and destruction of tetrachloroethylene by hydroxypropyl- β -cyclodextrin and iron. *Environ. Sci. Technol.*, 31(2): 472-478.
- Blesa, M.A., Borghi, E.B., Maroto, A.J.G. and Regazzoni, A.E., 1984. Adsorption of EDTA and Iron-EDTA complexes on magnetite and the mechanism of dissolution of magnetite by EDTA. *J. Colloid Interface Sci.*, 98(2): 295-305.
- Blesa, M.A., Morando, P.J. and Regazzoni, A.E., 1994. *Chemical Dissolution of Metal Oxides*. CRC Press, Ann Arbor, 401 pp.
- Bockris, J.O.M. and Khan, S.U.M., 1993. *Surface Electrochemistry. A Molecular Level Approach*. Plenum, New York, 1014 pp.
- Borghi, E.B., Regazzoni, A.E., Maroto, A.J.G. and Blesa, M.A., 1989. Reductive dissolution of magnetite by solutions containing EDTA and Fe(II). *J. Colloid Interface Sci.*, 130(2): 299-310.
- Burris, D.R., Campbell, T.J. and Manoranjan, V.S., 1995. Sorption of trichloroethylene and tetrachloroethylene in a batch reactive metallic iron-water system. *Environ. Sci. Technol.*, 29(11): 2850-2855.
- Cui, D.Q. and Eriksen, T.E., 1996a. Reduction of pertechnetate by ferrous iron in solution: Influence of sorbed and precipitated Fe(II). *Environ. Sci. Technol.*, 30(7): 2259-2262.
- Cui, D.Q. and Eriksen, T.E., 1996b. Reduction of pertechnetate in solution by heterogeneous electron transfer from Fe(II)-containing geological material. *Environ. Sci. Technol.*, 30(7): 2263-2269.
- Doong, R.-A. and Wu, S.-C., 1992. Reductive dechlorination of chlorinated hydrocarbons in aqueous solutions containing ferrous and sulfide ions. *Chemosphere*, 24(8): 1063-1075.

- dos Santos Afonso, M., Morando, P.J., Blesa, M.A., Banwart, S. and Stumm, W., 1990. The reductive dissolution of iron oxides by ascorbate. *J. Colloid Interface Sci.*, 138(1): 74-82.
- Dzombak, D.A. and Morel, F.M.M., 1990. *Surface Complexation Modeling: Hydrous Ferric Oxide*. John Wiley & Sons, New York.
- Fendorf, S.E. and Li, G.C., 1996. Kinetics of chromate reduction by ferrous iron. *Environ. Sci. Technol.*, 30(5): 1614-1617.
- Fredrickson, J.K. and Gorby, Y.A., 1996. Environmental processes mediated by iron-reducing bacteria. *Curr. Opin. Biotechnol.*, 7: 287-294.
- Frenier, W.W. and Kennedy, W.C., 1986. Passivation of steel in ammonium ethylenediaminetetraacetic acid solutions. *Corrosion*, 42(10): 613-622.
- Furrer, G. and Stumm, W., 1986. The coordination chemistry of weathering: I. Dissolution kinetics of α - Al_2O_3 and BeO. *Geochim. Cosmochim. Acta*, 50: 1847-1860.
- Gibbs, M.M., 1979. A simple method for the rapid determination of iron in natural waters. *Water Res.*, 13(3): 295-297.
- Gillham, R.W., 1996. In situ treatment of groundwater: Metal-enhanced degradation of chlorinated organic contaminants. *Recent Advances in Ground-Water Pollution Control and Remediation, NATO Advanced Study Institute, Kemer, Antalya, Turkey*, Kluwer Academic, pp. 249-274.
- Goldberg, S. and Glaubig, R.A., 1985. Boron adsorption on aluminum and iron oxide minerals. *Soil Sci. Soc. Am. J.*, 49(6): 1374-1379.
- Good, N.E. and Izawa, S., 1968. Hydrogen ion buffers. In: A. San Pietro (Editor), *Methods in Enzymology*. Academic, New York, pp. 53-68.
- Gorby, Y.A., Workman, D.J., Kennedy, D.W., Amonette, J.P. and Fruchter, J., 1997. Transformation of carbon tetrachloride by biogenic Fe(II) in crystalline Fe(III) oxides and layer sheet silicates. *Environ. Sci. Technol.*, submitted.
- Graham, M.J., Bardwell, J.A., Goetz, R., Mitchell, D.F. and MacDougall, B., 1990. Composition and growth of anodic oxide films on iron. *Corr. Sci.*, 31: 139-148.
- Gui, J. and Devine, T.M., 1991. In situ vibrational spectra of the passive film on iron in buffered borate solution. *Corr. Sci.*, 32(10): 1105-1124.
- Heron, G., Crouzet, C., Bourg, A.C.M. and Christensen, T.H., 1994. Speciation of Fe(II) and Fe(III) in contaminated aquifer sediments using chemical extraction techniques. *Environ. Sci. Technol.*, 28(9): 1698-1705.
- Hingston, F.J., Posner, A.M. and Quirk, J.P., 1971. Competitive adsorption of negatively charged ligands on oxide surfaces. *Discuss. Faraday Soc.*, 52: 334-342.
- Ho, F.C. and Ord, J.L., 1973. The anodic oxide of iron: its component layers and their properties. *J. Electrochem. Soc.*, 119(2): 139-145.
- Huennekens, F.M. and Chance, B., 1963. Enzyme reactions. In: S.L. Friess, E.S. Lewis and A. Weissberger (Editors), *Investigation of Rates and Mechanisms of Reactions. Technique of Organic Chemistry*. Interscience, New York, pp. 1231-1314.
- Janik-Czachor, M. and Kaszczyszyn, S., 1982. Effect of Cl^- ions on the passive film on iron. *Werkst. Korros.*, 33: 500-504.

- Johnson, T.L., Scherer, M.M. and Tratnyek, P.G., 1996. Kinetics of halogenated organic compound degradation by iron metal. *Environ. Sci. Technol.*, 30(8): 2634-2640.
- Johnson, T.L. and Tratnyek, P.G., 1994. A column study of carbon tetrachloride dehalogenation by iron metal. *Proceedings of the 33rd Hanford Symposium on Health & the Environment—In Situ Remediation: Scientific Basis for Current and Future Technologies*, Battelle Pacific Northwest Laboratories, Pasco, WA, Vol. 2. pp. 931-947.
- Johnson, T.L. and Tratnyek, P.G., 1995. Dechlorination of carbon tetrachloride by iron metal: The role of competing corrosion reactions. *209th National Meeting ACS, American Chemical Society*, Anaheim, CA, Vol. 35, No. 1. pp. 699-701.
- Joshi, P.S., Venkateswaran, G. and Venkateswarlu, K.S., 1992. Chelant enhanced passivation of carbon steel in deoxygenated alkaline aqueous solutions. *Brit. Corr. J.*: 200-206.
- Khudenko, B.M. and Gould, J.P., 1991. Specifics of cementation processes for metals removal. *Wat. Sci. Technol.*, 24(7): 235-246.
- Klausen, J., Trüber, S.P., Haderlein, S.B. and Schwarzenbach, R.P., 1995. Reduction of substituted nitrobenzenes by Fe(II) in aqueous mineral suspensions. *Environ. Sci. Technol.*, 29(9): 2396-2404.
- Kruger, J., 1989. The nature of the passive film on iron and ferrous alloys. *Corr. Sci.*, 29(2/3): 149-162.
- Macalady, D.L., Tratnyek, P.G. and Grundl, T.J., 1986. Abiotic reduction reactions of anthropogenic organic chemicals in anaerobic systems. *J. Contam. Hydrol.*, 1(1): 1-28.
- Matheson, L.J. and Tratnyek, P.G., 1994. Reductive dehalogenation of chlorinated methanes by iron metal. *Environ. Sci. Technol.*, 28(12): 2045-2053.
- Matthess, G., 1982. *The Properties of Groundwater*. Wiley, New York.
- McBride, M.B., 1987. Adsorption and oxidation of phenolic compounds by iron and manganese oxides. *Soil Sci. Soc. Am. J.*, 51: 1466-1472.
- Norvell, W.A., 1991. *Reactions of Metal Chelates in Soils and Nutrient Solutions, Micronutrients in Agriculture*. Soil Science Society of America, Madison, WI, pp. 187-227.
- Nowack, B., Lutzenkirchen, T., Behra, P. and Sigg, L., 1996. Modeling the adsorption of metal-EDTA complexes onto oxides. *Environ. Sci. Technol.*, 30(7): 2397-2405.
- Oblonsky, L.J. and Devine, T.M., 1995. A surface enhanced Raman spectroscopic study of the passive films formed in borate buffer on iron, nickel, chromium and stainless steel. *Corr. Sci.*, 37(1): 17-41.
- Phillips, E.J.P. and Lovley, D.R., 1987. Determination of Fe(III) and Fe(II) in oxalate extracts of sediment. *Soil Sci. Soc. Am. J.*, 51: 938-941.
- Pou, T.E., Murphy, O.J., Young, V. and Bockris, J.O.M., 1984. Passive films on iron: The mechanism of breakdown in chloride containing solutions. *J. Electrochem. Soc.*, 131(6): 1243-1251.
- Powell, R.M., Puls, R.W., Hightower, S.K. and Sabatini, D.A., 1995. Coupled iron corrosion and chromate reduction: Mechanisms for subsurface remediation. *Environ. Sci. Technol.*, 29(8): 1913-1922.

- Roberts, A.L., Totten, L.A., Arnold, W.A., Burris, D.R. and Campbell, T.J., 1996. Reductive elimination of chlorinated ethylenes by zero-valent metals. *Environ. Sci. Technol.*, 30(8): 2654-2659.
- Roden, E.E. and Zachara, J.M., 1996. Microbial reduction of crystalline iron(II) oxides: Influence of oxide surface area and potential for cell growth. *Environ. Sci. Technol.*, 30(5): 1618-1628.
- Ryan, J.N. and Gschwend, P.M., 1991. Extraction of iron oxides from sediments using reductive dissolution by titanium(III). *Clays Clay Miner.*, 39(5): 509-518.
- Sato, N., 1989. Toward a more fundamental understanding of corrosion processes. *Corrosion*, 45(5): 354-368.
- Scherer, M.M. and Tratnyek, P.G., 1995. Dechlorination of carbon tetrachloride by iron metal: Effect of reactant concentrations. *209th National Meeting ACS, American Chemical Society*, Anaheim, CA, Vol. 35, No. 1. pp. 805-806.
- Scherer, M.M., Westall, J.C., Ziomek-Moroz, M. and Tratnyek, P.G., 1997. Kinetics of carbon tetrachloride reduction at an oxide-free iron electrode. *Environ. Sci. Technol.*, in press.
- Shoesmith, D.W., 1987. Kinetics of aqueous corrosion. In: L.J. Korb and D.L. Olson (Editors), *Metals Handbook*. ASM, Metals Park, OH, pp. 45-49.
- Sims, J.R. and Bingham, F.T., 1968. Retention of boron by layer silicates, sesquioxides, and soil materials: II. Sesquioxides. *Soil Sci. Soc. Am. J.*, 32: 364-369.
- Sinniger, J., 1992. *Die inhibition der auflösung von eisen(III)(hydr)oxiden und ihre beziehung zur passivität von eisen*. Ph.D. Dissertation, Swiss Federal Institute of Technology, Zürich, 131 pp.
- Sivavec, T.M. and Horney, D.P., 1997. Reduction of chlorinated solvents by Fe(II) minerals. *213th National Meeting, Division of Environmental Chemistry, American Chemical Society*, San Francisco, CA, Vol. 37, No. 1. pp. 115-117.
- Sivavec, T.M., Horney, D.P. and Baghel, S.S., 1995. Reductive dechlorination of chlorinated ethenes by iron metal and iron sulfide minerals. *Emerging Technologies in Hazardous Waste Management VII, Extended Abstracts for the Special Symposium, Industrial & Engineering Chemistry Division, American Chemical Society*, Atlanta, GA, pp. 42-45.
- Sposito, G., 1984. *The Surface Chemistry of Soils*. Oxford, New York.
- Stratmann, M. and Müller, J., 1994. The mechanism of the oxygen reduction on rust-covered metal substrates. *Corr. Sci.*, 36(2): 327-359.
- Stucki, J.W., Komadel, P. and Wilkinson, H.T., 1987. Microbial reduction of structural iron(III) in smectites. *Soil Sci. Soc. Am. J.*, 51(6): 1663-5.
- Stumm, W. (Editor), 1987. *Aquatic Surface Chemistry: Chemical Processes at the Particle-Water Interface*. Wiley, New York.
- Stumm, W., 1992. *Chemistry of the Solid-Water Interface: Processes at the Mineral-Water and Particle-Water Interface of Natural Systems*. Wiley, New York.
- Stumm, W., 1993. From surface acidity to surface reactivity; inhibition of oxide dissolution. *Aquat. Sci.*, 55(5): 273-280.
- Stumm, W., Sulzberger, B. and Sinniger, J., 1990. The coordination chemistry of the oxide-electrolyte interface: the dependence of surface reactivity (dissolution, redox reactions) on surface structure. *Croat. Chem. Acta*, 63(3): 277-312.

- Tratnyek, P.G., 1996. Putting corrosion to use: Remediation of contaminated groundwater with zero-valent metals. *Chem. Ind. (London)*(13): 499-503.
- Uhlig, H.H., 1979. Passivity in metals and alloys. *Corr. Sci.*, 19: 777-791.
- Vasudevan, D. and Stone, A.T., 1996. Adsorption of catechols, 2-aminophenols, and 1,2-phenylenediamines at the metal (hydr)oxide/water interface: Effect of ring substituents on the adsorption onto TiO₂. *Environ. Sci. Technol.*, 30(5): 1604-1613.
- Wieland, E., Wehrli, B. and Stumm, W., 1988. The coordination chemistry of weathering: III. A generalization on the dissolution rates of minerals. *Geochim. Cosmochim. Acta*, 52: 1969-1981.
- Yamaguchi, M., Nishihara, H. and Aramaki, K., 1994. The inhibition of passive film breakdown on iron in a borate buffer solution containing chloride ions by organic anions inhibitors. *Corr. Sci.*, 36(3): 241-258.
- Zepp, R.G. and Wolfe, N.L., 1987. Abiotic transformation of organic chemicals at the particle-water interface. In: W. Stumm (Editor), *Aquatic Surface Chemistry: Chemical Processes at the Particle-Water Interface*. Wiley, New York, pp. 423-455.
- Zinder, B., Furrer, G. and Stumm, W., 1986. The coordination chemistry of weathering: II. Dissolution of Fe(III) Oxides. *Geochim. Cosmochim. Acta*, 50: 1861-1869.

VITA

The author was born October 2, 1966 in Hot Springs National Park, Arkansas and attended the Lakeside school system. He holds a Bachelor of Science degree from the University of Arkansas at Fayetteville in Geology which was granted in 1989.

The author has worked with a number of organizations including: Battelle Pacific Northwest Laboratories, Environmental Microbiology Group and Earth Sciences Group, Hanford Nuclear Reservation, Richland, WA; Office of Polar Programs, United States Geological Survey, Seal River Beach and Bering Glacier, Alaska; Office of Pesticide Programs, United States Environmental Protection Agency, Washington, D.C.; Institut für Allgemeine und Angewandte, Ludwig Maximilian Universität, Munich, Germany; and Foundation for Glacier and Environmental Research, Juneau Icefield, Alaska. Additional experience includes presentations and posters given at professional meetings such as Geological Society of America, American Chemical Society, Hanford Science Symposium on Health and the Environment, and Gordon Research Conference on Environmental Sciences. Awards include American Chemical Society-Division of Environmental Chemistry, 1995 Graduate Student Award; Association of Ground Water Scientists and Engineers: Graduate Student Fellowship; and Pacific Northwest National Laboratories/Department of Energy: Energy Research Fellowship. Selected publications include:

Johnson, T.L., W. Fish, Y.A. Gorby and P.G. Tratnyek. 1997. Degradation of carbon tetrachloride by iron metal: Complexation effects on the oxide surface. *J. Contam. Hydrol.*, in press:

Johnson, T.L., M.M. Scherer and P.G. Tratnyek. 1996. Kinetics of halogenated organic compound degradation by iron metal. *Environ. Sci. Technol.*, 30: 2634-2640.

Johnson, T.L. and P.G. Tratnyek. 1995. *Dechlorination of carbon tetrachloride by iron metal: The role of competing corrosion reactions*. 209th American Chemical Society National Meeting. Division of Environmental Chemistry Preprints of Papers, Anaheim, CA. Vol. 35, No. 1, pp. 699-701.

Johnson, T. L., and P. G. Tratnyek. 1994. A column study of carbon tetrachloride dehalogenation by iron metal. *Proceedings of the 33rd Hanford Symposium on Health & the Environment-In Situ Remediation: Scientific Basis for Current and Future Technologies*. Pasco, WA. pp 931-947.